10. SITE 543: OCEANIC REFERENCE SITE EAST OF THE BARBADOS RIDGE COMPLEX[1]

Shipboard Scientific Party[2,3]

HOLE 543

Date occupied: 28 February 1981

Date departed: 3 March 1981

Time on hole: 3 days, 14 hr.

Position: 15°42.74′; 58°39.22′

Water depth (sea level; corrected m, echo-sounding): 5633

Water depth (rig floor; corrected m, echo-sounding): 5643

Bottom felt (m, drill pipe): 5637.0

Penetration (m): 332

Number of cores: 34

Total length of core section (m): 324.0

Total core recovered (m): 228.4

Core recovery (%): 79.5

Oldest sediment cored:
Depth sub-bottom (m): 332
Nature: Claystone
Age: early Eocene
Measured velocity (km/s): 2.453 (543-34,CC—hard claystone)

Basement: Not reached

HOLE 543A

Date occupied: 3 March 1981

Date departed: 9 March 1981

Time on hole: 6 days, 1 hr.

Position: 15°42.74′; 58°39.22′

Water depth (sea level; corrected m, echo-sounding): 5633.0

Water depth (rig floor; corrected m, echo-sounding): 5643.0

Bottom felt (m, drill pipe): 5637.0

Penetration (m): 455.0

Number of cores: 16

Total length of core section (m): 142.5

Total core recovered (m): 69.4

Core recovery (%): 48.7

Oldest sediment cored:
Depth sub-bottom (m): 409
Nature: Ferruginous, calcareous claystone
Age: Campanian–Maestrichtian
Measured velocity (km/s): 1.671 (543A-10-1, 28–32 cm)

Basement:
Depth sub-bottom (m): 411.0 (top); 455 (bottom of hole)
Nature: Basalt
Velocity range (km/s): 4.910 to 5.621

Principal results: At Site 543 we penetrated a 411-m sequence of hemipelagic and pelagic sediments and 44 m of basaltic pillow lavas. The Recent sediments consist of ashy mud to a depth of 10 m. The subjacent sediments to 70.5 m are Pleistocene to upper Pliocene ashy nannofossil mud, transitional to a unit of lower Pliocene to lower Miocene mud and ashy mud that extends to 176 m sub-bottom. Radiolarian clay, initially with local ash layers, and subsequently with manganese stains, occurs from 176 to 322 m sub-bottom spanning the lower Miocene to Oligocene, respectively. Zeolitic clay–claystone is present from 322 to 379 m sub-bottom and overlies a basal calcareous, ferruginous, Maestrichtian to Campanian claystone that contacts basalt at 411 m. Plagioclase and plagioclase–olivine phyric pillow basalts extend to a total sub-bottom depth of 455 m.

Overall, the lithology at Site 543 records the birth and evolution of an open-ocean crustal sequence with its progressive approach to the Lesser Antilles volcanic arc. The upper 200 m of early Miocene and younger rocks are lithologically and paleontologically identical to the sequences cored at Sites 541 and 542, arguing for the oceanic derivation and hence offscraping of the latter at the deformation front of the Barbados Ridge complex. A marked increase in density and shear strength between about 180 and 200 m sub-bottom lies just under the seaward extension of a reflector separating the apparently offscraped and subducted units to the west. The observed changes in physical properties seemingly predict development of a décollement at 180 to 200 m sub-bottom as inferred from seismic data.

A downhole seismometer with temperature and tilt recorders was emplaced in the basaltic basement at Site 543. The instrument remained in the hole while a seismic refraction experiment was conducted. Malfunctioning of the seismometer necessitated retrieval of the downhole instrument and prevented deployment of the long-term recording package on the seafloor.

BACKGROUND AND OBJECTIVES

Site 543 lies on seismic line A1C about 22 km north-northeast of Sites 541 and 542 and 3.5 km seaward of the deformation front of the Barbados Ridge complex (Fig. 1-3). The substantial northward offset of Site 543 relative to Sites 541 and 542 was required in order to minimize the sediment penetration and therefore ensure reaching the ocean crust. Site 543 is on the northern

[1] Biju-Duval, B., Moore, J. C., et al., *Init. Repts DSDP*, 78A: Washington (U.S. Govt. Printing Office).

[2] Bernard Biju-Duval (Co-Chief Scientist), Institut Français du Pétrole, 92505 Rueil Malmaison, France (present address: Centre National pour l'Exploitation des Océans, 66 Avenue d'Iéna, 75116 Paris, France); J. Casey Moore (Co-Chief Scientist), Earth Sciences and Marine Studies, University of California at Santa Cruz, Santa Cruz, California; James A. Bergen, Department of Geology, Florida State University, Tallahassee, Florida; Grant Blackinton, Hawaii Institute of Geophysics, University of Hawaii at Manoa, Honolulu, Hawaii; George E. Claypool, Branch of Oil and Gas Resources, U.S. Geological Survey, Denver Federal Station, Denver, Colorado; Glenn Foss, Deep Sea Drilling Project, Scripps Institution of Oceanography, La Jolla, California; Rodolfo T. Guerra, Exploration Services Center, Mobil Exploration and Producing Services, Dallas, Texas; Christoph H. J. Hemleben, Institut und Museum für Geologie und Paläontologie, Universität Tübingen, D-7400 Tübingen 10, Federal Republic of Germany; Michael S. Marlow, U.S. Geological Survey, Menlo Park, California; James H. Natland, Deep Sea Drilling Project, Scripps Institution of Oceanography, La Jolla, California; Carol J. Pudsey, Department of Geology, University of Leicester, Leicester, United Kingdom; G. W. Renz, Deep Sea Drilling Project, Scripps Institution of Oceanography, La Jolla, California (present address: 5260 Angeles Crest, La Canada, California); Marc Tardy, Département de Sciences de la Terre, Université de Savoie, BP 1104, Chambéry, France; Douglas Wilson, Hawaii Institute of Geophysics, University of Hawaii at Manoa, Honolulu, Hawaii (present address: Department of Geophysics, Stanford University, Stanford, California); Audrey Wright, Earth Sciences and Marine Studies, University of California at Santa Cruz, Santa Cruz, California (present address: Deep Sea Drilling Project, Scripps Institution of Oceanography, La Jolla, California).

[3] With a contribution from Daniel Davis, Department of Earth and Planetary Sciences, Massachusetts Institute of Technology, Cambridge, Massachusetts.

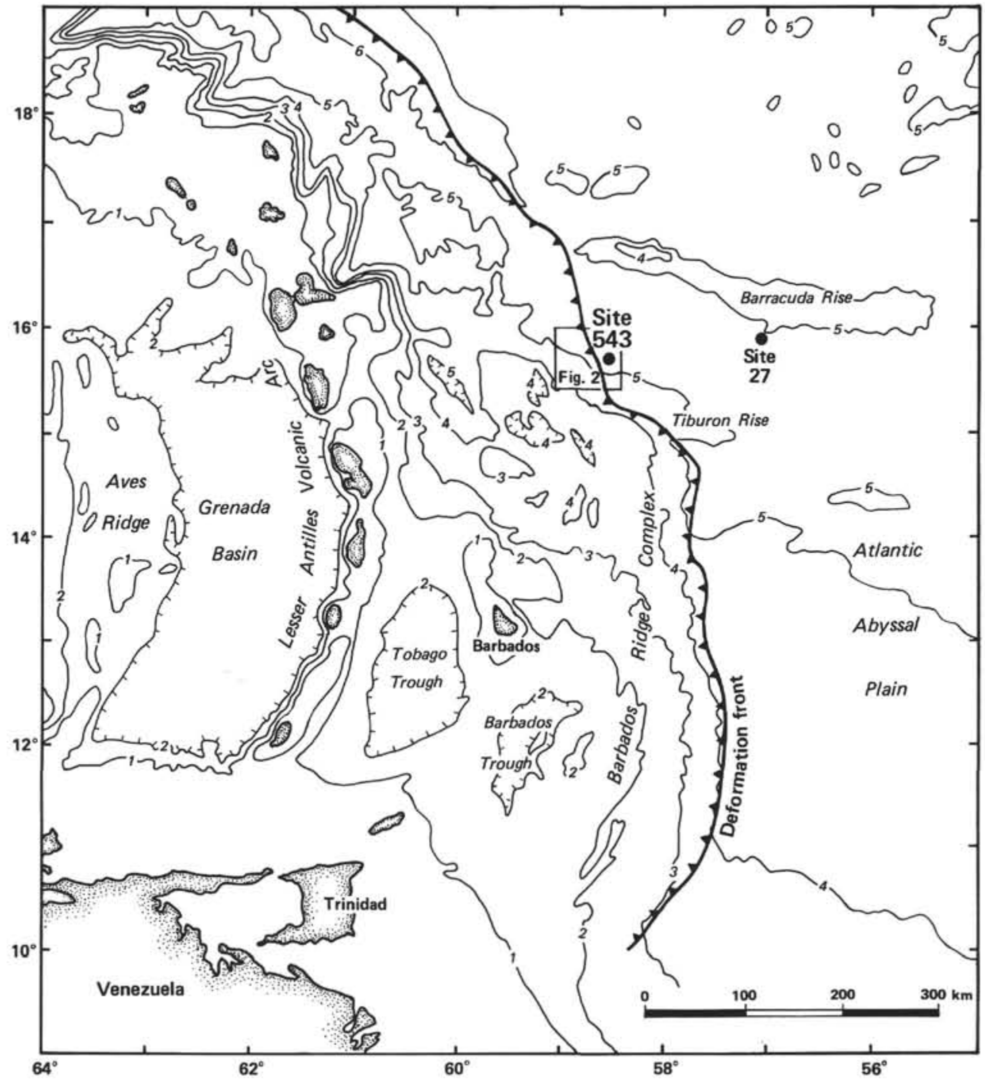

Figure 1. Regional location map. (Note position of deformation front defining eastward boundary of Barbados Ridge and Tiburon Rise underthrusting deformation front near Site 543. Contour intervals are in kilometers.)

flank of the Tiburon Rise and therefore penetrated a depositional sequence similar to that lying on the ocean plate seaward of Sites 541 and 542. Moreover, the principal acoustic reflectors noted at Sites 541 and 542 can be traced to Site 543 via the site survey seismic grid. Thus the demonstrable continuity in acoustic stratigraphy throughout the Leg 78A area permits Site 543 to be used as an oceanic reference site for Sites 541 and 542, despite their lateral offsets.

Both the Tiburon and Barracuda rises constitute prominent highs emerging from the Atlantic abyssal plain and presently intersecting the deformation front of the Barbados Ridge complex (Fig. 1). The sediment thickness near Site 543 is about 400 to 500 m and locally reaches at least 1100 m on the ocean plate in the Leg 78A area (Ngokwey et al., this volume). To the south on the Atlantic abyssal plain, sediments gradually attain a thickness of more than 4 km, suggesting derivation and lateral transport from the south (Biju-Duval et al., 1978; Mascle et al., in press). The damming effects of the Tiburon and Barracuda rises also contribute to the northward thinning of sediment on the Atlantic abyssal plain.

The principal goal of Site 543 was definition of an oceanic reference section that would allow multiple comparisons to the sequences cored landward of the deformation front at Sites 541 and 542. Specific objectives of drilling at Site 543 were: (1) to test by lithologic and paleontologic criteria whether the sections cored at Sites 541 and 542 are of ocean-plate origin and thereby offscraped from the Tiburon Rise area; (2) to provide a physical-property profile through the undisturbed ocean-plate section and thereby a basis for measuring the tectonic consolidation of any offscraped rocks of similar lithology; (3) to date and establish physical and lithologic contrasts across the seaward projection of the reflector separating the apparently off-scraped and underthrust sequences landward of the deformation front (here we hoped to determine the physical basis for their apparent

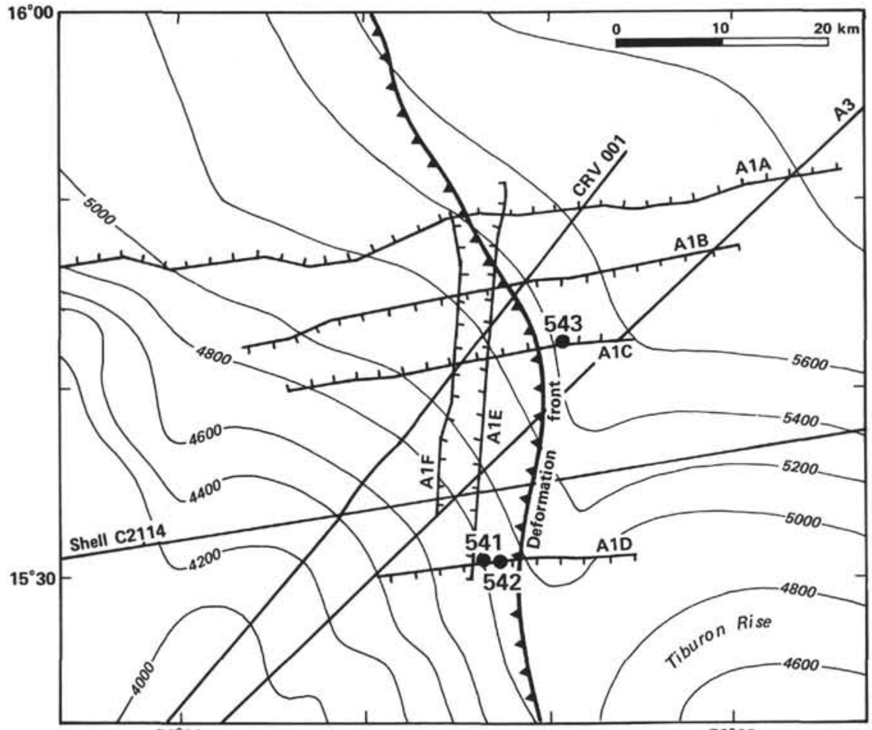

Figure 2. Detailed site location map (box, Fig. 1). (Note position of deformation front and location of seismic reflection lines used for site survey. Bathymetry is in meters. Lines A1A to A1D from IFP/CNEXO survey [from Ngokwey et al., this volume].)

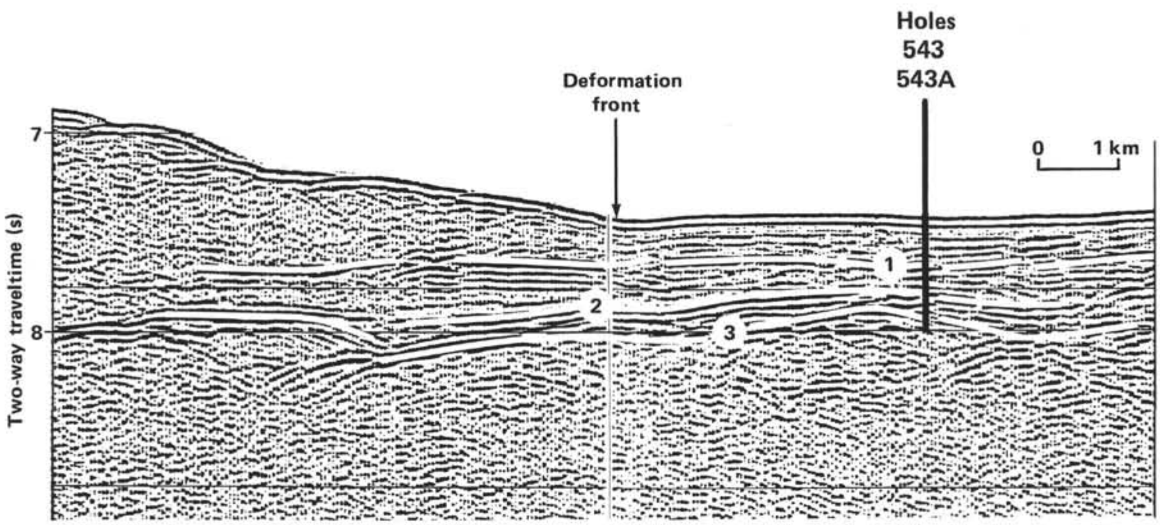

Figure 3. Seismic reflection line A1C. (From Ngokwey et al., this volume.) Reflector 1 is equivalent to the boundary between a discontinuously reflective (deformed) unit and an acoustically layered unit at Sites 541 and 542. Reflector 2 separates seismic units of tabular (above) and irregular (below) thicknesses. Reflector 3 is top of oceanic crust.

décollement surface); (4) to sample the section underthrust deeply beneath the Barbados Ridge complex (because we failed to penetrate this underthrust sequence at either Site 541 or Site 542, sampling it at Site 543 was crucial); and (5) to date the ocean crust and emplace a downhole seismometer in the basement.

OPERATIONS

Hole 543

Site 543 is located about 12 mi. north-northeast of Site 542 and seaward of the toe of the trench slope. Its primary purpose was to provide an undisturbed reference section for comparison with the disturbed and accreted sediments cored on the slope. The inability to penetrate to basement at Sites 541 and 542 dictated that Site 543 would also be the location for the downhole seismometer implantation.

The move and site approach consumed only 2 hr., and a positioning beacon was launched at 0450 hr., 28 February. The seismic gear was retrieved and on-site stationing began while the beacon was still falling. The beacon signal, which had never been strong, faded completely after 1 hr., and a second beacon (of alternate frequency) was dropped to replace it.

The pipe trip was extended by about 4.25 hr. to assemble a new bottom-hole assembly (BHA) to replace the one lost in Hole 542B. Several satellite navigation fixes were received during the trip, and a positioning offset of 910 m to the south was made to move the vessel onto seismic profile.

Using the corrected precision depth recorder (PDR) reading of 5653 m as a guide, an initial seafloor punch core was taken by lowering the bit to 5655.5 m. Signs of "taking weight" were first noted on the rig weight indicator at about 5649 m. On recovery the inner core barrel was filled to its top, which had penetrated to 5646 m. Water depth was therefore estimated at 5645 m. Continuous coring then continued to 324 m sub-bottom without significant difficulty. Coring and recovery data are given in Table 1.

As Core 34 was being recovered, the inner barrel suddenly became jammed in the drill pipe about 1500 m above the bit. The overshot shear pin failed during attempts to free the inner barrel and the sand line was retrieved. A second inner barrel was pumped down to jar the first barrel loose, but without success. A second wireline recovery attempt also failed to move the stuck core barrel. It was then necessary to pull about 4200 m of drill pipe to recover the core. The barrel was found to be jammed in place by a steel ball that had fallen down the pipe from the latch of the adjustable line wiper.

Hole 543A

With the drill string cleared of obstructions, it was tripped back to the seafloor. A second attempt to recover a "mud-line" punch core and to verify water depth was then made by lowering the bit to 5647 m. On recovery, sediment was again found packed to the top of the barrel, and water depth was revised to 5637 m. Again, coring and recovery data are presented in Table 1.

The hole was drilled, without coring, to 332 meters sub-bottom. Considerable hole problems occurred below about 260 m. Torquing and vertical sticking of the pipe, along with annular plugging, nearly forced us to abandon the hole at one point. The problems were attributed to adherence of sticky clay to the drill collars. Fortunately firmer sediments were reached near the end of the drilled interval and an improvement in hole conditions was noted after "working" the pipe and circulating mud slugs. The "wash" core barrel was recovered, and continuous coring commenced. Core recovery for the lower sediment section was consistently below normal for unknown reasons. Basaltic basement was reached at 411 m sub-bottom. Good hole conditions and 81% core recovery prevailed in the basement rocks, with penetration at a slow 2 m/hr. Coring operations were terminated at 455 m sub-bottom due to time and scheduling considerations.

The core bit and associated components were released by activating the mechanical bit release with a wire-line shifting tool. The open-ended drill string was then pulled to 280 m sub-bottom for logging. Because of the soft nature of the sediment, the pipe was left fairly deep in the hole to avoid the bridging and plugging tendencies of soft clay that have often frustrated logging attempts.

The temperature-density-gamma ray sonde was rigged and run down the pipe to 5600 m, the starting point for the temperature log. When only about 20 m of temperature log had been recorded—and before seafloor depth had been reached—a downhole electrical problem devel-

Table 1. Coring summary, Site 543.

Core no.	Date (1981)	Time	Depth from drill floor (m) top bottom	Depth below seafloor (m) top bottom	Length cored (m)	Length recovered (m)	Amount recovered (%)
Hole 543							
1	Feb. 28	2150	5635.0–5645.5	0–10.5	10.5	9.12	90
2	Feb. 28	2342	5645.5–5655.0	10.5–20.0	9.5	7.86	83
3	Mar. 1	0148	5655.0–5664.5	20.0–29.5	9.5	9.73	102
4	Mar. 1	0334	5664.5–5674.0	29.5–39.0	9.5	9.71	102
5	Mar. 1	0524	5674.0–5683.5	39.0–48.5	9.5	6.51	69
6	Mar. 1	0706	5683.5–5693.0	48.5–58.0	9.5	9.49	100
7	Mar. 1	0850	5693.0–5702.5	58.0–67.5	9.5	5.20	55
8	Mar. 1	1041	5702.5–5712.0	67.5–77.0	9.5	7.43	78
9	Mar. 1	1225	5712.0–5721.5	77.0–86.5	9.5	9.60	101
10	Mar. 1	1410	5721.5–5731.0	86.5–96.0	9.5	6.62	70
11	Mar. 1	1600	5731.0–5740.5	96.0–105.5	9.5	4.47	47
12	Mar. 1	1741	5740.5–5750.0	105.5–115.0	9.5	9.78	103
13	Mar. 1	1925	5750.0–5759.5	115.0–124.5	9.5	9.72	102
14	Mar. 1	2120	5759.5–5769.0	124.5–134.0	9.5	8.12	85
15	Mar. 1	2307	5769.0–5778.5	134.0–143.5	9.5	3.59	39
16	Mar. 2	0109	5778.5–5788.0	143.5–153.0	9.5	6.83	61
17	Mar. 2	0258	5788.5–5797.5	153.0–162.5	9.5	6.81	72
18	Mar. 2	0448	5797.5–5807.0	162.5–172.0	9.5	9.03	95
19	Mar. 2	0630	5807.0–5816.5	172.0–181.5	9.5	8.54	90
20	Mar. 2	0816	5816.5–5826.0	181.5–191.0	9.5	5.98	63
21	Mar. 2	1010	5826.0–5835.5	191.0–200.5	9.5	0.0	0
22	Mar. 2	1155	5835.5–5845.0	200.5–210.0	9.5	Tr.	0
23	Mar. 2	1350	5845.0–5854.5	210.0–219.5	9.5	3.61	38
24	Mar. 2	1610	5854.5–5864.0	219.5–229.0	9.5	6.74	71
25	Mar. 2	1815	5864.0–5873.5	229.0–238.5	9.5	3.51	37
26	Mar. 2	2030	5873.5–5883.0	238.5–248.0	9.5	9.02	95
27	Mar. 2	2325	5883.0–5892.5	248.0–257.5	9.5	8.87	93
28	Mar. 3	0150	5892.5–5902.0	257.5–267.0	9.5	7.91	83
29	Mar. 3	0340	5902.0–5911.5	267.0–276.5	9.5	9.82	103
30	Mar. 3	0530	5911.5–5921.0	276.5–286.0	9.5	8.96	94
31	Mar. 3	0715	5921.0–5930.5	286.0–295.5	9.5	1.88	20
32	Mar. 3	0945	5930.5–5940.0	295.5–305.0	9.5	7.12	73
33	Mar. 3	1230	5940.0–5949.0	305.0–314.5	9.5	4.02	44
34	Mar. 3	2358	5949.5–5959.0	314.5–324.0	9.5	2.80	29
Total					324.0	228.4	79.5
Hole 543A							
1	Mar. 4	0827	5627.0–5637.0	0–10.0	10.0	7.87	79
H1[a]	Mar. 4	1808	5637.0–5959.0	10.0–332.0	Washed	5.21	—
2	Mar. 4	2050	5659.0–5968.5	332.0–341.5	9.5	2.44	26
3	Mar. 4	2245	5968.5–5978.0	341.5–351.0	9.5	2.92	31
4	Mar. 5	0150	5978.0–5987.5	351.0–360.5	9.5	3.98	42
5	Mar. 5	0307	5987.5–5997.0	360.5–370.0	9.5	4.21	44
6	Mar. 5	0510	5997.0–6006.5	370.0–379.5	9.5	1.25	13
7	Mar. 5	0745	6006.5–6016.0	379.5–389.0	9.5	4.91	52
8	Mar. 5	1045	6016.0–6025.5	389.0–398.5	9.5	1.11	12
9	Mar. 5	1315	6025.5–6035.0	398.5–408.0	9.5	0.97	11
10	Mar. 5	1805	6035.0–6044.5	408.0–417.5	9.5	3.12	32
11	Mar. 5	2105	6044.5–6047.0	417.5–420.0	2.5	2.27	91
12	Mar. 6	0145	6047.0–6054.0	420.0–427.0	7.0	4.17	60
13	Mar. 6	0710	6054.0–6063.0	427.0–436.0	9.0	8.53	95
14	Mar. 6	1011	6063.0–6065.0	436.0–438.0	2.0	0.85	43
15	Mar. 6	1724	6065.0–6072.0	438.0–445.0	7.0	6.61	94
16	Mar. 7	0102	6072.0–6082.0	445.0–455.0	10.0	9.0	90
Total					142.5	69.4	48.7

[a] Core 543A-H1 is a wash core that recovered material from 10 to 332 m sub-bottom with the core barrel in place; percent recovery data are not given for this core.

oped that caused the loss of temperature logging capability. The equipment was switched to the density-caliper-gamma ray mode, but the problems remained. The logging tool was recovered and the trouble was traced to seawater in the DSDP-furnished sinker bar. A backup sinker bar was installed and a second attempt was made. An open-hole bridge was encountered just 2 m below the end of the pipe. The sonde was worked through this and two other obstructions as temperature was logged to 375 m sub-bottom. A more substantial bridge at this point could not be penetrated after several attempts. A static temperature measurement was then recorded and the logging mode was switched to the density mode to log up to the pipe. It was then found that the density log detectors had apparently been damaged by the rough treatment the tool had received in getting through obstructions. The logging sonde became stuck upon reentering the drill string and could be moved neither up nor down. During attempts to dislodge it, the tool suddenly came free while under considerable pull. It was subsequently found that the caliper backup arm had been broken off and left in the hole. The caliper and gamma ray curves were good, however, and verified that the borehole was badly eroded, with an average diameter of 13 to 14 in. Density or sonic logs would therefore have been of little value in the sediment section. Because insufficient operating time remained to clean the hole and log the basement interval, the logging cable was then reheaded for the attachment of the Hawaii Institute of Geophysics (HIG) ocean sub-bottom seismometer (OSS) package.

While the reheading and final instrument package tests were in progress, the power sub was picked up and the hole was cleaned to 4 m above total depth. To avoid plugging the end of the pipe, high pump rates were used to clean the hole, and downward progress was stopped at the first sign of contact on the weight indicator. Two joints of drill pipe were then set back, leaving just 22 m of open hole.

At just past midnight on 8 March, the seismometer was started down the pipe. Unfortunately, the instrument met an obstruction at the end of the drill string and would not pass into open hole. It was concluded that, despite precautions, the end of the bit release top connector had become plugged with sediment and/or drill cuttings and that pump circulation was through the "windows" in the side of the top connector. After a few minutes of unsuccessful effort to get the instrument out of the pipe, it was recovered for an attempt to unplug the pipe. A specially weighted junk inner core barrel section was assembled and pumped down the pipe at maximum pump rate. Pump pressure was abnormally high and no change in pressure was noted after an adequate interval of pumping. With a great deal of anxiety, we again lowered the seismometer package through the pipe on the logging cable. At 0905 hr., the instrument passed out of the pipe. It was then successfully emplaced in the open basalt hole and a series of tests were run.

With the seismometer finally in place, the logging cable was clamped off at the top of the drill pipe and cut. A special cable slip-pulling neck assembly was attached to the end of the in-hole portion of the cable. This was latched up to an overshot-swivel assembly on the sand line, the weight of the cable was taken by the sand line, and the clamp was removed. The logging sheaves were then rigged down, and the slow process of stripping the pipe out of the hole begun. The pipe trip proceeded smoothly, however, and over 6 km of pipe were pulled past the cable in 16 hr.

The cable in the hole was then responsed to the remainder on the winch by means of a "torpedo" connection. Following tests of the downhole instrument package, the cable on the winch was slowly payed out while the ship was offset a total of 3.6 km from the hole. As this exceeded the maximum offset capability of the positioning system, it was necessary to drop a new acoustic beacon for station-keeping at the new location.

The accompanying vessel, *North Star*, had emplaced an array of five ocean bottom seismometers (OBS) several miles across and centered on Site 543. Test charges were then fired to test the response of the OSS and communications between the two vessels in preparation for refraction profiling. At this point, the downhole seismometer data were found to be garbled and not usable. The data from one shooting line was taped in the hope that some data could be retrieved.

The *Challenger* was then slowly moved back to the drill site as the logging cable was retrieved. The OSS was pulled from the hole without undue difficulty, despite the inability to retract the caliper arm. The instrument was on deck at 1945 hr., 9 March, and the vessel got underway at 2006 hr.

Site 543 to San Juan

The *Challenger* steamed about 20 mi. north to rendezvous with the *North Star*, which was engaged in refraction shooting for the OBS array. Following transfer of personnel back to the *North Star*, the profiling gear was streamed and the *Challenger* began postsite profiling that passed over Site 543. At 0056 hr., 10 March, the survey was completed and course was set for the return to San Juan.

SEDIMENT LITHOLOGY

Lithostratigraphy

Site 543, the oceanic reference site, was drilled in 5627 m water depth, 3.5 km east of the toe of the accretionary prism. Two holes were drilled at Site 543: Hole 543 was continuously cored for 324 m before a core barrel jammed in the drill pipe and the hole had to be abandoned. Hole 543A was cored continuously below 332 m and penetrated 44 m of basaltic basement. The first sediment continuously cored at Hole 543A (Core 2) is just beneath the deepest sediment cored at Hole 543 (Core 34). The sediment recovery from Holes 543 and 543A was sufficient to permit good lithostratigraphic definition of the oceanic reference site sediments.

Based on macroscopic core descriptions, smear slide analyses, and calcium carbonate bomb data, the sequence of sediments and rock units drilled at Site 543 can be divided into seven lithologic units (Fig. 4). A summary of these units is shown in Table 2. Downhole percentages

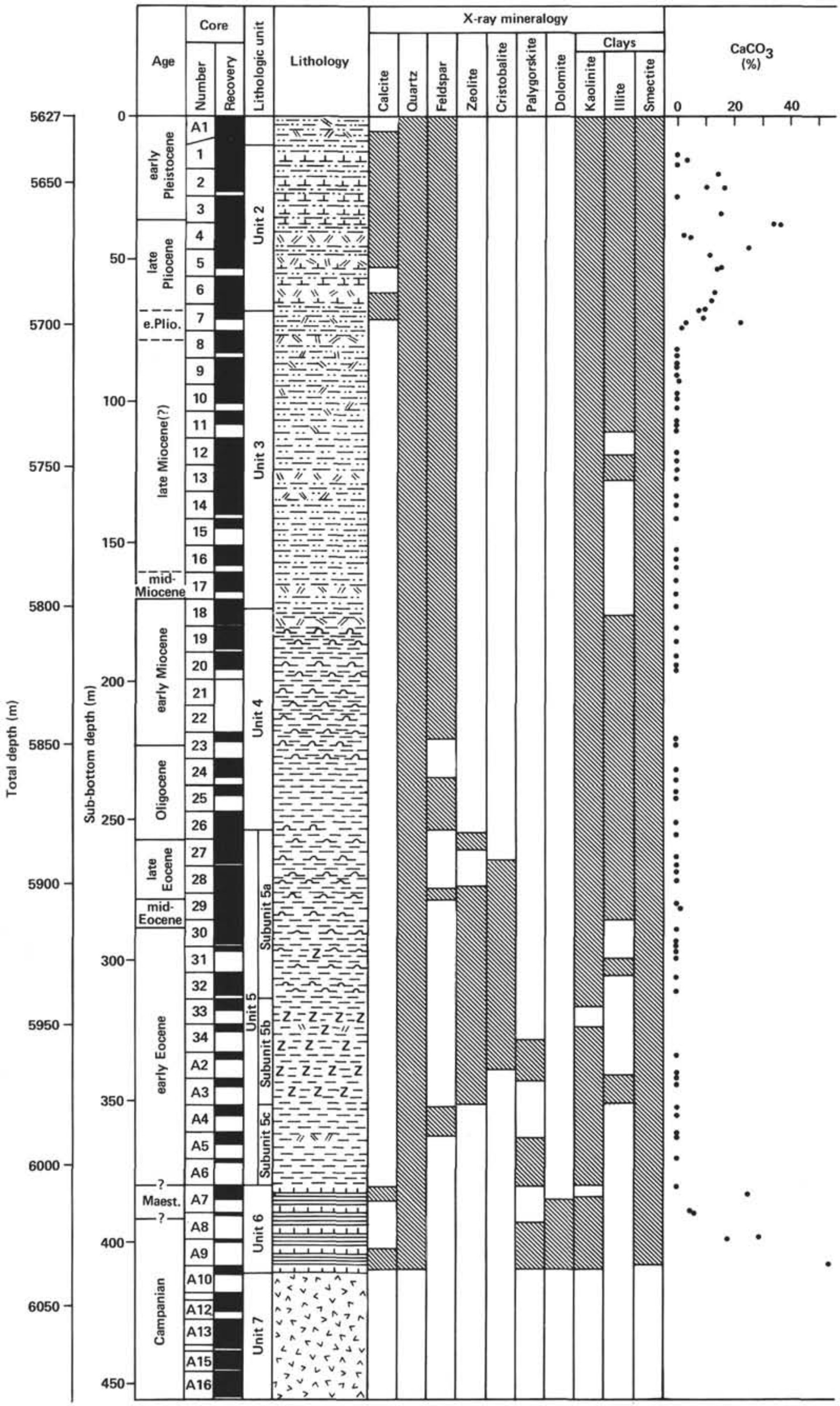

Figure 4. Summary lithology, sediment composition, structure, physical properties, and seismic stratigraphy, Site 543. (In X-Ray Mineralogy column blackened areas simply show presence.)

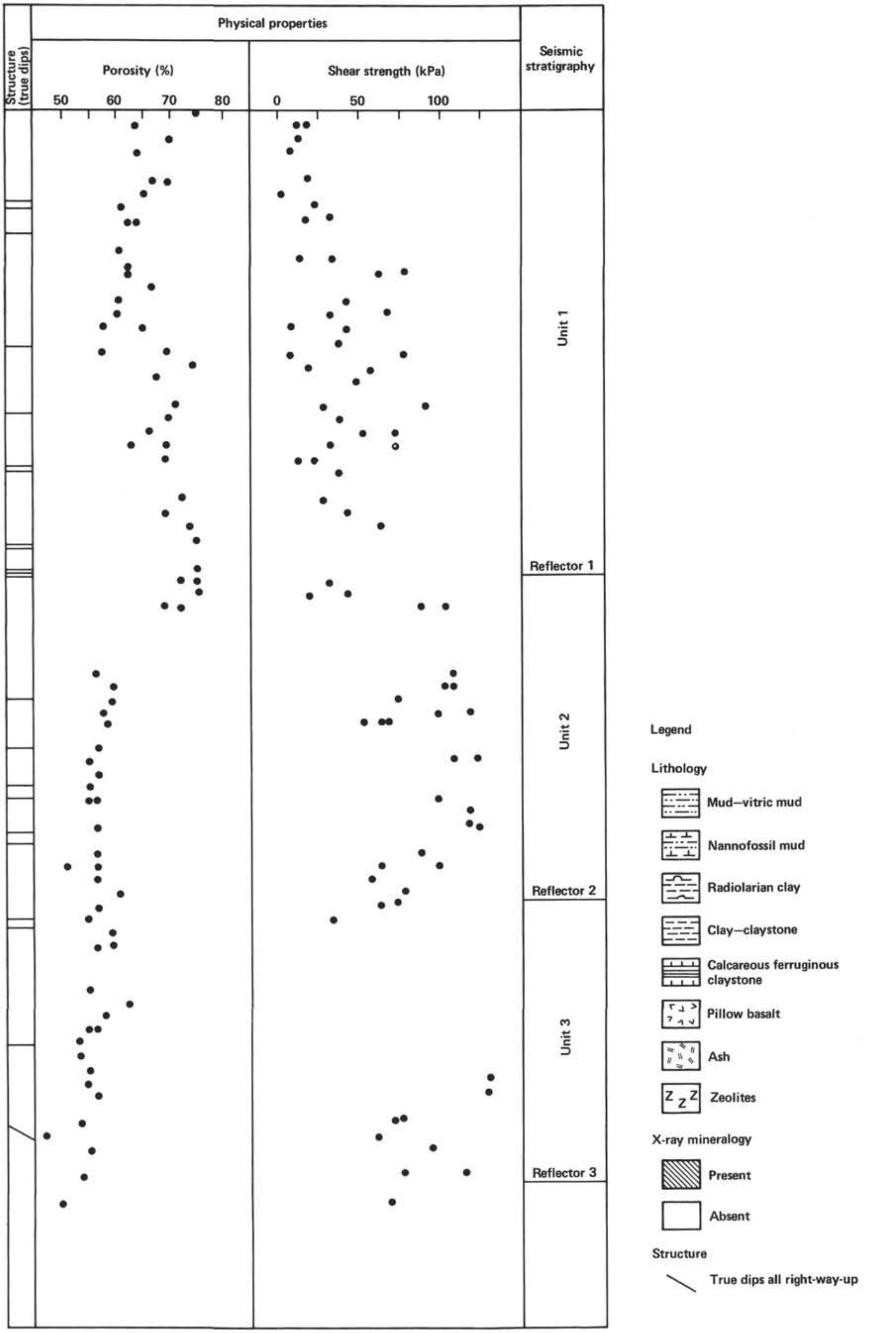

Figure 4. (Continued).

Table 2. Lithologic units, Site 543.

Unit, subunit	Hole 543 Sample (core-section, cm level)	Hole 543 Sub-bottom depth (m)	Hole 543A Sample (core-section, cm level)	Hole 543A Sub-bottom depth (m)	Dominant lithology	Age
1	—	—	1	0–8	Ashy mud	Quaternary
2	1 to 7-2, 100	8–68.5	—	—	Ashy nannofossil mud and vitric mud with ash layers	early Pleistocene–late Pliocene
3	7-2, 100 to 18-3, 50	68.5–174.0	—	—	Mud and vitric mud with ash layers	early Pliocene-early Miocene(?)
4	18-3, 50 to 26-5, 100	174.0–253.0	—	—	Radiolarian clay with ashy layers	early Miocene–Oligocene
5a	26-5, 100 to 32	253.0–313.0	—	—	Mn-stained radiolarian clay	Oligocene–middle late Eocene
5b	33 to 34	313.0–322.0	2 to 3	322.0–351.0	Zeolitic clay–claystone and clay–claystone	Eocene
5c	—	—	4 to 6	351.0–379.5	Claystone	Eocene
6	—	—	7 to 10-2, 100	379.5–411.0	Calcareous ferruginous claystone	Cretaceous (early Maestrichtian–early Campanian)
7	—	—	10-2, 100 to 16	411.0–455.0	Pillow basalts	Cretaceous

Note: — indicates no data.

of calcium carbonate at Site 543 were determined with the shipboard carbonate bomb (Fig. 4).

Lithologic Unit 1 is an 8-m-thick, Quaternary ashy mud drilled in the mud-line core (Core 1) of Hole 543A that overlies and is younger than the first sediment drilled at Hole 543. It is primarily brown (10YR 5/3) with dark grayish brown (10YR 4/2) to light brownish gray (10R 6/2) ashy layers and patches, vague streaking, and slight color variations throughout. The entire unit has been intensely deformed and swirled by drilling.

Lithologic Unit 2 is a 60-m-thick, lower Pleistocene to upper Pliocene, brown (10YR 5/3) ashy nannofossil mud with interbedded grayish brown (10YR 5/2) vitric muds and gray to dark gray (5Y 5/1-5Y 3/1) ash layers. The color of this unit gradually changes downhole to olive gray (5Y 5/2) and gray (5Y 5/1-5Y 6/1). It has been moderately to intensely deformed by drilling throughout.

Lithologic Unit 3 is a 105-m-thick, lower Pliocene to lower Miocene, mottled and bioturbated mud and vitric mud with ash layers. It is differentiated from the overlying unit by an absence of calcareous components, indicating deposition below the CCD. The clay is primarily olive gray (5Y 5/2) with some brown (10YR 5/3) to grayish brown (10YR 5/2) layers in the top 35 m, gradually changing to greenish gray (5GY 5/2) below Core 12. The ash layers and patches range from medium dark gray (N4) to very dark gray (10YR 3/1) to brownish black (5YR 2/1) to black and often have distinctive greenish gray (5G 6/1) alteration halos around them. The unit has been intensely deformed by drilling that has greatly disturbed original bedding and burrows.

Lithologic Unit 4 is a 79-m-thick, bioturbated, lower Miocene to Oligocene radiolarian clay with ashy patches and ash layers. It is differentiated from the overlying unit by the presence of more than 10% radiolarians. The greenish gray (5GY 5/1) with olive (5Y 5/3) and olive gray (5Y 5/2) mottles in the upper 10 m, gradually changing to primarily olive gray (5Y 5/2-5Y 6/2) and olive (5Y 5/3), with greenish gray (5GY 5/1) layers below Core 19, Section 2. The ash beds vary from 1 to 10 cm thick, range from dark gray to grayish brown (10YR 4/1-10YR 4/2) to black (N2.5), and are frequently associated with pale blue green (5BG 7/2) to greenish gray (5G 6/1) alteration halos. Bioturbation is faint except near the upper contacts of the ash layers. Though the unit has been moderately deformed by drilling, horizontal layering is observed in Core 25. A white 5-mm-thick layer of rhodochrosite is found in Core 24, Section 4.

Lithologic Unit 5 is a 124-m-thick, Oligocene to lower Eocene pelagic unit that is divisible into three subunits (5a, 5b, and 5c) on the basis of macroscopic core descriptions, smear slide analyses, and shipboard XRD results (see the section on X-Ray Diffraction, this chapter).

Subunit 5a is a 60-m-thick Oligocene(?) to middle upper Eocene, burrowed and mottled, manganese-stained radiolarian clay. It is differentiated from the overlying unit by the presence of abundant manganese-oxide stains. The clay is light yellowish brown (10YR 6/4) to very pale brown (10YR 6/3-10YR 7/3) and contains abundant gray (10YR 6/1) to dark grayish brown (10YR 4/2) to black (20YR 2.5/1) manganese-oxide stains. Distinctive parallel laminations are observed in Core 32, Section 1.

Subunit 5b is a 38-m-thick, Eocene interbedded zeolitic clay–claystone and clay–claystone unit. It is differentiated from the overlying subunit by a scarcity (less than 10%) or absence of radiolarians, rather than by the presence of zeolites in the sediment (zeolites first appear in XRD analyses of the sediments in the radiolarian clay of Core 30, Hole 543; see the X-Ray Diffraction section, this chapter). The zeolitic clays or claystones in this unit are light yellowish brown (10YR 6/4) to pale brown (10YR 6/3); the interbedded clays or claystones are yellowish red (5YR 4/6-5YR 6/6). Rare blebs and approximately 1-cm-thick layers of greenish gray (5GY 6/1-5GY 7/1) altered ash are found throughout the unit. Dark gray (N4) to very dark grayish brown manganese-oxide stains occur in Core 3, Hole 543A. The entire unit has been intensely deformed by drilling, consisting of pancake-shaped coherent lumps ("biscuits") separated by thin shear zones ("rotational shear zones"), which are an artifact of drilling and are spaced every 2 to 5 cm down the core. Laminations and burrows are found in the firm, coherent "biscuits."

Subunit 5c is a 28-m-thick, Eocene, predominantly reddish brown (2.5YR 4/4-2.5YR 4/5) burrowed claystone. It is differentiated from the overlying subunit by an absence of zeolites (see the section on X-Ray Diffraction). The upper portion of the subunit (Core 4, Hole 543A) contains some yellowish brown (10YR 5/4) to brown (7.5YR 5/4) layers and has some dark grayish brown (10YR 4/2) to very dark grayish brown (10YR 3/2) manganese-oxide stains. It has been very deformed by drilling, consisting of coherent "biscuits" embedded in a highly brecciated, sheared, and slickensided matrix of the same material.

Lithologic Unit 6 is a 31.5-m-thick, lower Maestrichtian to lower Campanian, horizontally laminated, bioturbated, calcareous ferruginous claystone deposited on top of Cretaceous basement (see Hemleben and Troester, this volume). It is differentiated from the overlying sediment by the presence of calcareous and ferruginous components. The unit is variegated dark brown (7.5YR 3/2) to reddish brown (5YR 4/3-5YR 4/4) and contains yellowish red (5YR 5/4) nannofossil-rich layers. Cores 7, 8, and 9 (Hole 543A) contain authigenic dolomite.

Lithologic Unit 7 consists of Cretaceous basement pillow basalts (see the section on Basalts, this chapter).

All of the sediments cored at Site 543 were deposited below the lysocline (see the section on Paleoenvironments, this chapter). The vast majority of sediments accumulated by pelagic–hemipelgic settling in quiet, deep water on top of Cretaceous basement (Lithologic Unit 7). Evidence for deposition of some material by gravity flows was found in a 4-cm-thick, foraminifer-rich layer in Core 3, Section 5, Hole 543. Ash beds found in Lithologic Units 1 to 4 do not appear to have been redeposited as turbidites, but probably settled to the seafloor following volcanic eruptions on the Lesser Antilles island arc. The relatively great amounts of ash particles in Lithologic Units 1 to 4 indicate a substantial input of volcanic material from the Lesser Antilles island arc as the Atlantic crust moved toward the arc.

Bioturbation

Bioturbation is prevalent in the Site 543 cores, but there are fewer recognizable forms than at either Sites 541 or 542. The uppermost 70 m of sediment are too badly swirled by drilling to detect any original sedimentary features. Slight burrow mottling first appears in Core 8 (543) and becomes a little more pronounced in Core 12. Core 18 contains burrowed ash beds and all further cores down to 29 are burrow mottled, but without recognizable ichnogenera. Core 30 is mottled at the top and base only. Core 31 contains rather large "mottles" 1 to 3 cm across instead of the normal burrows less than 1 cm in diameter. Some of these may be diagenetic nodules rather than burrows. Core 32 contains sporadic burrows of *Planolites* type. The lowest two, Cores 33 and 34 at Hole 543, contain drilling biscuits in a deformed matrix. The biscuits preserve lamination and bioturbation. The sedimentation rate was high enough that burrowing animals did not have time to rework the sediment completely.

In Hole 543A, Cores 2 to 4 are not conspicuously burrowed. Together with the lack of arenaceous benthic foraminifers, this characteristic may indicate anoxic or at least oxygen-poor bottom conditions. Cores 5 and 6 are burrow mottled, and the variegated ferruginous clays of Cores 7 to 9 exhibit spectacular burrowing (Fig. 5). Abundant *Planolites*, a few *Zoophycus*, tiny *Chondrites*, and a pelleted oblique burrow (?*Teichichnus*) were identified in Core 7. Core 9 contains laminae of lighter and darker brown sediment, and the tops and bases of the laminae are burrowed on a minute scale.

There are two possible reasons for the preservation of lamination in these basal ferruginous sediments deposited near the ridge crest: (1) the sedimentation rate was too high to allow complete reworking; (2) the environment may have been fairly rugged, with the water full of noxious exhalations and ferruginous manganiferous brines and vapors (c.f., Galapagos Rift), and not many animals lived there.

X-Ray Mineralogy

Fifty-six samples were analyzed from this site, using the same method as described for Site 541. The minerals identified include quartz, alkali feldspar, plagioclase, calcite, zeolites (clinoptilolite and ?heulandite), cristobalite, palygorskite, kaolinite, illite, smectite and dolomite, plus traces of apatite and hematite. A thin white vein in Sample 543-24-4, 92 cm was identified as rhodochrosite. Results are summarized in Figure 4 and described in more detail in Pudsey (this volume).

Quartz occurs throughout. Feldspars occur from 0 to 250 m sub-bottom, and in general the peak for alkali feldspar is higher than that for plagioclase. Calcite is present in the Pleistocene and Pliocene muds above 75 m sub-bottom, and sporadically in the Eocene and Cretaceous below 380 m. Zeolites are present from 250 to 350 m and cristobalite from 280 to 320 m. Palygorskite occurs from 335 m to the base of the sediments, but its peak height fluctuates wildly and it is not present in all samples in this interval. Dolomite occurs only in Cores 543A-7, -8 and -9 (385–410 m), but is an important constituent of Core 9. Of the nonfibrous clay minerals, kaolinite is present throughout, but its peak height is relatively low from 100 to 200 m. Illite is an important constituent only from 0 to 100 m and is absent from 135 to 170 m and below 355 m; smectite is most abundant from 100 to 200 meters, and it decreases noticeably in the lowest 70 m of sediment.

In the manganiferous Lithologic Subunit 5a, black layers contain much more clay and less quartz than orange layers. Manganese oxides are presumably amorphous, because they do not give a peak on the diffractograms.

Volcanic Ash

Core disturbance was extreme throughout most of the upper 150 m of the sediment section (Cores 543-1 to -13, and 543A-1, covering part of the upper Miocene, the Pliocene, and the Quaternary), which made ash beds difficult to identify and sample. Fortunately, the corresponding interval was much less disturbed at Site 541.

Despite the disturbance, ashy intervals were prominent in many of the upper 14 cores of Hole 543. These are sufficiently disturbed that they have been somewhat mixed with mud, hence they are described as ashy mud,

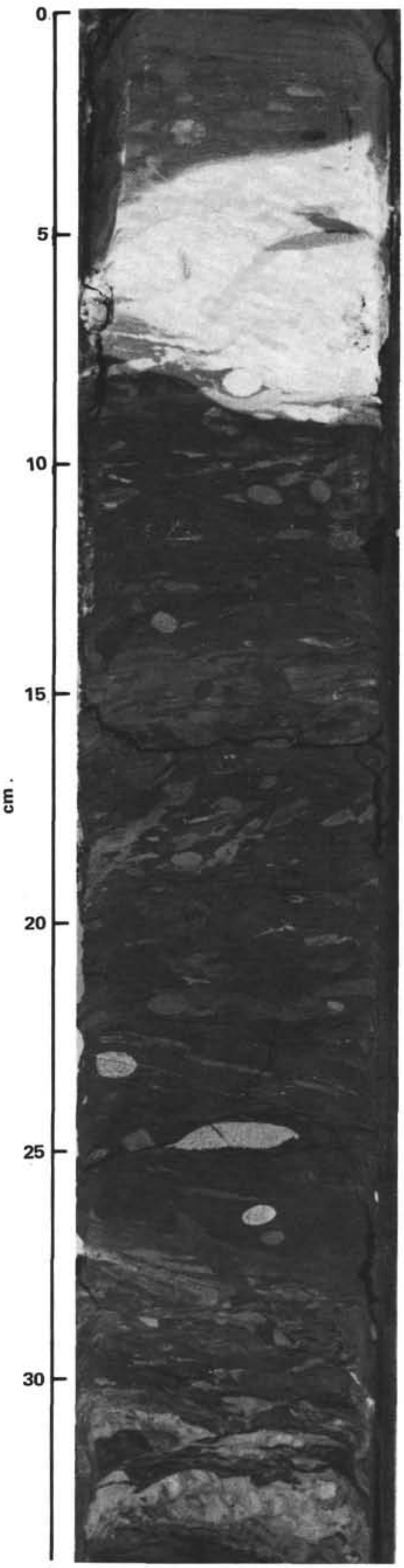

Figure 5. Bioturbated ferruginous clay, Sample 543A-7-3, 0–34 cm. (*Planolites* burrows are filled with lighter material than the surrounding mud.)

for the most part, on the core barrel sheets. In a few intervals, there are relatively undisturbed major ash beds up to 5 cm thick that must correlate with those found at Sites 541 and 542, although the disturbance may make precise correlation nearly impossible.

The principal addition to the ash record that Hole 543 provides is documentation of a significant pulse of explosive volcanism on the Lesser Antilles arc in the early and early middle Miocene (Cores 17–20). Below these cores, there are only scattered and very minor ash occurrences, mostly completely altered to clays. There is one ash deposit in the Oligocene (Core 27). There are none in the middle and upper Eocene. The lower Eocene has 10 thin wisps of altered ash beds that may correspond to the oldest volcanism known from highly altered and restricted outcroppings in the limestone Caribbees. Site 543 was quite a bit further from the arc in the early Eocene than it is now, hence no comparison of the volume of explosive volcanism between the Eocene and modern Lesser Antilles arc is possible with these cores.

The Lesser Antilles arc thus has had three periods of major explosive volcanic activity, corresponding to the early Miocene, early Pliocene, and Quaternary ash beds recovered by drilling at Sites 541, 542, and 543, as well as in surface piston cores. This finding is a significant improvement in resolution of ash chronology compared with the sketchy data available from the islands. These topics are discussed further by Natland (this volume).

STRUCTURAL GEOLOGY AND DRILLING DEFORMATION

Most, if not all, of the small-scale structures we observed in cores from Site 543 can be interpreted as drilling-induced. However, there is an apparent correlation between material response and sediment composition that may be a clue to how this stratigraphic section would behave if it were deformed *in situ*.

Numerous horizontal layers were observed in Cores 543-1 through -31 and in Cores 543A-2 and -3. The base of an ash layer in Section 543A-4-1 at 62 cm dips 5°. Burrow-mottled layering in Sample 543A-7-2, 80–130 cm dips up to 30° in biscuits but varies in magnitude and sense from biscuit to biscuit, partly due to rotation along horizontal drilling fractures. However, some of the dip is probably primary and may reflect deposition on irregular basement topography or faulting near the ridge crest in newly formed basement.

Cores 543-1 to -13 display swirling patterns that are typically produced by drilling in the shallowest, least consolidated sediments. In parts of Cores 543-14 and -16 we noticed firm, coherent chunks of mud separated by softer, more highly deformed mud. Most of Cores 543-17 to -19 and Sections 1 and 2 of Core 543-20 consist of these firm chunks and soft "matrix." Some coherent chunks, when broken open, showed slickensided, polished curviplanar surfaces spaced <1 cm apart. Soft portions between chunks have polished surfaces spaced >1 cm, and locally they have been churned into a hash of small irregular chips averaging a few millimeters in length. The overall alternation of coherent pieces and softer matrix is reminiscent of sections in which ordinary drilling biscuits are separated by rotational disc fractures induced by drilling. Randomly oriented, polished surfaces spaced between about 1 mm and 1 cm were also noted in some cores from Sites 541 and 542 (see Sites 541 and 542 reports, this volume), but they occur in firm, sticky mud and clearly predate drilling disc fractures. In Core 543-23 we again noted swirling.

Sediments in Core 543-26 through part of Core 543-32 are manganese-stained pelagic clays that are locally rich in radiolarians. A dip-slip fault dipping 40°, with steps on the polished surface suggesting normal faulting, occurs in Section 5 of Core 29. The first development of well-defined disc fractures and biscuits roughly coincides with the lithologic change from clay to pelagic clay in Core 26. In Hole 543A, Cores 2 through 7 contain pelagic clays devoid of radiolarians. These sediments occur in variably sized, firm, relatively undeformed chunks and lumps, separated and locally surrounded by coherent, highly deformed mud. Some chunks contain polished surfaces spaced >1 cm, but many bear no signs of internal deformation. The deformed zones between these biscuits range from 2 mm to at least 20 cm in thickness. As freshly cut surfaces of cores dry out, tiny hairline cracks form and reflect an internal fabric defined by subparallel polished surfaces spaced about 1 mm apart. This *crude* scaly foliation is easily visible when samples of deformed mud are broken apart. In thin, well-defined zones between biscuits, the minicracks (and foliation) are horizontal, but in thicker zones they have variable orientations. Some deformed zones also display wispy and contorted patches of mud that are colored differently from their more voluminous host. Compared with the scaly clays occurring in the bottom few cores at Site 541, the foliation in the deformed zones in Cores 2 through 7 of Hole 543A is less penetrative and less strongly oriented. In addition, these zones in Hole 543A are still sticky and coherent, rather than flaky.

The change from well-defined biscuits separated by thin disc fractures to chunks separated by wider zones of deformed mud coincides approximately with the transitions above and below the radiolarian pelagic clay to pelagic clays at Site 543. This coincidence suggests that deformational response may depend partly on sediment composition. The deformed zones in Cores 543-14 to 20 and 543A-2 to 7 are probably due to drilling rather than *in situ* deformation. In these cores, we can generally see a complete range in thickness of deformed zones. The thinnest are clearly rotational shear fractures, separating well-formed biscuits; thicker zones (<1 cm) are identical in their fabric and composition. The material constituting the thickest zones is very similar to deformed sediment in drilling laminations. It is possible, but unlikely that some of this sheared material in the thickest zones formed *in situ*. Even if all of the deformation in Cores 543-14 to -20 and Cores 543A-2 to -7 can be ascribed to drilling, it is clear that these clay-rich parts of the sedimentary section are weaker and more easily deformed than the radiolarian mudstone, which we obtained in Cores 543-21 to -32, and are thus more likely to serve as horizons of natural décollement. Notably the upper boundary of the radiolarian mudstone coincides approximately with Reflector 1, which apparently represents a décollement surface separating offscraped and subducted deposits landward of the deformation front.

PORE FLUID CHEMISTRY

Nine samples were taken for interstitial water geochemistry at Site 543, six from Hole 543, and three from Hole 543A. The data are listed, plotted versus depth, and summarized in Gieskes et al. (this volume). Prominent features of the data are an initial drop in pH from 0 to 273 m sub-bottom, then an increase below that to just above basalt, steady decrease of Ca^{2+} with depth, and an initial decline of Mg^{2+} to about 150 m, then a slight increase and leveling off between 250 m to the top of basalts at 408 m. The excess Mg^{2+} may be reflected in the lowermost sediments by an abundance of palygorskite and the occurrence of dolomite (Pudsey, this volume). The causes for these variations are discussed elsewhere (Gieskes et al., this volume), but migration of fluids similar to those below 350 m along the shear zone at Sites 541 and 542 could cause the perturbations in Mg^{2+} abundances observed at those sites.

ORGANIC GEOCHEMISTRY

Organic carbon content in Site 543 sediments decreases regularly with depth, as was the case for Sites 541 and 542 sediments. C_1 to C_6 hydrocarbons are just detectable at 100 to 400 standard gas volumes per 10^9 volumes of sediment. A minor show of nonhydrocarbon gas was confirmed at a depth of about 245 m in Hole 543. A similar observation at a depth of about 240 m in Hole 541 was discounted and attributed to core disturbance and air contamination. Subsequent shore-based analyses of this gas (Claypool, this volume) show nitrogen and argon contents in excess of atmospheric content. The origin of this minor nitrogen gas show is unknown at this time.

BIOSTRATIGRAPHY

A biostratigraphic summary for all microfossil groups examined on board ship is given in Figure 6. The biostratigraphy described here is based on shipboard investigations. For more refined discussions of nannofossils and radiolarians see Bergen (this volume) and Renz (this volume), respectively.

Nannofossils

Hole 543

Samples from Cores 1 through 8, Section 1 contain nannofossil assemblages as old as early Pliocene. The preservation in these samples is noticeably worse than in samples of equivalent age from Sites 541 and 542.

Cores 1 through 3 are zoned as early Pleistocene *Pseudoemiliania lacunosa* is found in all samples from these cores in which nannofossils occur. The presence of *Cyclococcolithina macintyrei* in Samples 543-1-1, 60–61 cm to 543-3-2, 62–63 cm place this interval in the *Cyclococcolithina macintyrei* Zone of Gartner (1977). No *Gephyrocapsa* are useful in age determinations.

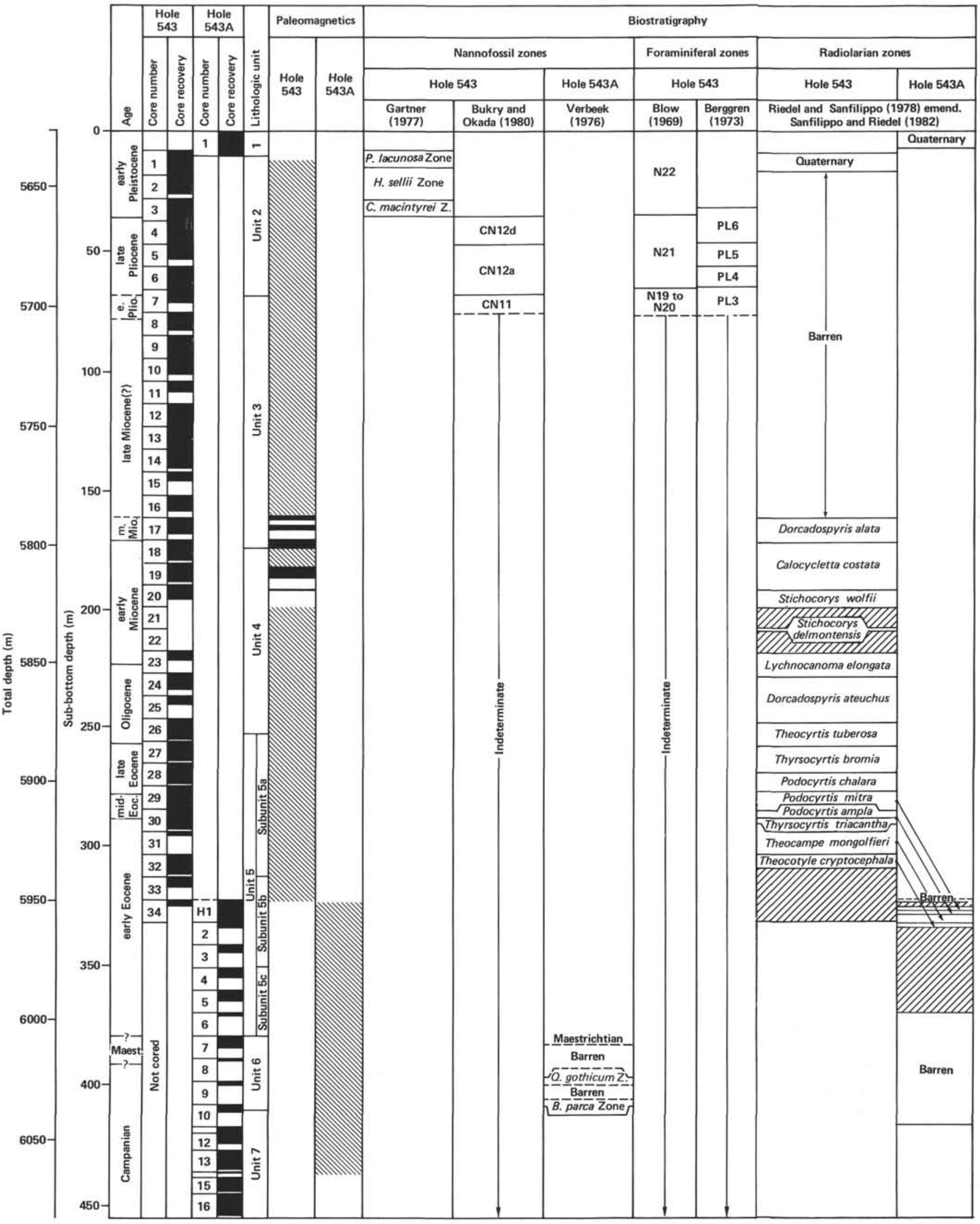

Figure 6. Summary biostratigraphy and magnetostratigraphy, Site 543. (Polarity normal intervals are black, polarity reversed intervals are white, and polarity uncertain intervals [or intervals with no data] are diagonally striped.)

Cores 4 through 7, Section 2 are late Pliocene. *Discoaster tamalis, D. surculus,* and *D. pentaradiatus* have their last occurrences in Sample 543-5-2, 100–101 cm. Therefore, a hiatus exists between that sample and Sample 543-5-1, 100–101 cm. Samples 543-5-2, 100–101 cm to 543-7-2, 55–56 cm are placed in the *Discoaster tamalis* Subzone (CN12a). Core 4 through Sample 543-5-1, 100–101 cm are assigned to the *Calcidiscus macintyrei* Subzone (CN12d). The *Discoaster surculus* and *Discoaster pentaradiatus* Subzones (CN12b,c) are not recognized in this hole.

Samples 543-7-3, 55–56 cm through 543-8-1, 65–66 cm are placed in the *Reticulofenestra pseudoumbilica* Zone (CN11), based on the extinctions of *Amaurolithus tricorniculatus* and *R. pseudoumbilica. Sphenolithus neoabies,* whose extinction is used in addition to *R. pseudoumbilica,* is last seen in Sample 543-7-2, 55–56 cm. *S. abies* becomes extinct in this same sample.

This hole is barren below Sample 543-8-1, 65–66 cm.

Hole 543A

Nannofossils recovered from Hole 543A are poorly preserved, but are unusually common when found. Cores 1 through 6 and Core 8 are barren.

Core 7, Section 1 is barren, except for the occurrence of very rare *Micula mura* and *Ceratolithoides kamptneri* in very poorly preserved assemblages. If not reworked, this section is from the very top of the Maestrichtian.

Core 7, Section 3 and the lower part of Core 7, Section 2 all contain *C. aculeus, Arkangelskiella,* and large *Prediscosphaera cretacea.* The absence of *Broinsonia parca* in this interval suggests that it is not Campanian; it is most likely early Maestrichtian. Core 7, Section 4 is barren.

Sample 543A-9,CC and the bottom part of Section 543-9-1 are barren. Assemblages containing *Quadrum nitidum, Q. geothicum, C. aculeus,* and *B. parca constricta* are found near the top of Core 9, Section 1. This interval is assigned to the early late Campanian, based on the presence of the above species, but also on the absence of *Q. trifidum.*

Samples from Core 10, which include the contact with basement, are dated as early Campanian. This assignment is based on the co-occurrence of *B. parca* and *Marthasterites furcatus.*

Radiolarians

Radiolarians in varying abundances and states of preservation were recovered from both holes. The most significant recovery is a Cenozoic sequence ranging from lower Eocene to middle Miocene in the first hole.

Hole 543

A sparse Quaternary assemblage of radiolarians showing strong dissolution occurs in Section 543-1,CC. Cores 2 through 16 are barren. Radiolarians occur again in Section 543-17-1 and continue through the last core (34,CC).

At the beginning of this long sequence (Sample 543-17-1, 10–12 cm) a few fragments are seen. One of these is identified as *Calocycletta costata,* dating the sample as no younger than the *Dorcadospyris alata* Zone (Riedel and Sanfilippo, 1978) of the middle Miocene. Sample 543-17-2, 10–12 cm through 543-18-1, 30–32 cm show increasing abundances and better states of preservation. They are placed in the *Dorcadospyris alata* Zone. The following species are present: *C. costata, Cyrtocapsella cornuta, D. alata, Stichocorys delmontensis,* and *S. wolffii.*

In Samples 543-18-2, 31–33 cm through 543-20-1, 70–72 cm, *D. dentata* is consistently more abundant than its descendent, *D. alata.* This fact, along with the continuing occurrence of *Calocycletta costata* as well as *C. virginis, Phormostichoartus corona,* and *Cannartus violina,* places these samples in the *Calocycletta costata* Zone of the early Miocene. This correlates well with the beginning radiolarian sequence found at Site 541 (Core 48, Section 5).

Samples 543-20-2, 70–72 cm through 543-20,CC are assigned to the *Stichocorys wolffii* Zone because of the presence of *S. wolffii, C. virginis, Carpocanopsis bramlettei,* and *Cyrtocapsella cornuta,* and the absence of *Calocycletta costata.* Specimens are very abundant, occurring in highly diverse assemblages of moderate to good preservation.

There was no recovery from Core 21. What little was recovered from Core 22 (Section 543-22-1, top—approximately 25 cm^3) is assigned to the *Stichocorys delmontensis* Zone. *S. delmontensis, C. virginis, Carpocanopsis bramlettei, Calocycletta serrata, Cyrtocapsella cornuta, C. tetrapera, D. ateuchus,* and *Eucyrtidium diaphanes* are present. *S. wolffii* and *Theocyrtis annosa* are notably absent. Specimens are abundant and well preserved.

Samples 543-23-1, 145–147 cm through 543-24-1, 2–4 cm have common to abundant radiolarians, and the quality of preservation remains moderately good. This sequence is placed in the *Lychnocanoma elongata* Zone (straddling the Oligocene/Miocene boundary) because of the presence of *L. elongata, Calocycletta virginis, D. ateuchus,* and *T. annosa* and the absence of *C. serrata, Cyrtocapsella cornuta,* and *C. tetrapera.* This assignment indicates that the *Cyrtocapsella tetrapera* Zone may have occurred in the sediment lost in Core 22.

Samples 543-24-2, 40–42 cm through 543-26-1, 64–66 cm show a rapid decrease in the quality of preservation and great variability in abundance. The assemblage has a very low diversity that is dominated by *D. ateuchus, L. elongata* and *T. annosa* are absent. This places the samples in the *Dorcadospyris ateuchus* Zone.

The *Theocyrtis tuberosa* Zone occurs in Sample 543-26-2, 43–45 cm through 543-27-2, 126–128 cm. The following species are noted: *D. ateuchus, Lithocyclia angusta* (C), *L. aristotelis* (R), *T. tuberosa,* and *Tristylospyris triceros.* Abundance and quality of preservation are increasing.

The Eocene/Oligocene boundary occurs between Sample 543-27-2, 126–128 cm and 543-27-3, 53–55 cm. Samples 543-27-3, 53–55 cm through 543-28-3, 73–75 cm are assigned to the *Thyrsocyrtis bromia* Zone. *L. angusta* drops out above the sequence, whereas *L. aristotelis* occurs with greater frequency. *Lophocyrtis jacchia* and *Lychnocanoma amphitrite* appear consistently and increase in abundance. *Calocyclas turris* and *Thyrsocyrtis bromia* occur in Sample 543-27-5, 104–106 cm through the end of the sequence. Both species are dominant members of the assemblage. Radiolarians are common to abundant and moderately well preserved.

No assemblage is assigned to the *Podocyrtis goetheana* Zone, although specimens of *P. goetheana* are frequently found in Sample 543-28-2, 40–42 cm.

Samples 543-28-4, 110–112 cm through 543-29-2, 72–74 cm are assigned to the *Podocyrtis chalara* Zone. *P. chalara* appears consistently with common or greater abundance. *Rhandolithus pipa* occurs rarely. *P. goetheana* is absent. Specimens are common to abundant and moderately well preserved.

Sample 543-28,CC contains displaced material from the *Thyrsocyrtis bromia* zone.

Samples 543-29-3, 6–8 cm through 543-30-1, 10–12 cm are assigned to the *Podocyrtis mitra* Zone. *P. chalara* continuously decreases in abundance until it disappears in the middle of the sequence, whereas *P. mitra* is ever present with a fluctuating abundance. *P. sinuosa* is absent until the very end of the sequence. Specimens range from common to abundant and are moderately well preserved.

Samples 543-30-1, 38–40 cm through 543-30-3, 7–9 cm are assigned to the *Podocyrtis ampla* Zone. *P. sinuosa* is consistently more abundant than *P. mitra,* which disappears in the middle of the sequence. *P. ampla* is present throughout; *P. phyxis* is absent. Radiolarians are abundant to common and moderately well preserved.

Samples 543-30-3, 132–134 cm through 543-30-5, 129–131 cm are assigned to the *Thyrsocyrtis triacantha* Zone. *P. phyxis* and *Eusyringium Fistuligerum* are absent, whereas *Theocotyle venezuelensis* appears with increasing abundance. Radiolarians are common and moderately well preserved.

Sample 543-30-6, 60–62 cm through Section 543-31,CC are assigned to the *Theocampe mongolfieri* Zone due to the common presence of *T. mongolfieri* and to the absence of *E. lagena*. Specimens are abundant and moderately well preserved.

Samples 543-32-1, 37–39 cm through 543-32-5, 68–70 cm have abundant, very well preserved assemblages (for the most part). Specimens superficially similar to *T. mongolfieri* are common, but they lack strict longitudinal pore alignment and ribs. *Calocycloma castum* appears with increasing abundance. According to the zonal definition, these facts place the samples in the *Theocotyle cryptocephala* Zone (Riedel and Sanfilippo, 1978, amend.; Sanfilippo and Riedel, 1982).

Sections 543-32,CC through 543-34,CC show assemblages with decreasing abundances and all in very poor states of preservation. Specimens of *C. castum, Calocyclas hispida, Lithochytris vespertilio, Phormocyrtis striata striata,* and *T. cryptocephala* are seen rarely and cannot be used with confidence for zonation. Species of the genera *Amphicraspedum* and *Spongodiscus* dominate the assemblages.

Hole 543A

Offset drilling recovered one core from the surface, washed down to 332 m and continuously cored to 411 m at basement and 44 m into basalt.

Sections 543A-1-3 and 543A-1,CC contain a Quaternary radiolarian assemblage of low to moderate diversity, showing breakage and signs of dissolution.

Section 543A-H1-1 is barren of radiolarians.

After voids in the recovery, Samples 543A-H1-4, 95–97 cm through 543A-2-1, 95–97 cm contain common to few radiolarians in moderate to poor states of preservation. Sample 543A-H1-4, 95–97 cm contains specimens of *Podocyrtis mitra* (C), *P. trachodes* (R), and *Sethochytris triconiscus,* which bracket the sample, placing it in the upper half of the *Podocyrtis mitra* Zone. This correlates best with samples from Section 543-29-7.

The presence of rare specimens of *Eusyringium fistuligerum* and *P. dorus* and the common occurrence of *P. sinuosa* place Sample 543A-H1-5, 85–87 cm at the boundary of the *Podocyrtis ampla/Thyrsocyrtis triacantha* Zones. This correlates closest with Section 543-30-3. Radiolarians are abundant and moderately well preserved.

Sample 543A-H1-6, 64–66 cm contains no diagnostic species to indicate its zone. Specimens are few and very poorly preserved. *Lithochytris vespertilio, P. sinuosa,* and *Rhandolithus pipa* are dominant.

Section 543A-H1,CC contains both specimens of *Theocorys anaclasta* and *Theocampe mongolfieri,* which bracket it in the *Theocampe mongolfieri* Zone. Specimens of *Thyrsocyrtis triacantha* are rare with respect to those of *T. tensa. Periphaena delta* is absent. This places the sample near the middle of the zone, which correlates best with Section 543-31-1.

These correlations for Core H1 illustrate the characteristic of a washed core to collect samples from different intervals in the sediment column.

Sample 543A-2-1, 95–97 cm contains an assemblage of high diversity, common abundance, and poor preservation. *T. mongolfieri* is absent, and *Calocycloma castum* and *Theocotyle cryptocephala* are present. This sample is assigned to the *Theocotyle cryptocephala* Zone and correlates best with Section 543-32-4.

Section 543A-2-2 and 543A-2,CC contain radiolarians in common abundance but very poorly preserved. Several specimens of *Calocycloma castum* and *Buryella clinata* are seen throughout.

Cores 3, 4, and 5 contain radiolarians in varying abundances (C–R) but so poorly preserved that specimens are unrecognizable. Fragments of three specimens in Section 543A-5,CC are probably contaminants. Cores 6 through basement are barren. Rare fragments found at the contact are again thought to be contaminants.

Foraminifers

Hole 543

Hole 543 was drilled to 324 m sub-bottom. The upper 10 cores (approximately 96 m of section) contain foraminifers varying from sparse to abundant.

Cores 1 through 3 are assigned to the lower Pleistocene Zone N22 of Blow. Specimens of *Globorotalia (G.) truncatulinoides, G. (T.) tosaensis,* and *Globigerinoides obliquus obliquus* are present throughout. Sample 543-3-4, 30–32 cm contains *G. obliquus extremus* and is assignable to Berggren's Zone PL6. As seen at Site 541, the top of Zone PL6 appears to occur in the lower Pleistocene.

The interval from Sample 543-3-4, 30–32 cm to Sample 543-4-6, 147–149 cm is assigned to Zone PL6. The Pliocene/Pleistocene boundary is placed below Section 543-3,CC on the basis of the nannofossil data.

Globorotalia (G.) miocenica occurs in Section 543-4,CC. This section is assigned to the upper Pliocene Zone PL5 (i.e., Zone N21 of Blow). Cores 4 and 5 are assigned to Zone PL5.

Core 6 is assigned to the upper Pliocene Zone PL4 (i.e., Zone N21 of Blow) on the basis of the presence of *Globorotalia (G.) multicamerata.*

Core 7 is assigned to that part of Zone N19 to N20 (i.e., PL3) below the extinction datum of *Sphaeroidinellopsis subdehiscens paenedehiscens.* The foraminifers in Core 7 are sparse. The lower/upper Pliocene boundary is placed above Sample 543-7-3, 55–56 cm, on the basis of the nannofossil data (Bergen, this volume).

Cores 8 to 10 contain only sparse foraminifers; most of which are broken. Thus no zonal assignments are attempted.

Cores 11 through 34 are barren of foraminifers.

Hole 543A

In Hole 543A, the first 10 m below the seafloor are cored. The hole was then washed to 332 m and continuously cored to 455 m.

No diagnostic planktonic foraminifers were observed throughout the cored interval. Some benthic foraminifers assignable to the Upper Cretaceous, Campanian to Maestrichtian (Hemleben and Troester, this volume), are found from Cores 6 to 10.

PALEOENVIRONMENT

Recent seafloor sediments of Site 543 were deposited about 450 m below the local calcite compensation depth (CCD). As a consequence, the top of Core 1 of Hole 543 is barren of calcareous fossils and Cores 1 through 8, Section 1 contain mostly moderate to poorly preserved assemblages of planktonic foraminifers. In general the sedimentation rate of Site 543 is considerably lower compared with Site 541. Thus it is not possible to obtain the same resolution of events such as climatic changes. However, changes in preservation of calcareous fossils in Cores 1 through 3 may reflect the glacial and interglacial phases during the Quaternary. Core 3 seems to represent mostly the Nebraskan (Berger, 1977) interval. A comparison of the Nebraskan preservational peaks at Sites 541 and 543 demonstrates a slight shift (Site 541) toward the Pliocene; however, this shift may be influenced more by gravity flow deposits than by climatic changes. Samples of glacial intervals (e.g., Nebraskan) contain cold-water species (e.g., *G. truncatulinoides, G. inflata,* and *Neogloboquadrina* cf. *pachyderma*) along with the normal tropical assemblage. The cooling of the water mass is less rapid at the Pliocene/Pleistocene boundary in low latitudes than in high latitudes. The first appearance of the subtropical species *G. truncatulinoides* coincides with the Nebraskan glacial interval and not necessarily with the Pliocene/Pleistocene boundary.

Compared with Site 541, the preservation is less, indicating earlier deposition closer to the CCD during the late Pliocene. Sediments of Sections 543-7,CC through 543-10,CC were deposited close to or below the CCD. Siliceous microfossils first appear in Core 17, Section 1, indicating a depositional environment definitely below the CCD.

Sediments of Hole 543A (Cores 1 through 6) contain no calcareous microfossil assemblages and thus are deposited below the CCD. In these cores little or no bioturbation can be seen. The occurrence of numerous arenaceous and calcareous benthic foraminifers together with increasing bioturbation in Cores 6 to 10, Section 1 indicates better bottom conditions than seen in Cores 4 to 5. The first occurrence of calcareous benthic foraminifers in Core 7, Section 2 may indicate a depositional environment above the CCD. However, the abundance of benthic foraminifers or the ratio of arenaceous–calcareous foraminifers changes rather drastically in each core (Cores 7 through 10) and may reflect the relative movement of the CCD. In addition, the total lack of planktonic foraminifers (tests or even fragments) points toward a relict fauna of abyssal, benthic species. Thus the depositional environment can be placed close to the CCD. In comparing Holes 541, 542, and 543A with the Barbados outcrops in respect to the foraminiferal abundance, it is obvious that the depositional environment of Barbados, especially the Oceanic Formation, must be placed several thousand meters higher up the slope than the sites of Leg 78A.

BASALTS

Lithology

Altogether, 35.9 m of basalt were recovered in Hole 543A, out of 44 m cored, for a recovery rate of 81%. This is one of the highest rates of recovery for a single-bit hole into basement ever obtained by DSDP, and remarkably, was even higher than the rate of recovery in the sediments. The recovery was so exceptional that it was possible to log each pillow recovered on the igneous rock description forms, and determine that a total of 59 separate cooling units had been cored. Coring in basaltic basement began 3 m into the interval encompassed by Core 10 of Hole 543A, and proceeded through Core 16. It was terminated in order to leave sufficient time for logging and downhole experiments.

The reasons for the exceptional basalt recovery were (1) alteration was sufficient to have "healed" the abundant fractures typical of pillowed basalts, and (2) interpillow voids were largely filled, or at least lined, with spectacular, virtually geoidal calcite, which preserved entire glass selvages on many pillows. The pillows themselves are fairly small, rarely more than 1 m thick, and usually only a few tens of centimeters thick. Glass selvages were commonly curved, and were recovered on both the top and bottom, as well as the sides, of pillows. Some pillows were cored precisely on their edges, resulting in strikingly curved marginal glass zones that extend for several tens of centimeters through several pieces of rock. There were also three glass rinds that changed trend abruptly, curving sharply back upon themselves, representing places where the pillows formed "buds" one from another, during eruption.

The basalts vary from sparsely to strongly phyric, with plagioclase phenocrysts being most abundant and clinopyroxene and olivine phenocrysts occurring in some samples. The distribution of these phenocrysts varies mainly on a sample to sample basis, making it difficult to define distinctive petrographic units. However, phenocrysts are most abundant in Core 10, and again in Cores 14 to 16.

The most important downhole lithologic variations concern alteration and the distribution of interpillow sediments. Alteration is quite extensive in Cores 10 through 12. The rocks are pervasively altered to a dark grayish brown color, and some, mainly at pillow margins, are an almost brick-colored orange brown, highlighting the pale gray plagioclase phenocrysts. Through Core 13, calcite is the major mineral lining fractures, which, even in pillow interiors, can be 1 to 2 cm wide. Below this core, fractures are narrower—never more than 0.5 cm wide—and are lined either with calcite or green clays. Below Core 12, Section 4, the extent of the grayish brown zones of oxidative alteration diminishes, and most of the basalts are gray and dark gray in color. Clays identified by X-ray diffraction in these cores are primarily celadonite, mixed-layer clays, and dioctahedral smectite, all of which occur in the same samples, suggesting predominantly oxidative conditions of alteration. Trioctahedral smectite was found in only one sample. The celadonite-mixed-layer clay association forms distinctive dark bluish green encrustations on fracture surfaces, and is especially prevalent in Cores 14 and 15, with an additional occurrence in Core 16, Section 5. Primarily, there are only very narrow veins of calcite in the latter core.

Inter- and intrapillow sediments occur only in Cores 10 to 13. They include one sample with brown claystone between two pieces of glass, calcite-cemented basaltic sands, and one example of a wide fracture partially filled with brown claystone, then completely filled with calcite above the claystone. The claystone/calcite contact is horizontal, implying that clays partly filled the fracture well after it had formed in the solidified rock. The sediments in the basalts therefore probably only filled in void spaces as they were deposited. The pillows did not "intrude" soft sediments.

Petrography

Seventeen thin sections reveal the Hole 543A basalts to be petrographically typical of many previously described basalts from the Mid-Atlantic Ridge. They have the textures and crystal morphologies typical of pillows, namely zones of spherulites adjacent to glassy rinds becoming coarser grained and more microlitic toward pillow interiors. The principal variations occur in the abundances and, to some extent, the varieties of phenocrysts, and in the types of alteration. Plagioclase phenocrysts occur in all thin sections, and are as abundant as 15% in some of the sections from Cores 14 to 16. There are two types: large plagioclase megacrysts, often having inclusions of spherulitic devitrified glass and sharp exterior normal zones, and euhedral or tabular smaller phenocrysts, which are more numerous. Both types can occur as glomerocrysts, although the larger megacrysts form rather massive glomerocrysts and the smaller type frequently is only loosely clumped. Rare altered olivine is associated with the megacrysts, and clinopyroxene occurs with the smaller euhedral plagioclase phenocrysts. Single spinel crystals occur in three samples. The abundance of clinopyroxene phenocrysts, the rarity of olivine, and the rarity of chrome spinel, imply that the basalts are fairly extensively fractionated. The groundmass consists of plagioclase microlites or spherulites, spherulitic to dendritic clinopyroxene, and titanomagnetite, almost invariably altered to reddish iron hydroxides.

The phenocryst distribution in the cores can be summarized as follows: (1) Cores 10 to 11, Section 1: moderately plagioclase-olivine phyric basalt; (2) Core 11, Section 1 to Core 12, Section 2: sparsely to moderately plagioclase phyric basalt with rare augite phenocrysts and no calcic plagioclase megacrysts or glomerocrysts; (3) Core 12, Section 2 to Core 14: sparsely to moderately plagioclase-olivine phyric basalts; and (4) Cores 15 and 16: moderately to strongly plagioclase-clinopyroxene-olivine phyric basalt.

The other striking petrographic feature of these basalts is the distribution and type of secondary minerals. In Cores 10 and 11, there has been significant replacement of plagioclase by K-feldspar and calcite, with associated almost complete oxidation of groundmass titanomagnetite. The K-feldspar and calcite replacements are intimately associated texturally, and there is strong crystallographic control in the plagioclases on the occurrence of these secondary minerals.

Below Core 12, alteration is confined to partial replacement of the groundmass and olivines by green or blue green clays and iron hydroxides, filling in of vesicles by clays, iron hydroxides, and pyrite, ofttimes strikingly zoned, and veining by calcite with or without clays. Formation of iron hydroxides in the groundmass or in vesicles is more extensive near cracks. This phenomenon can even be seen macroscopically by tracing narrow calcite veinlets into pillow interiors. No matter how narrow these veinlets are, they are usually accompanied by narrow parallel zones 1 to 2 mm wide of oxidative alteration and iron hydroxide coloration. In some cases, particularly deeper in the cored basement, the calcite veins themselves either line or are lined with reddish iron hydroxide fillings. Overall, the alteration in Hole 543A basalts is very similar to that of basalts from Hole 417A, drilled during Leg 51, particularly in regard to the formation of K-feldspar near the top of basement, and the generally oxidative character of alteration elsewhere. The primary petrology and a summary of the features of alteration are presented in more detail in chapters by Natland et al. (this volume) and Bougault et al. (this volume).

PHYSICAL PROPERTIES

The physical properties of cores recovered from Site 543 are similar to the properties measured in cores from Sites 541 and 542.

Sonic Velocity

An average of two ultrasonic velocity measurements were made on samples from each core from Site 543 (Table 3). The variation in compressional velocity throughout the entire site, excluding the basaltic basement rocks at the bottom of the hole, is uniform and generally small. As can be seen in Figure 7, the increase in velocity down to basement in the hole is very slight, very gradual, and linear (except for a few scattered points).

We converted the vertical components of sonic velocities to acoustic impedance, defined as

$$z = \rho \cdot V_p$$

where ρ = density and V_p = vertical velocity. As can be seen in Figure 7, the acoustic impedance at Site 543 increases uniformly down the hole, starting at about 2.0×10^5 g/cm²s near the seafloor and increasing to about 3.0×10^5 g/cm²s near the bottom of the hole.

In order to describe the variations in velocity with depth, we calculated mean velocities for given depth measurements as well as for the entire site above basaltic basement (Table 4). The average velocities parallel and perpendicular to the cores (exclusive of basalt basement samples) are virtually indistinguishable for the entire site. This relationship suggests that sedimentary material from the site is acoustically isotropic.

In order to test whether sedimentary samples from Site 543 are indeed acoustically isotropic, we computed relative anisotropy for each core sample from the relationship:

$$\text{Anisotropy } A_n\ (\%) = 100 \times (V_{\parallel} - V_{\perp}/V_{\parallel} + V_{\perp})$$

where $V_{\parallel}$ and $V_{\perp}$ are the velocity values parallel and perpendicular to bedding, respectively. The results of these calculations are shown in Table 5. For all 61 computations, the average anisotropy, $\bar{A}_n$, is 0.395% with a standard deviation of 1.103%. The average anisotropy is slightly positive albeit very small. A cursory examination of Table 5 suggests that the slightly positive anisotropic effect discovered at Site 543 is confined to the sedimentary section below 300 m. Above 300 m, the drilled section at Site 543 is isotropic, as are the drilled sections at adjacent Sites 541 and 542.

Porosity, Density, and Water Content

Plots of water content, porosity, and density are shown in Figure 8. Porosity is also plotted versus depth in Figure 4. The density averages about 1.50 g/cm³ from the seafloor to a sub-bottom depth of about 190 m. We have no sample data between about 190 and 210 m at

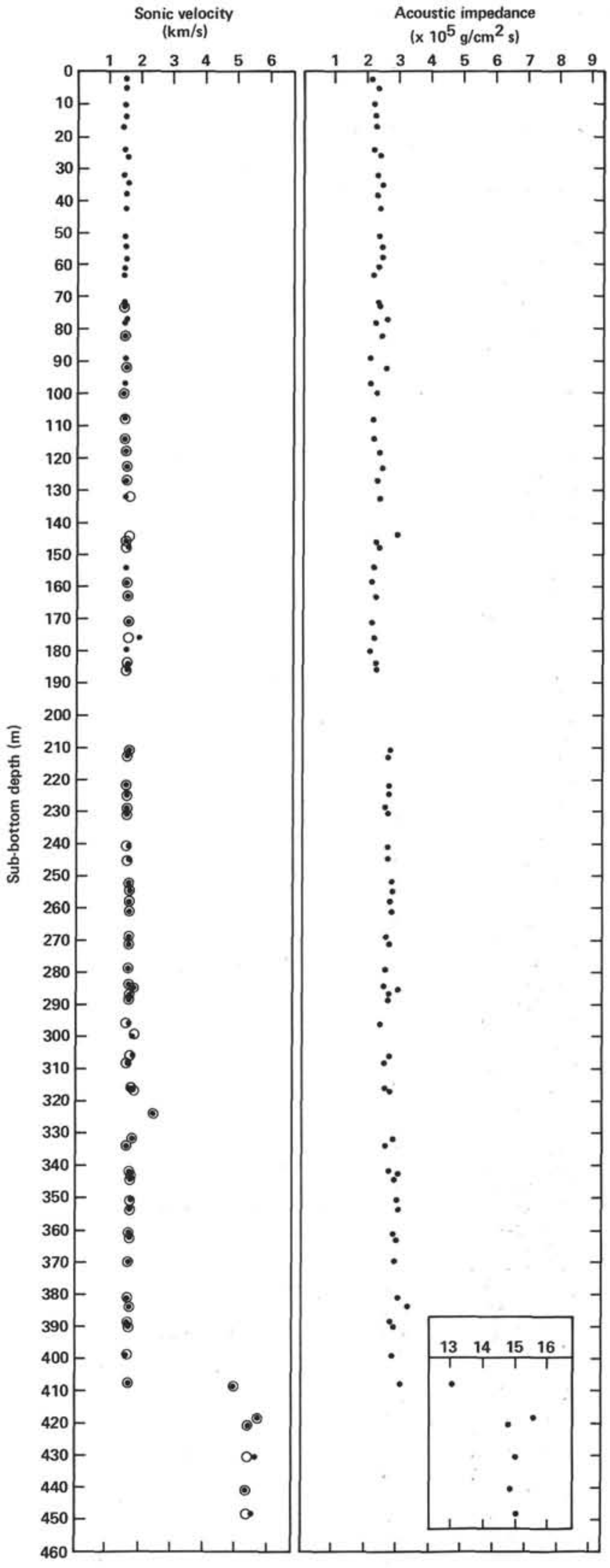

Figure 7. Plot of acoustic impedance and sonic velocity versus sub-bottom depth at Site 543. (Sonic velocities are calculated from recovered core samples and are *not* corrected to *in situ* values. Acoustic impedance values also are *not* corrected to *in situ* values.)

Table 3. Summary of physical properties for Site 543.

Sample (core-section, interval in cm)	Sub-bottom depth (m)	Sonic velocity (km/s) H^a	Sonic velocity (km/s) V^a	2-min. GRAPE Wet-bulk density (g/cm^3) H^a	2-min. GRAPE Wet-bulk density (g/cm^3) V^a	2-min. GRAPE Porosity (%) H^a	2-min. GRAPE Porosity (%) V^a	Gravimetrics Wet-bulk density (g/cm^3)	Gravimetrics Porosity (%)	Gravimetrics Water content (%)	Acoustic impedance ($\times 10^5$ g/cm^2 s) V^a	Shear strength (kPa)	Thermal conductivity [$\times 10^{-3}$ (cal/cm · s · deg)]
Hole 543													
1-2, 56–59	2	1.490		1.35		80.6		1.41	76.2	55.6	2.10		
1-2, 105–108	3											18.1	
1-4, 116–118	5	1.499		1.50		71.6		1.54	65.3	43.4	2.31		
1-4, 105–108	6											17.3	
1-7, 90–93	10	1.493		1.49		72.2		1.50	70.8	48.3	2.24		
1-7, 103–106	10											13.2	
2-2, 17–20	12											9.1	
2-3, 44–47	14	1.490		1.49		72.2		1.52	64.6	43.6	2.26		
2-5, 29–32	17											9.1	
2-5, 44–47	17	1.545		1.49		72.2		1.57	64.7	42.2	2.28		
3-3, 120–123	24	1.480		1.49		72.2		1.48	71.1	49.2	2.19		
3-4, 13–16	25											18.5	
3-5, 40–43	26	1.545		1.52		70.5		1.55	67.9	44.9	2.39		
3-7, 19–22	29											6.6	
4-2, 60–63	32	1.492		1.56		71.6		1.54	66.7	44.3	2.30		
4-3, 100–103	34											27.2	
4-4, 60–63	35	1.519		1.57		67.5		1.60	61.9	39.6	2.43		
4-6, 97–100	38											35.0	
4-6, 130–133	38	1.504		1.49		72.2		1.53	65.6	44.0	2.30		
5-3, 13–16	42	1.500		1.50		71.0		1.56	63.3	41.7	2.34		
5-3, 21–25	42											18.1	
5-3, 40	42												2.533
6-2, 135–137	51	1.496		1.43		75.8		1.56	61.4	40.4	2.33		
6-4, 70–72	54	1.506		1.58		66.9		1.61	63.8	40.6	2.42		
6-4, 82–86	54											17.3	
6-6, 97–100	57											32.5	
6-7, 13–16	58											63.0	
6-7, 21–23	58	1.519		1.58		66.9		1.60	63.2	40.5	2.43		
7-2, 86–89	60											21.4	
7-2, 94–97	61	1.482		1.55		68.7		1.58	63.8	41.4	2.34		
7-3, 138–141	62											77.8	
7-4, 41–44	63	1.471		1.56		68.1		1.55	67.3	44.4	2.28		
7-4, 47–50	63											26.4	
8-3, 104–107	72											44.9	
8-3, 124–128	72	1.485		1.55		68.7		1.60	62.2	39.9	2.38		
8-4, 50–54	73	1.488	1.493	1.57		67.5		1.61	62.4	39.6	2.40		
8-4, 69–72	73											72.1	
8,CC (5–8)	77											37.1	
8,CC (10–13)	77	1.523		1.63		63.9		1.71	55.8	33.3	2.60		
9-1, 92–95	78											12.4	
9-1, 104–107	78	1.482		1.47		72.2		1.53	65.8	44.1	2.27		
9-4, 65–68	82	1.493	1.502	1.50	1.56	71.6	68.1	1.65	59.0	36.6	2.48		
9-4, 73–76	82											45.3	
9-6, 82–85	85											39.5	
9-6, 120	86												2.644
10-2, 82–86	89	1.480		1.37		79.4		1.41	71.2	51.8	2.09		
10-2, 92–95	89											11.8	
10-4, 81–84	92	1.529	1.529	1.66	1.65	62.1	62.7	1.68	59.1	36.1	2.57		
10-4, 98–101	92											82.4	
10-5, 6–9	93											59.3	
11-1, 101–103	97											19.8	
11-1, 119–123	97	1.470		1.43		75.8		1.40	74.9	54.8	2.06		
11-3, 49–52	100											48.0	
11-3, 59–63	100	1.463	1.489	1.51	1.52	71.0	70.4	1.51	69.3	46.9	2.25		
12-2, 110–113	108											31.3	
12-2, 117–121	108	1.485	1.477	1.41	1.44	77.0	75.2	1.46	72.3	50.6	2.16		
12-4, 82–85	111											96.4	
12-6, 100	114												2.644
12-6, 117–120	114											41.2	
12-6, 125–129	114	1.487	1.497	1.44	1.44	75.2		1.49	71.1	48.9	2.23		
13-2, 104–107	118											53.5	
13-2, 116–120	118	1.499	1.505	1.52	1.56	71.0	68.1	1.54	67.8	45.0	2.32		
13-3, 144–147	119											73.3	
13-6, 63–66	123											76.6	
13-6, 70–74	123	1.520	1.511	1.69	1.60	60.3	65.7	1.63	65.4	41.1	2.46		
14-1, 83–86	125											32.9	
14-2, 80–83	127	1.520	1.512	1.49	1.50	72.2	71.6	1.52	71.7	48.4	2.30		
14-3, 103–106	129											24.7	
14-5, 97–100	132											13.2	
14-5, 110–113	132	1.500	1.662	1.39		78.2		1.43	70.9	50.6	2.38		

Table 3. (Continued).

Sample (core-section, interval in cm)	Sub-bottom depth (m)	Sonic velocity (km/s) H[a]	Sonic velocity (km/s) V[a]	2-min. GRAPE Wet-bulk density (g/cm^3) H[a]	2-min. GRAPE Wet-bulk density (g/cm^3) V[a]	2-min. GRAPE Porosity (%) H[a]	2-min. GRAPE Porosity (%) V[a]	Gravimetrics Wet-bulk density (g/cm^3)	Gravimetrics Porosity (%)	Gravimetrics Water content (%)	Acoustic impedance ($\times 10^5$ g/cm^2 s) V[a]	Shear strength (kPa)	Thermal conductivity [$\times 10^{-3}$ (cal/cm · s · deg)]
Hole 543 (Cont.)													
15-3, 36–39	137											39.5	
15,CC	144		1.643	1.77	1.80	55.5	53.7	1.77	58.5	33.9	2.91		
16-2, 73–76	146											28.8	
16-2, 92–95	146	1.526	1.533	1.47	1.50	73.4	71.6	1.49	74.4	51.3	2.28		
16-4, 24–27	148	1.551	1.506	1.56	1.56	68.1		1.54	71.0	47.3	2.32		
16-4, 76–79	149											43.2	
17-1, 70–73	154	1.527		1.49	1.49	72.2		1.44	76.2	54.1	2.20		
17-1, 77–80	154											62.6	
17-4, 135–138	159	1.518	1.505	1.34	1.35	81.2	80.6	1.41	76.5	55.7	2.12		
18-1, 65–68	163	1.581	1.565	1.40	1.46	77.6	74.0	1.46	74.9	52.6	2.28		
18-6, 99–102	171	1.604	1.598	1.40	1.34	74.0	81.7	1.40	76.2	55.8	2.24		
19-3, 10–13	175											32.9	
19-3, 93–97	176	1.946	1.592	1.34	1.33	81.2	81.8	1.39	76.4	56.4	2.21		
19-3, 80–84	176	1.596	1.564	1.40	1.36	77.6	80.0	1.43	73.6	52.6	2.24		
19-5, 8–11	178											42.8	
19-6, 8–11	180											19.8	
19-6, 13–16	180	1.514		1.41		77.0		1.39	76.5	56.2	2.10		
20-2, 88–91	184											105.4	
20-2, 98–101	184	1.556	1.551	1.47	1.38	73.4	78.8	1.44	74.1	52.7	2.23		
20-3, 88–92	186	1.547	1.536	1.42	1.42	76.4		1.49	71.5	49.2	2.29		
20-3, 94–97	186											90.6	
20-4, 85–88	187											>118.6	
20-4, 100	187												2.384
23-1, 128–131	211											112.0	
23-1, 138–142	211	1.619	1.580	1.66	1.74	62.1	57.3	1.70	58.9	35.5	2.69		
23-2, 99–103	213	1.578	1.579	1.64	1.59	63.3	66.3	1.68	61.9	37.9	2.65		
23-2, 108–111	213											112.0	
24-2, 95–97	222											75.8	
24-2, 108–111	222	1.563	1.560	1.66	1.70	62.1	58.9	1.68	62.1	37.9	2.62		
24-3, 98–100	224											118.6	
24-4, 103–106	225	1.572	1.575	1.74	1.76	57.3	56.1	1.71	61.1	36.7	2.69		
24-4, 108–110	225											101.3	
25-1, 7–10	229											54.4	
25-1, 11–15	229	1.578	1.539	1.65	1.68	62.7	60.9	1.67	61.9	37.9	2.57		
25-2, 55–59	231	1.557	1.551	1.65	1.68	62.7	60.9	1.68	60.2	36.5	2.61		
25-2, 65–68	231											67.5	
25-3, 15–18	232											66.7	
26-2, 54–57	241	1.604	1.541	1.72	1.72	58.5		1.71	59.3	35.5	2.64		
26-2, 102–105	241											106.2	
26-4, 79–82	244											112.0	
26-5, 55–58	245	1.620	1.570	1.63	1.63	61.9		1.70	57.9	34.8	2.67		
26-6, 70–73	247											125.2	
27-3, 120–123	252	1.625	1.610	1.68	1.63	60.9	61.9	1.70	59.2	35.8	2.74		
27-5, 27–30	254											79.1	
27-5, 83–86	255	1.613	1.612	1.67	1.61	61.5	65.1	1.70	58.1	35.1	2.74		
28-1, 71–74	258	1.629	1.622	1.54	1.61	69.3	65.1	1.66	59.2	36.5	2.69		
28-2, 101–104	260											102.1	
28-3, 59–62	261	1.646	1.607	1.76	1.70	56.1	59.7	1.73	57.0	33.8	2.78		
28-4, 97–100	263											117.8	
28-4, 125	263												2.588
29-2, 56–60	269	1.643	1.617	1.53	1.53	69.9		1.61	59.3	37.6	2.60		
29-2, 65–68	269											121.9	
29-3, 50–53	271											123.5	
29-3, 61–65	271	1.623	1.610	1.56	1.55	68.1	68.7	1.66	58.5	36.1	2.67		
29-6, 72–75	275											>115.3	
30-2, 110–113	279	1.603	1.618	1.55	1.50	68.7	71.6	1.61	59.6	38.0	2.60		
30-2, 118–120	279											>120.3	
30-4, 38–41	281											90.6	
30-5, 125–128	284	1.634	1.641	1.48	1.47	72.8	73.4	1.58	52.7	34.3	2.59		
30-5, 134–137	284											102.1	
30-6, 82–88	285	1.784	1.731	1.56	1.57	68.1	67.5	1.70	53.0	32.0	2.94		
31-1, 45–48	286											62.6	
31-1, 77–81	287	1.631	1.634	1.53	1.54	69.4	69.3	1.63	58.3	36.6	2.66		
31-2, 8–11	288	1.604	1.630	1.46	1.51	74.0	71.0	1.62	58.7	37.1	2.64		
31-2, 17–20	288											59.3	
32-1, 50–53	296											79.1	
32-1, 81–84	296	1.614	1.548	1.46	1.41	74.0	77.0	1.55	63.6	42.1	2.40		
32-2, 94–96	298											74.9	
32-3, 85–87	299											64.2	
32-4, 43–47	300	1.755	1.824	1.47	1.54	73.4	69.3	1.62	58.3	36.9	2.95		

Table 3. (Continued).

Sample (core-section, interval in cm)	Sub-bottom depth (m)	Sonic velocity (km/s) H[a]	Sonic velocity (km/s) V[a]	2-min. GRAPE Wet-bulk density (g/cm^3) H[a]	2-min. GRAPE Wet-bulk density (g/cm^3) V[a]	2-min. GRAPE Porosity (%) H[a]	2-min. GRAPE Porosity (%) V[a]	Gravimetrics Wet-bulk density (g/cm^3)	Gravimetrics Porosity (%)	Gravimetrics Water content (%)	Acoustic impedance ($\times 10^5$ g/cm^2 s) V[a]	Shear strength (kPa)	Thermal conductivity [$\times 10^{-3}$ (cal/cm · s · deg)]
Hole 543 (Cont.)													
33-1, 106-111	306	1.785	1.681	1.43	1.52	75.8	70.4	1.62	57.3	36.3	2.72		
33-2, 80-82	307											33.4	
33-3, 22-26	308	1.588	1.592	1.51	1.52	71.0	70.4	1.58	62.1	40.3	2.52		
33-3, 63	308												2.339
34-1, 146-148	316	1.683	1.661	1.49	1.36	72.2	80.0	1.54	61.6	40.9	2.56		
34-2, 94-97	317	1.776	1.711	1.47	1.48	73.4	72.8	1.61	59.3	37.7	2.75		
34,CC	324	2.426	2.453										
Hole 543A													
H1-4, 18-21	327											119.4	
2-1, 8-11	332	1.707	1.704	1.55	1.55	68.7		1.66	57.2	35.4	2.83		
2-2, 52-55	334	1.589	1.569	1.52	1.60	70.4	65.7	1.61	63.7	40.6	2.53		
2,CC	342	1.638	1.624	1.58	1.63	66.9	63.9	1.64	59.2	36.9	2.66		
3-1, 148-150	343	1.749	1.689	1.66	1.67	62.1	61.5	1.74	55.9	33.0	2.94		
3-2, 101-104	344	1.706	1.674	1.81	1.57	53.1	67.5	1.73	58.3	34.6	2.90		
4-1, 6-9	351	1.690	1.646	1.79	1.88	54.3	49.0	1.79	55.2	31.5	2.95		
4-3, 36-39	354	1.689	1.566	1.63	1.81	63.9	53.1	1.80	55.6	31.7	2.98		
5-1, 84-87	361	1.662	1.636	1.30	1.74	83.6	57.3	1.76	56.6	32.9	2.88		
5-2, 58-61	363	1.686	1.651	1.81	1.78	53.1	54.9	1.77	56.6	32.7	2.92		
5-2, 70-73	363											128.5	
6-1, 49-52	370	1.634	1.598	1.61	1.79	65.1	54.3	1.76	57.8	33.8	2.81		
6-1, 66-68	370											130.1	
6-1, 105	371												3.041
7-1, 96-100	381	1.629	1.628	1.89	1.95	48.4	44.8	1.83	55.2	31.0	2.98		
7-1, 101-104	381											70.8	
7-2, 27-30	381											73.7	
7-3, 91-94	384											59.7	
7-3, 100-104	384	1.697	1.672	2.06	1.91	38.2	47.2	1.94	48.4	25.6	3.24		
7-4, 10	384												3.578
8-1, 10-13	389											95.1	
8-1, 17-20	389	1.610	1.586					1.76	56.4	32.9	2.79		
8-1, 87-91	390	1.638	1.587					1.78	56.5	32.5	2.82		
8,CC (5-8)	399											114.9	
9-1, 6-10	399	1.617	1.597					1.80	54.8	31.1	2.87		
9-1, 33-36	399											74.5	
9-1, 50-54	399	1.568	1.585					1.81	54.6	30.9	2.87		
10-1, 14-17	408											71.7	
10-1, 28-32	408	1.664	1.671					1,85	52.3	28.9	3.09		
10-1, 120-124	409	4.910	4.932	2.74	2.72			2.65	8.5	3.3	13.07		
11-2, 30-34	419	5.621	5.561	2.96	2.97			2.81	5.6	2.1	15.57		
12-1, 80-84	421	5.358	5.287	2.99	2.90			2.80	6.1	2.2	14.80		
13-3, 55-58	431	5.580	5.314	3.06	3.06			2.83	5.7	2.1	15.04		
15-3, 7-11	441	5.293	5.284	3.02	2.91			2.8	4.5	1.6	14.90		
16-3, 46-50	449	5.471	5.327	3.06	2.97			2.82	4.6	1.7	15.02		

Note: Some shear strength measurements exceeded instrumentation limits and are indicated by a greater than (>) symbol. These values are not plotted in any figures and the values are considered below failure strength of the material.

[a] H = horizontal; V = vertical.

Table 4. Average sonic velocities, in Holes 543 and 543A.

Sub-bottom depth range (m)	$\overline{V}_{\parallel}$[a] (km/sec)	S	N	$\overline{V}_{\perp}$[a] (km/sec)	S	N
0-100	1.494	0.021	25	1.495	0.021	29
100-200	1.533	0.037	16	1.544	0.051	18
200-300	1.624	0.055	21	1.610	0.066	21
300-400	1.703	0.176	21	1.676	0.183	21
Total	1.589	0.135	86	1.580	0.120	86

Note: Values listed here are exclusive of measurements in basement. $\overline{V}_{\parallel}$ = velocity parallel to bedding; $\overline{V}_{\perp}$ = velocity perpendicular to bedding. S = standard deviation and N = number of samples.

[a] Includes $V_{\parallel}$ presumed to be equal to $V_{\perp}$ in the upper section of semiconsolidated material.

the site, but below the gap in data, the density has increased significantly and averages about 1.70 to 1.75 g/cm^3. There is a slight decrease in density from about 260 to 340 m sub-bottom.

The porosity and water content values for the upper 200 m of Site 543 are quite variable, often decreasing or increasing up to 20% in a few tens of meters. Similar trends in the variation in density can be noted in the upper 200 m of Site 543 (Fig. 8). Below the gap in data near 200 m, both the water content and porosity decrease gradually toward the bottom of the hole, as might be expected due to increasing compaction and overburden pressure.

We should note here that there is a great deal more scatter in the water content, porosity, and density values

Table 5. Calculated sonic velocity anisotropy values for individual samples, Site 543 (see text for derivation).

Section (core-section)	Sub-bottom depth (m)	Anisotropy (%)
Hole 543		
8-4	73	−0.17
9-4	82	−0.30
10-4	92	0.0
11-3	100	−0.88
12-2	108	0.27
12-6	114	−0.34
13-2	118	−0.20
13-6	123	0.30
14-2	127	0.26
14-5	132	−5.12
16-2	146	−0.23
16-4	148	1.47
17-4	159	0.43
18-1	163	0.51
18-6	171	0.19
19-3	176	1.01
20-2	184	0.16
20-3	186	0.36
23-1	211	1.22
23-2	213	−0.03
24-2	222	0.10
24-4	225	−0.10
25-1	229	1.25
25-2	231	0.19
26-2	241	2.00
26-5	245	1.57
27-3	252	0.46
27-5	255	0.03
28-1	258	0.22
28-3	261	1.20
29-2	269	0.80
29-3	271	0.40
30-2	279	−0.47
30-5	284	−0.21
30-6	285	1.51
31-1	287	−0.09
31-2	288	−0.80
32-1	296	2.09
32-4	300	−1.93
33-1	306	−3.00
33-3	308	−0.13
34-1	316	0.66
34-2	317	1.86
34,CC	324	−0.55
Hole 543A		
2-1	332	0.09
2-2	334	0.63
2,CC	342	0.43
3-1	343	1.75
3-2	344	0.95
4-1	351	1.32
4-3	354	1.02
5-1	361	0.79
5-2	363	1.05
6-1	370	1.11
7-1	381	0.03
7-3	384	0.74
8-1	389	0.75
8-1	390	1.58
9-1	399	0.62
9-1	399	−0.54
10-1	408	−0.21

for the upper 200 m at Site 543 than for strata drilled at equivalent depths at Sites 541 and 542.

Shear Strength

Shear strength values for cores From Site 543 are listed in Table 3 and are shown in Figures 8 and 4. Unlike shear strengths measured at Sites 541 and 542, the values obtained at Site 543 are quite scattered and variable throughout the drilled section, although the average shear strength values tend to increase down the hole. The scattered data points, especially at depth, for shear strength are very unlike the generally constant (or slightly decreasing), uniform values measured at the other two sites. The difference in data suggests that consolidation or tectonic processes that may be active at Sites 541 and 542 are apparently not currently active at Site 543, or that some other processes are acting on the strata at Site 543.

Thermal Conductivity

Eight conductivity measurements were made at Site 543 (Table 3). The conductivity values measured at site 543 are generally slightly less (about 10%) than values measured for equivalent depths at Sites 541 and 542. Conductivity is nearly constant at Site 543 and averages about 2.5×10^{-3} cal/cm · s · deg, except near the bottom of the hole, where conductivity values increase to slightly more than 3.5×10^{-3} cal/cm · s · deg.

Some Related Findings

Figure 9 is a plot of porosity versus density measurements from cores taken at Site 543. Also shown is the empirically derived equation from DSDP, relation density and porosity:

$$\rho_b = 2.70 - 1.675\phi$$

where ϕ = porosity of a sample.

The porosity and density values from Site 543 are scattered but do show a generally linear relationship. However, the scatter in the data from Site 543 is considerably greater than density-porosity data from Sites 541 and 542. Data from Sites 541 and 542 consistently plot above the empirically derived function from DSDP, whereas data from Site 543 generally plot below the DSDP equation. Thus for a given porosity, strata from Sites 541 and 542 are generally more dense than equivalent rocks from Site 543.

Earlier, we speculated that the uniform physical properties observed at sites 541 and 542 in a so-called subduction zone may be related to a tectonic overprint. Convergence and subsequent deformation have apparently allowed a relatively irregular physical property profile, as at Site 543, to be transformed to a uniform profile, as at Sites 541 and 542.

PALEOMAGNETICS

The objectives for paleomagnetic sampling at Site 543 were to use polarity stratigraphy for age control and to determine the magnetic properties of the basalts. Refer to the paleomagnetism chapter (Wilson, this volume)

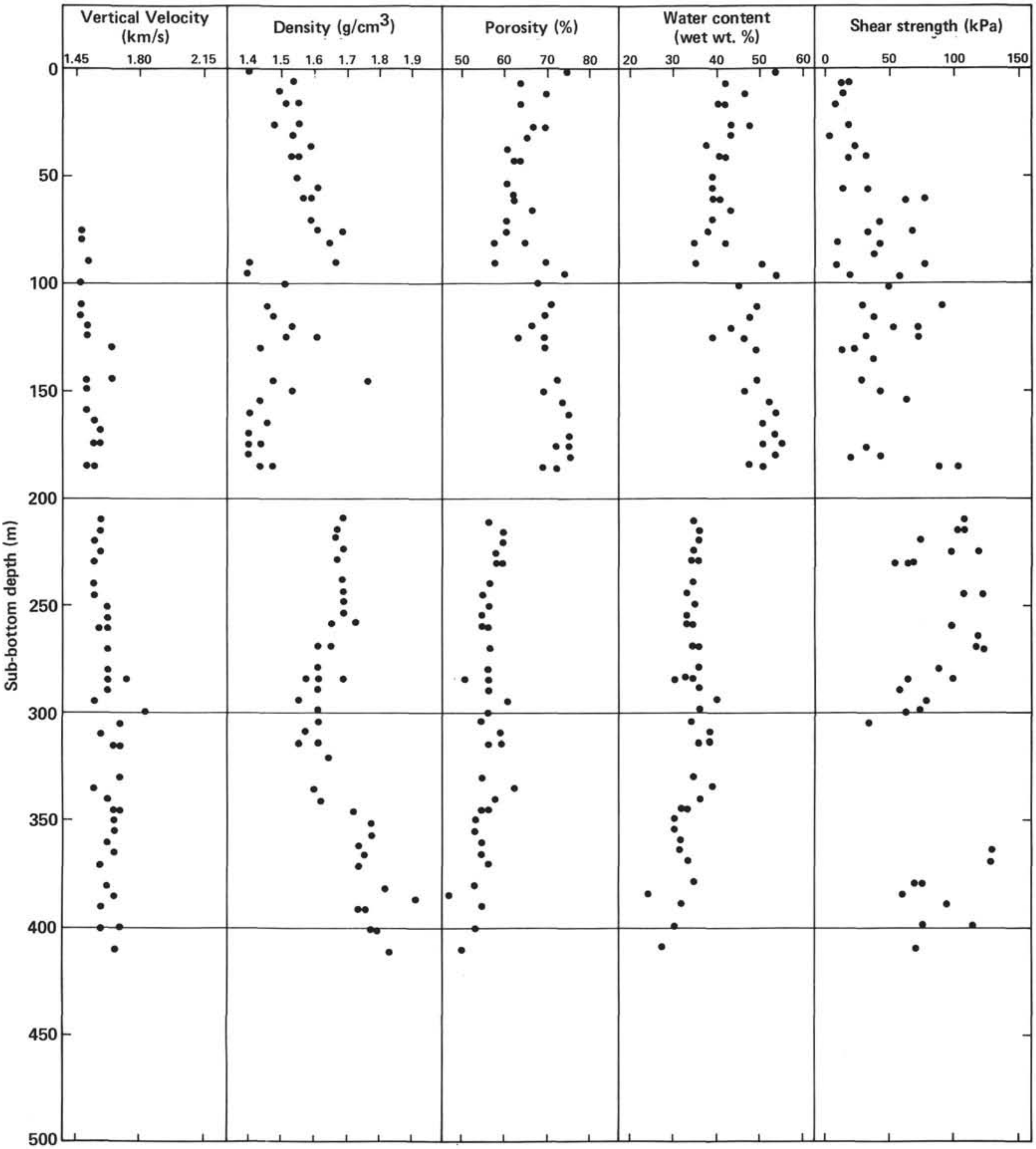

Figure 8. Plot of water content (wet wt.%), porosity (%), density (gm/cm$_3$), vertical velocity (km/s), and shear strength (kPa) values versus depth at Site 543.

for a complete discussion. Drilling deformation was, again, a major problem in the upper part of the sedimentary section. No samples at all were collected in the interval from Cores 1 to 5, and samples were very sparse from Cores 6 to 16—completely inadequate for polarity stratigraphy. Sample density and stability were adequate for Cores 17 to 20 (161–199 m sub-bottom).

The reversed intervals in Cores 18 and 20 should correlate to polarity epochs 16 and 18, respectively (Fig. 10). The radiolarian dates for this range strongly support these identifications, based on the correlation of Theyer and Hammond (1974).

The correlation between core polarity epochs and the marine magnetic anomalies is not rigorous in this inter-

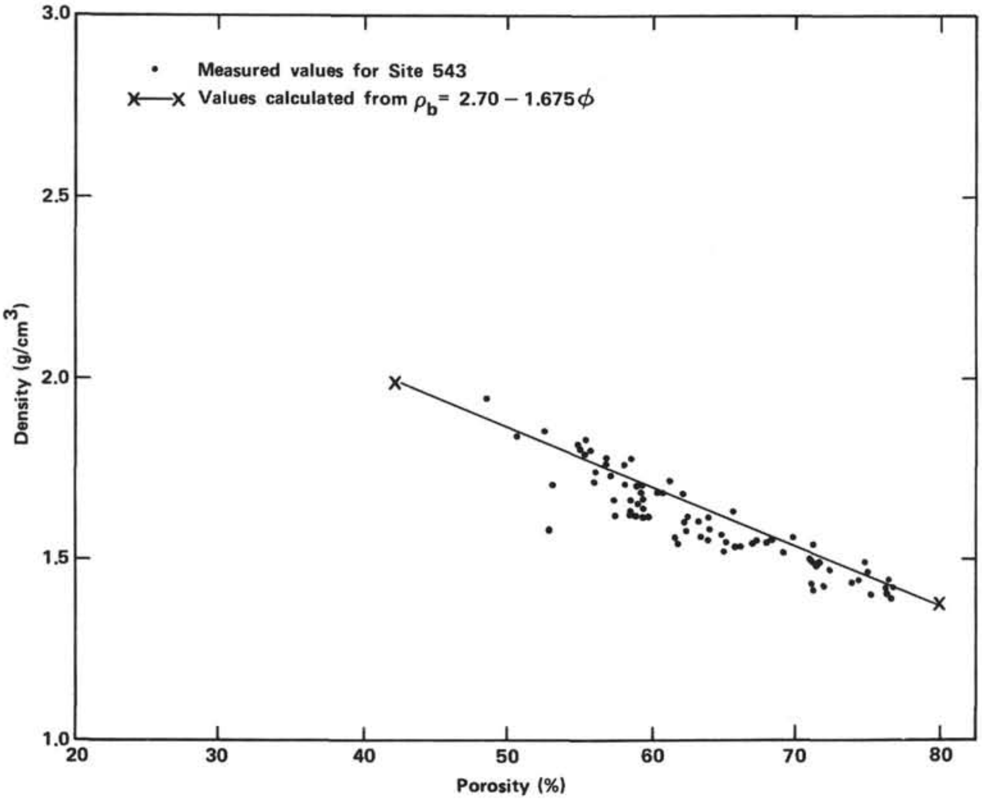

Figure 9. Plot of density versus porosity for core samples from Site 543. (See text for discussion.)

val, but if we have a nearly constant sedimentation rate, these four cores would correspond very nicely to Marine Anomalies 5C and 5D (age range 16 to 18 Ma, from Ness et al., 1980).

Cores 24 to 34 present an interesting problem. Drilling deformation was minimal and recovery was good, so sample density was adequate. Of over 40 samples, more than 30 are confidently judged to be reversed, and only one is normal. This pattern is not remotely compatible with any time scale and indicates remagnetization during a predominantly reversed interval. There is little hope for drawing any useful conclusions from the sediments in Hole 543A due to poor recovery and low paleolatitude.

The basalts are extremely stably magnetized and show very good internal consistency. NRM intensities are fairly strong, generally 5 to 10 Å/m. Directions change less than 2° with AF demagnetization, and median destructive fields are 15 to 30 nT. Inclinations divide neatly into three groups: Section 543A-10-1, −11°; Sections 543A-11-1 to 543A-12-1, −35° ±1°; and Sections 543A-12-2 to 543A-16-7, 25° ±4°. These correspond to basalts of differing petrography and composition, hence probably represent separate eruptions that recorded secular variation during a single reversed polarity epoch (Natland, this volume; Wilson, this volume).

TEMPERATURE MEASUREMENTS

A temperature logging run was made in Hole 543A using the Gearhart-Owen logging tool. The run extended past the end of the pipe, but stopped short of basement due to bridging in the hole. The results, complicated by an upward flow of warm water from the bottom of the hole, suggest a smaller undisturbed thermal gradient (roughly 20°/km) than that found to the west of the deformation front at Site 541. For more details, see Davis et al. (this volume).

SEISMIC STRATIGRAPHY—CORRELATIONS WITH LITHOLOGY AND PHYSICAL PROPERTIES

In the abyssal plain north of the Tiburon Rise the A1C seismic section is characterized by flat or gently dipping, more or less continuous reflectors of low amplitude and generally low continuity. Nevertheless it is possible to define several units within the sequence.

Seismic unit 1 occurs between seafloor and Reflector 1 and is composed of flat-lying layered sediments passing westward into the toe of the Barbados Ridge complex. Note in profile A1C that the uppermost part of this unit could be slightly folded at the deformation front (Fig. 3).

Seismic unit 2 occurs between Reflectors 1 and 2, is relatively transparent, and shows few thickness variations. This unit passes below the discontinuously reflective sequence of the prism.

Seismic unit 3 occurs between Reflectors 2 and 3 (the top of the acoustic basement) and exhibits rapid variation of thickness due to the paleotopography as well as variations in seismic character.

The location of Site 543 was chosen over a basement high, between the deformation front and the proposed

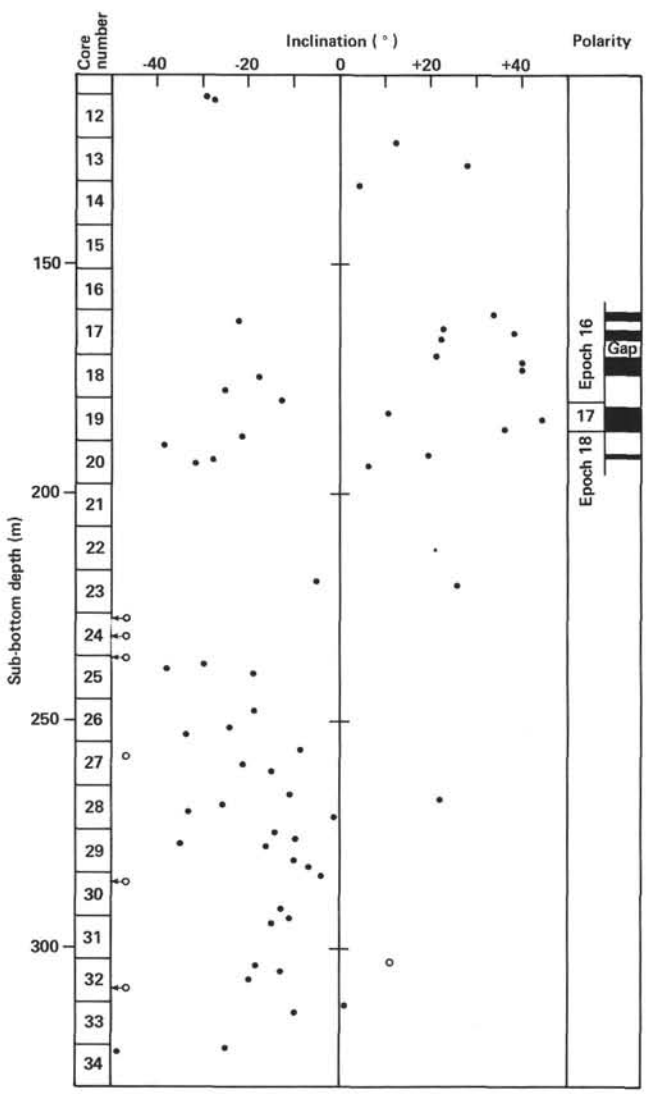

Figure 10. Stable magnetic inclination in sediments of Hole 543 versus sub-bottom depth, and polarity interpretation. (Black areas indicate normal polarity; white areas show reversed polarity. Open circles represent data judged to be less reliable than the data represented by filled circles; open circles with arrows indicate data that are off the graph.)

reference hole (CAR-1D). Due to navigational difficulties the location of Site 543 is estimated to be 0.5 km north of the Profile A1C (Fig. 2). At shot point 380 on Profile A1C the sedimentary sequence is 0.490 s thick (two-way traveltime), where seismic unit 1 is 220 m/s thick, seismic unit 2 is 150 m/s thick, and seismic unit 3 is 120 m/s thick.

Despite the southern displacement of Profile A1C from Site 543, correlation between the observed seismic stratigraphy and the drilled section is good (Fig. 11):

1) From 0 to 174 m (sub-bottom), the well-layered Pleistocene–Pliocene–upper Miocene sequence (Lithological Units 1, 2, and 3) corresponds to seismic unit 1 (using an average velocity of 1.57 km/s, the thickness of this seismic unit should be about 173 m). We can correlate the prominent Reflector 1 with the significant decrease in porosity and increase in density and shear strength, which occurs between 180 and 200 m sub-bottom at the uppermost part of the lower Miocene radiolarian muds; the same Reflector 1 was penetrated at Site 541, where the bit entered the very top of the underthrust sequence.

2) From 174 m to the bottom of Hole 543, Lithological Units 4, 5, and 6 correspond to seismic units 2 and 3. A lack of significant change in the physical properties of the cored section in unit 2 makes it difficult to correlate the seismic stratigraphy with the cored section. Nevertheless, using a velocity of 1.68 km/s between 200 and 300 m, we can correlate Reflector 2 at the bottom of seismic unit 2 to the top of zeolitic clays (Unit 5b) of the middle Eocene.

3) The depth to oceanic layer 2 at Site 543 was difficult to predict because of the lack of good velocity analyses from seismic reflection data. The cored contact is estimated at 411 m sub-bottom, a depth close to the calculated depth (404 m) based on core velocity measurements (around 390 m using an average velocity of 1.75 km/s).

SUMMARY AND CONCLUSIONS

Site 543 is located on the Tiburon Rise 3.5 km seaward of the deformation front of the Barbados Ridge complex. Here we penetrated a 411-m sequence of hemipelagic and pelagic sediments and 44 m of basaltic basement.

The recent sediments consist of ashy mud to a depth of 8 m at Site 543. The subjacent sediments to 70.5 m are Pleistocene to upper Pliocene ashy nannofossil mud that is transitional to a unit of lower Pliocene to lower Miocene mud and ashy mud that extends to 176 m sub-bottom. Radiolarian clay initially with local ash layers, subsequently with manganese stains, occurs from 170 to 322 m sub-bottom, spanning the lower Miocene into the Oligocene. Zeolitic clay–claystone is present from 322 to 379 m sub-bottom and overlies a basal calcareous, ferruginous Maestrichtian to Campanian claystone that contacts basalt at 411 m. Plagioclase as well as plagioclase–olivine phyric pillow basalts extend to a total depth of 455 m.

Overall the lithology at Site 543 records the birth and evolution of an oceanic crustal sequence with its progressive juxtaposition with an active volcanic source. The pillow basalts recovered at the base of Site 543 are typical of those found at the Mid-Atlantic Ridge, and they are succeeded by altered sediments commonly formed during hydrothermal activity at ridges. The claystones and zeolitic clay–claystone and manganese-rich radiolarian clays record slow sedimentation under open-ocean conditions, removed from any significant terrigenous or volcanic source. Notable quantities of ash occur in the lower Miocene and are also present through the Neogene, suggesting proximity to the Lesser Antilles arc. The carbonate content and occurrence of nannofossils and foraminifers suggest that Site 543 was above the CCD in the Late Cretaceous and the early Pliocene to Pleistocene. In general the Miocene and younger sediments at Site 543 are similar to those cored at Sites 541 and 542.

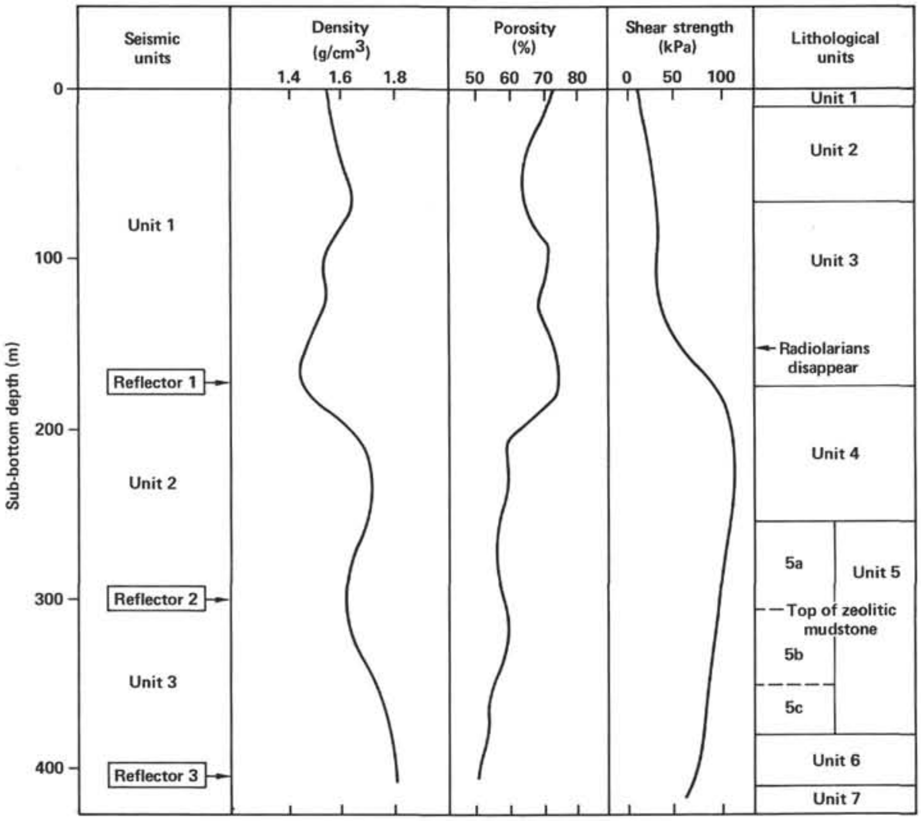

Figure 11. Correlations between physical properties, lithological units, and main reflectors of profile A1C (Fig. 3).

The structural features observed in the cores from Site 543 are principally induced by drilling. As such, these features provide an excellent reference section and allow separation of drilling induced and natural structures in the tectonically deformed sequences at Sites 541 and 542. Notably, the clay-rich sediments above 191 m and below 315 to 380 m at Site 543 are more easily deformed by drilling than the radiolarian-bearing sediments separating them, suggesting the former may constitute favored zones for décollement when this oceanic section is underthrust beneath the trench slope.

At Site 543 sonic velocity increased uniformly with depth in the sedimentary section. Density and porosity show a sharp increase and decrease, respectively, between 180 and 200 m. An increase in shear strength also occurs at this interval. This marked variation in physical properties correlates with the transition from mud to radiolarian mudstone and the approximate seaward extension of the reflector separating the apparently offscraped and underthrusted units to the west.

A key characteristic of Site 543 is the overall equivalence of its Miocene and younger sediments to the sequences cored at Sites 541 and 542; as such, we may infer oceanic derivation and offscraping of the deformed and faulted sequence penetrated at these latter sites. A second critical result is the association between 165 and 200 m of the top of the radiolarian-bearing mud, the increase in density and strength, and the reflection separating the apparently offscraped and subducted units west of the deformation front. The observed changes in physical properties, while subtle, favor the development of a décollement at this level, as inferred from the seismic data.

A downhole seismometer with temperature and tilt recorders was emplaced in the basaltic basement at Site 543. The instrument remained in the hole while a seismic refraction experiment was conducted. Malfunctioning of the seismometer necessitated retrieval of the downhole instrument and prevented deployment of the long-term recording package on the seafloor.

REFERENCES

Berger, W. H., 1977. Carbon dioxide excursion and the deep-sea record, aspects of the problem. *In* Anderson, N. R., and Malahoff, A. (Eds.), *The Fate of Fossil Fuel CO_2 in the Oceans.* Mar. Sci., 6: 505–542.

Berggren, W. A., 1973. The Pliocene time scale: calibration of planktonic foraminiferal and calcareous nannoplankton zones. *Nature,* 243:391–397.

Biju-Duval, B., Mascle, A., Montadert, L., and Wanneson, J., 1978. Seismic investigations in the Columbia, Venezuela, and Grenada Basins, and on the Barbados Ridge for future IPOD drilling. *Geol. Mijnbouw,* 57:105–116.

Blow, W. H., 1969. Late middle Eocene to Recent planktonic foraminiferal biostratigraphy. *In* Bronnimann, P., and Renz, H. H. (Eds.), *Proc. First Int. Conf. Planktonic Microfossils, Geneva, 1967.* 1: 199–422.

Bukry, D., and Okada, H., 1980. Supplementary modification and introduction of code numbers to the low-latitude Coccolith biostratigraphic zonation. *Mar. Micropaleontol.*, 5:321–325.

Gartner, S., 1977. Calcareous nannofossil biostratigraphy and revised zonation of the Pleistocene. *Mar. Micropaleontol.*, 2:1–25.

Mascle, A., Lajat, D., and Nely, G., in press. Sediment deformation linked to subduction and argilokinesis in the southern Barbados

Ridge from multichannel seismic surveys. *Trans. 4th Latin Am. Geol. Congr.*

Ness, G., Levi, S., and Couch, R., 1980. Marine magnetic anomaly time scales for the Cenozoic and Late Cretaceous: a precis, critique, and synthesis. *Rev. Geophys. Space Phys.*, 18:753–770.

Riedel, W. R., and Sanfilippo, A., 1978. Stratigraphy and evolution of tropical Cenozoic radiolarians. *Micropaleontology*, 23:61–69.

Sanfilippo, A., and Riedel, W. R., 1982. Revision of the radiolarian genera *Theocotyle, Theocotylissa,* and *Thyrsocyrtis. Micropaleontology*, 28(2):170–188.

Theyer, F., and Hammond, S. R., 1974. Paleomagnetic polarity sequence and radiolarian zones, Brunhes to Polarity Epoch 20. *Earth Planet. Sci. Lett.*, 22:307–319.

Verbeek, J. W., 1976. Calcareous nannoplankton biostratigraphy of Middle and Upper Cretaceous deposits in Tunisia, Southern Spain, and France. *Utrecht Micro. Bull.*, 16:1–157.

SITE 543 HOLE CORE 1 CORED INTERVAL 5635.0–5645.5 (mbsl) 8.0–18.5 (mbsf)

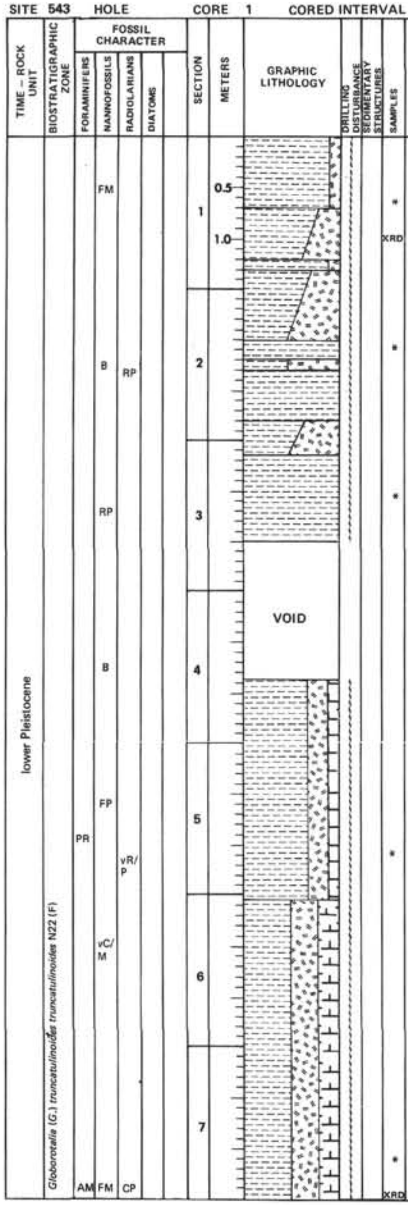

LITHOLOGIC DESCRIPTION

VITIRC MUD, CALCAREOUS VITRIC MUD

- Colors are brown (10YR 5/3) and grayish brown (10YR 5/2), generally more ashy. Locally dark gray (5Y 3/1). Ashy zones represent originally discrete ash fall layers mixed up by drilling. Core is intensely swirled by drilling. Carbonate content is greater in Sections 4–7.

SMEAR SLIDE SUMMARY (%):

	1, 67	2, 60	3, 55	5, 110	7, 110
	D	D	D	D	D
Texture:					
Sand	10	1	3	5	7
Silt	20	9	10	10	10
Clay	70	90	87	85	83
Composition:					
Quartz	1	1	2	2	1
Feldspar	2	3	3	3	2
Clay	42	85	60	40	72
Volcanic glass	30	10	15	10	25
Foraminifers	–	–	–	5	–
Calc. nannofossils	25	2	20	40	–

$CaCO_3$ Bomb (%):
2, 56 = 0.5
3, 55 = 3.4
4, 111 = 1.0
7, 90 = 14.9

SITE 543 HOLE CORE 2 CORED INTERVAL 5645.5–5655.0 (mbsl) 18.5–28.0 (mbsf)

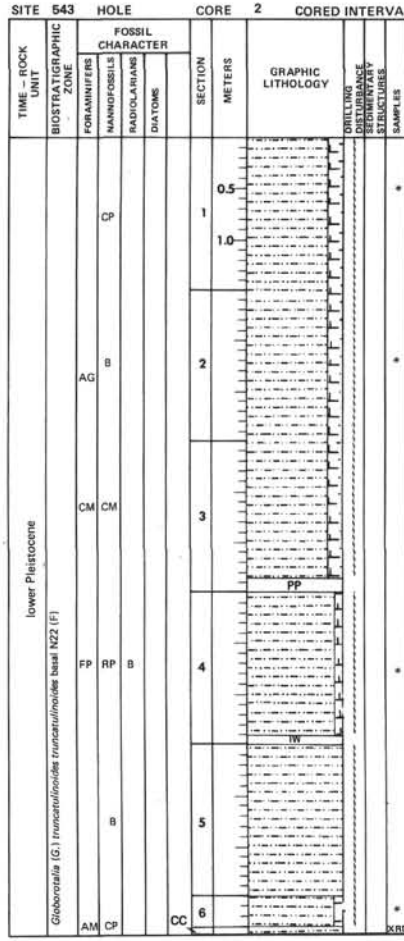

LITHOLOGIC DESCRIPTION

VITRIC MUD, CALCAREOUS VITRIC MUD and MINOR ASH

- Colors are dominantly brown (10YR 5/3) and pale brown (10YR 6/3–6/4) with blebs of black (N7), and grayish brown (2.5Y 5/2), and yellowish brown (10YR 5/4) ash. Intimately mixed and swirled by drilling. Ash was probably originally discrete beds, now is blebs, blotches, spots, swirls,and etc.

SMEAR SLIDE SUMMARY (%):

	1, 50	2, 70	4, 75	6, 15
	D	D	D	D
Texture:				
Sand	2	3	3	3
Silt	8	10	7	7
Clay	90	87	90	90
Composition:				
Quartz	1	1	1	1
Feldspar	2	2	2	2
Clay	41	50	47	43
Volcanic glass	10	5	7	5
Foraminifers	1	2	3	4
Calc. nannofossils	45	40	40	45

$CaCO_3$ Bomb (%):
3, 44 = 10.4
3, 58 = 16.8
5, 44 = 0.0

SITE 543 HOLE CORE 3 CORED INTERVAL 5655.0–5664.5 (mbsl) 28.0–37.5 (mbsf)

TIME-ROCK UNIT: lower Pleistocene

BIOSTRATIGRAPHIC ZONE: *Globorotalia (G.) truncatulinoides truncatulinoides* basal N22 (F); *Cyclococcolithina macintyrei* zone (N)

Section	Foraminifers	Nannofossils	Radiolarians
1		FP	
2		FP	
3	CM	CM	
4	AG	CM	
5		vC/M	B
6	CM	vC/M	
7		vC/P	
CC	AG	vC/P	

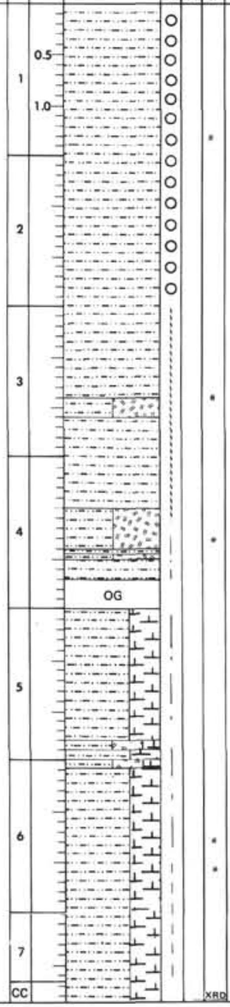

LITHOLOGIC DESCRIPTION

VITRIC MUD, CALCAREOUS VITRIC MUD, MUDDY ASH, and MINOR ASH

- Colors are pale brown (10YR 6/3), pale olive (5Y 6/4) and olive gray (5Y 5/2) toward top of core, changing to more ashy gray (5Y 6/1) and olive gray (5Y 6/2) near the bottom. Blebs and streaks of gray and dark gray (N4) ash.
- Sections 1 and 2 are mainly compacted mud breccias. Distinct ashy zones more nearly horizontal occur lower in the core. Otherwise, it is pretty disturbed by coring.

SMEAR SLIDE SUMMARY (%):

	1, 135 D	3, 90 D	4, 80 M	6, 80 D	6, 110 D
Texture:					
Sand	2	3	25	5	3
Silt	8	6	15	10	10
Clay	90	91	60	85	87
Composition:					
Quartz	1	1	1	1	1
Feldspar	2	2	3	3	2
Clay	42	62	42	36	38
Volcanic glass	10	—	50	15	6
Foraminifers	Tr	Tr	—	5	3
Calc. nannofossils	45	30	5	40	50

$CaCO_3$ Bomb (%):
3, 120 = 15.5
5, 40 = 34.2
5, 56 = 37.6

SITE 543 HOLE CORE 4 CORED INTERVAL 5664.5–5674.0 (mbsl) 37.5–47.0 (mbsf)

TIME-ROCK UNIT: upper Pliocene

BIOSTRATIGRAPHIC ZONE: *Globorotalia (G.) multicamerata–Pulleniatina obliquiloculata obliquiloculata–Globorotalia (T.) tosaensis* N20–21 (F); *Discoaster brouweri* subzone CN12d (N)

Section	Foraminifers	Nannofossils	Radiolarians	Diatoms
1		FP		
2	RP	B		
3		FP		
4		FP		
5			FP	B
6		FP		
7		FP		
CC	CM	FP		

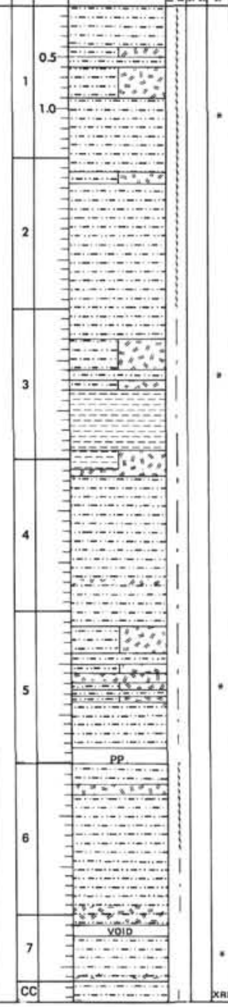

LITHOLOGIC DESCRIPTION

VITRIC MUD, MUDDY ASH, and MINOR ASH

- Colors: mainly olive gray (5Y 5/2) to olive (5Y 5/3) with more ashy zones gray (5Y 6/1) and light olive gray (5Y 6/2). Lesser light brownish gray (10YR 6/2). Also dark gray (N4) ash.
- The core consists of alternating ash-rich and ash-poor zones, pretty intensely deformed by drilling. Ashes were probably originally discrete, but now have been mixed by coring. They are more coherent near the bottom of the core. The core is sporadically somewhat calcareous.

SMEAR SLIDE SUMMARY (%):

	1, 110 D	3, 65 D	5, 75 D	7, 40 D
Texture:				
Sand	3	1	2	7
Silt	10	5	8	10
Clay	87	94	90	83
Composition:				
Quartz	1	1	1	1
Feldspar	3	2	3	3
Clay	90	60	60	65
Volcanic glass	—	2	5	10
Foraminifers	—	—	1	1
Calc. nannofossils	Tr	35	30	20
Sponge spicules	—	—	Tr	—

$CaCO_3$ Bomb (%):
2, 60 = 2.5
2, 89 = 5.0
4, 60 = 25.2
6, 130 = 11.9

SITE 543 HOLE CORE 5 CORED INTERVAL 5674.0–5683.5 (mbsl) 47.0–56.5 (mbsf)

TIME – ROCK UNIT	BIOSTRATIGRAPHIC ZONE	FORAMINIFERS	NANNOFOSSILS	RADIOLARIANS	DIATOMS	SECTION	METERS
upper Pliocene	*Globorotalia (G.) multicamerata–Pulleniatina obliquiloculata obliquiloculata* N20 (F); *Discoaster pentaradiatus* subzone CN12c (N); *Discoaster tamalis* subzone CN12a (N)		RP			1	0.5, 1.0
		CM	vC/P			2	
			CP			3	
			vC/M	B		4	
						5	
		FP	CP			CC	

GRAPHIC LITHOLOGY; DRILLING DISTURBANCE; SEDIMENTARY STRUCTURES; SAMPLES

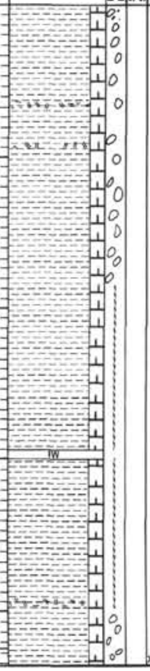

LITHOLOGIC DESCRIPTION

CALCAREOUS VITRIC MUD

- Colors: olive gray (5Y 5/2) and olive (5Y 5/3), swirled with gray (5Y 5/1) and gray (N4) swirls.
- Core is intensely disturbed by coring. Upper two sections are compacted mud breccia. Pipe rust is at top of Section 1.
- Core has gas bubbles (~3%).

SMEAR SLIDE SUMMARY (%):

	1, 100	3, 80	5, 20
	D	D	D
Texture:			
Sand	Tr	1	2
Silt	5	7	8
Clay	95	92	90
Composition:			
Quartz	1	1	2
Feldspar	3	3	6
Clay	92	80	79
Volcanic glass	5	6	5
Calc. nannofossils	–	10	8

$CaCO_3$ Bomb (%):
3, 13 = 15.3
3, 81 = 14.3

SITE 543 HOLE CORE 6 CORED INTERVAL 5683.5–5693.0 (mbsl) 56.5–66.0 (mbsf)

TIME – ROCK UNIT	BIOSTRATIGRAPHIC ZONE	FORAMINIFERS	NANNOFOSSILS	RADIOLARIANS	DIATOMS	SECTION	METERS
upper Pliocene	*Sphaeroidinella dehiscens–Globoquadrina altispira*–lower *G. (G.) multicamerata–P. obliquiloculata obliquiloculata* N19–basal N20 (F); *Discoaster tamalis* subzone CN12a (N)		CP			1	0.5, 1.0
			vC/P			2	
			CP			3	
			vC/P	B		4	
			vC/P			5	
			vC/M			6	
						7	
		RP	FP			CC	

GRAPHIC LITHOLOGY; DRILLING DISTURBANCE; SEDIMENTARY STRUCTURES; SAMPLES

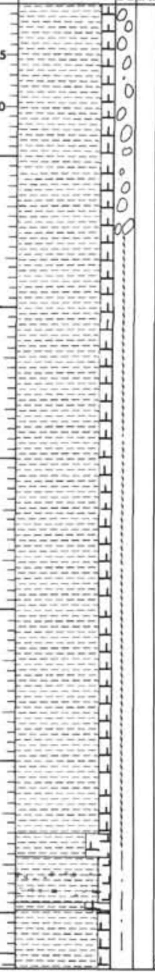

LITHOLOGIC DESCRIPTION

CLAY and CALCAREOUS CLAY, traces of ASH

- Colors: olive (5Y 5/3) and olive gray (5Y 5/2) with minor black (5Y 2.5/1) and dark gray (N4) spots (ashy). One dusky yellow green (5GY 5/2) layer in Section 6.
- Compacted mud breccia Sections 1 and 2 intensely deformed below that, but coherent bedding can be made out in Section 6.
- Ash content is diminished compared with previous (higher) cores.

SMEAR SLIDE SUMMARY (%):

	1, 90	3, 75	5, 75	1, 90
	D	D	D	M
Texture:				
Sand	–	2	1	–
Silt	5	10	8	–
Clay	95	88	91	–
Composition:				
Quartz	1	2	1	1
Feldspar	4	4	3	3
Clay	55	44	58	38
Volcanic glass	Tr	10	8	5
Foraminifers	–	Tr	Tr	3
Calc. nannofossils	40	40	30	50

$CaCO_3$ Bomb (%):
2, 135 = 13.8
4, 70 = 12.3
6, 70 = 9.9

SITE 543 HOLE CORE 7 CORED INTERVAL 5693.0–5702.5 (mbsl) 66.0–75.5 (mbsf)

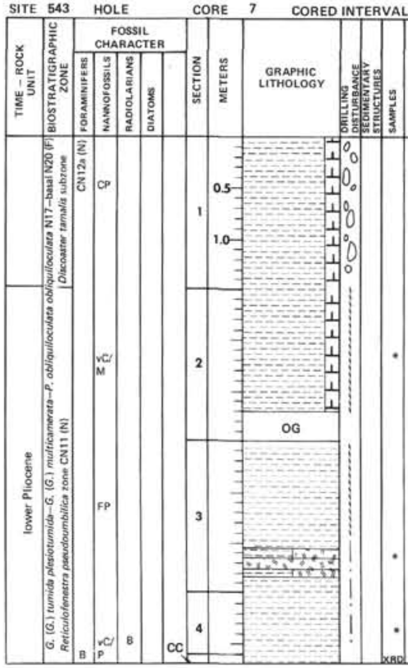

LITHOLOGIC DESCRIPTION

CLAY, ASHY MUD, and ASH, locally CALCAREOUS
- Colors: gray (5Y 5/1), light gray (5Y 6/1), and olive gray (5Y 5/2), with lesser olive (5Y 5/3). One ash is very dark gray (10YR 3/1).
- Compacted mud breccia Section 1. Below that intensely disturbed, swirled and agitated. Sections 3 and 4 have some coherent bedding and ash layers.

SMEAR SLIDE SUMMARY (%):

	2, 68	3, 117	4, 36
	D	M	D
Texture:			
Sand	Tr	3	Tr
Silt	5	95	4
Clay	95	2	96
Composition:			
Feldspar	3	93	3
Heavy minerals	–	1	Tr
Clay	40	–	96
Volcanic glass	–	5	1
Carboante unspec.	1	–	–
Foraminifers	1	–	–
Calc. nannofossils	55	–	–
Fish remains	Tr	–	–
Fe-oxides	–	1	–

$CaCO_3$ Bomb (%):
2, 94 = 9.4
3, 74 = 3.9
3, 92 = 22.2
4, 41 = 2.0

SITE 543 HOLE CORE 8 CORED INTERVAL 5702.5–5712.0 (mbsl) 75.5–85.0 (mbsf)

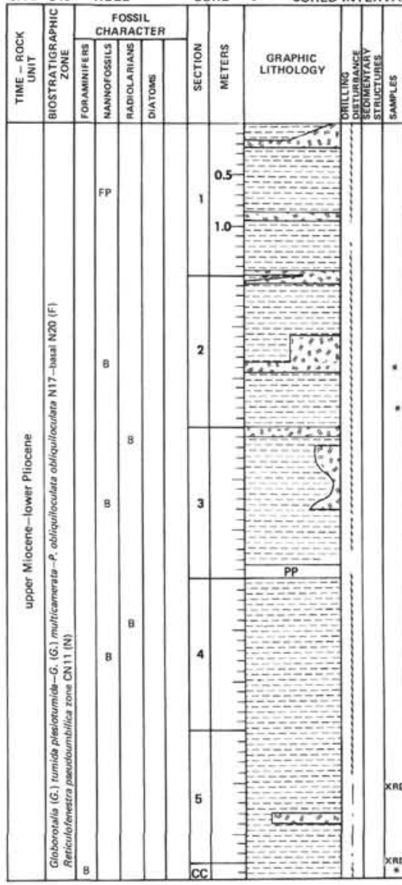

LITHOLOGIC DESCRIPTION

CLAY, VITRIC MUD, and MINOR ASH
- Colors: mainly olive gray (5Y 5/2), with lesser gray (5Y 4/1) and swirls of dark gray (N3), medium dark gray (N4), and brownish black (5YR 2/1) ash. Swirls not necessarily ashy are gray (10YR 6/1) and olive (5Y 4/4).
- Core is intensely disturbed throughout, with local concentrations of ash, probably once discrete beds, now mixed up by drilling.

SMEAR SLIDE SUMMARY (%):

	2, 91	2, 130	CC
	M	D	D
Texture:			
Sand	40	3	1
Silt	30	10	10
Clay	30	87	89
Composition:			
Feldspar	45	1	1
Heavy minerals	Tr	Tr	Tr
Clay	30	87	89
Volcanic glass	25	12	10
Calc. nannofossils	–	–	Tr

$CaCO_3$ Bomb (%):
3, 116 = 0.0
3, 124 = 0.0
4, 50 = 0.0
CC, 10 = 0.0

SITE 543 HOLE CORE 9 CORED INTERVAL 5712.0–5721.5 (mbsl) 85.0–94.5 (mbsf)

TIME – ROCK UNIT: upper Miocene–lower Pliocene

BIOSTRATIGRAPHIC ZONE: *G. (G.) plesiotumida–G. (G.) multicamerata–P. obliquiloculata obliquiloculata* N17–basal N20 (F)

FOSSIL CHARACTER: FORAMINIFERS, NANNOFOSSILS, RADIOLARIANS, DIATOMS — B B B

SECTION: 1 2 3 4 5 6 7 CC — METERS: 0.5, 1.0

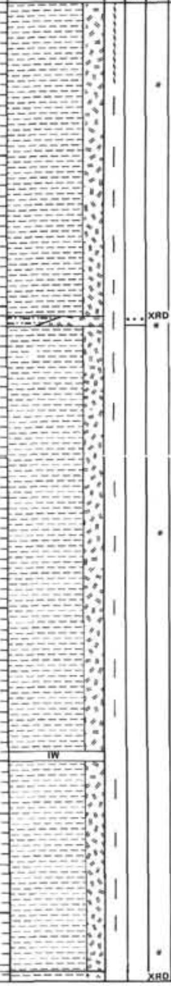

LITHOLOGIC DESCRIPTION

VITRIC MUD and and ASH TRUBIDITE (I)

- Colors: pale brown (10YR 6/3), light brownish gray (10YR 6/2), grayish brown (10YR 5/2), brown (10YR 5/3), olive gray (5Y 5/2) (turbidite), dusky yellow green (5GY 5/2), and olive (5Y 5/3). Generally intensely swirled and deformed mud except near bottom which is faintly mottled. Turbidite rests in an island of coherence in an otherwise deformed interval.

SMEAR SLIDE SUMMARY (%):

	1, 80 D	2, 20 M	4, 75 D	7, 40 D
Texture:				
Sand	Tr	30	Tr	–
Silt	25	65	8	25
Clay	75	5	92	75
Composition:				
Feldspar	4	2	2	10
Heavy minerals	Tr	–	–	Tr
Clay	75	–	92	75
Volcanic glass	19	93	6	14
Carbonate unspec.	2	–	Tr	1
Calc. nannofossils	Tr	–	–	–

$CaCO_3$ Bomb (%):
1, 104 = 0.0
3, 84 = 0.0
4, 65 = 0.0

SITE 543 HOLE CORE 10 CORED INTERVAL 5721.5–5731.0 (mbsl) 94.5–104.0 (mbsf)

TIME – ROCK UNIT: upper Miocene–lower Pliocene

BIOSTRATIGRAPHIC ZONE: *G. (G.) plesiotumida–G. (G.) multicamerata–P. obliquiloculata obliquiloculata* N17–basal N20 (F)

FOSSIL CHARACTER: FORAMINIFERS, NANNOFOSSILS, RADIOLARIANS, DIATOMS — R B B B

SECTION: 1 2 3 4 5 CC — METERS: 0.5, 1.0

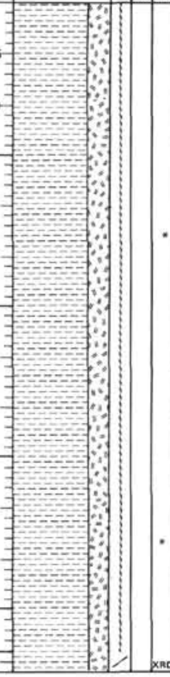

LITHOLOGIC DESCRIPTION

VITRIC MUD with spots of ASH

- Colors: mainly olive gray (5Y 5/2) with minor pale brown (10YR 6/3) (top Section 1), and greenish gray (5GY 6/1). Also brownish gray (2.5Y 5/2) ash spots. Intensely deformed throughout, with minor ash spots amidst the swirl.

SMEAR SLIDE SUMMARY (%):

	2, 80 D	4, 80 D
Texture:		
Silt	25	15
Clay	75	85
Composition:		
Feldspar	7	5
Clay	75	85
Volcanic glass	18	10
Carbonate unspec.	–	Tr

$CaCO_3$ Bomb (%):
1, 60 = 0.0
2, 82 = 0.0
4, 81 = 0.0

SITE 543 HOLE CORE 11 CORED INTERVAL 5731.0–5740.5 (mbsl) 104.0–113.5 (mbsf)

FOSSIL CHARACTER: FORAMINIFERS, NANNOFOSSILS, RADIOLARIANS, DIATOMS — B B B

SECTION: 1 2 3 CC — METERS: 0.5, 1.0

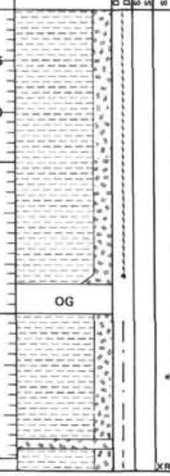

LITHOLOGIC DESCRIPTION

VITRIC MUD and an ASH BED

- Colors: olive gray (5Y 5/2) and gray (5Y 5/1). Brownish black (5YR 2/1) ash.
- Core is intensely deformed and swirled throughout, except near ash bed in Section 3. Ashy patches are distributed elsewhere.

SMEAR SLIDE SUMMARY (%):

	3, 60 D
Texture:	
Sand	Tr
Silt	8
Clay	92
Composition:	
Feldspar	2
Clay	92
Volcanic glass	6

$CaCO_3$ Bomb (%):
1, 119 = 0.0
2, 90 = 0.0
3, 59 = 0.0

SITE 543 HOLE CORE 12 CORED INTERVAL 5740.5–5750.0 (mbsl) 113.5–123.0 (mbsf)

TIME – ROCK UNIT	BIOSTRATIGRAPHIC ZONE	FORAMINIFERS	NANNOFOSSILS	RADIOLARIANS	DIATOMS	SECTION	METERS	GRAPHIC LITHOLOGY	DRILLING DISTURBANCE	SEDIMENTARY STRUCTURES	SAMPLES
						1	0.5, 1.0				*
						2					*
						3					XRD
						4		PP			*
		B	B	B		5					
						6					
						7					*
						CC					XRD

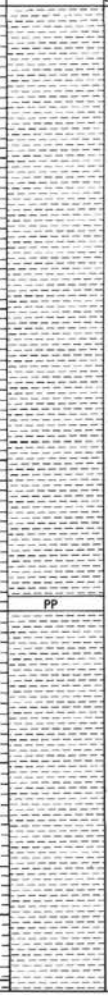

LITHOLOGIC DESCRIPTION

CLAY, with traces of VITRIC MUD

- Colors: mainly brown–yellowish brown (10YR 5/3-5/4) swirled at top, with olive gray (5Y 5/2), olive (5Y 5/3), and gray (5Y 5/1) near bottom. Ashy intervals are gray (10YR 5/2), brown (7.5Y 5/2), and 10YR 4/1 burrowed.
- Quite deformed and swirled into Section 3, less deformed below. Burrow mottling evident lower half of core. Tends to have redistributed ash.
- No major ash beds.

SMEAR SLIDE SUMMARY (%):

	1, 10 D	2, 90 D	4, 100 D	7, 13 D
Texture:				
Sand	–	–	–	Tr
Silt	4	5	2	4
Clay	96	95	98	96
Composition:				
Feldspar	2	4	2	3
Heavy minerals	Tr	Tr	Tr	1
Clay	96	95	98	96
Volcanic glass	2	1	Tr	Tr
Carbonate unspec.	–	–	Tr	Tr
Fish remains	–	–	Tr	Tr

$CaCO_3$ Bomb (%):
2, 117 = 0.0
4, 70 = 0.0
6, 125 = 0.0

SITE 543 HOLE CORE 13 CORED INTERVAL 5750.0–5759.5 (mbsl) 123.0–132.5 (mbsf)

TIME – ROCK UNIT	BIOSTRATIGRAPHIC ZONE	FORAMINIFERS	NANNOFOSSILS	RADIOLARIANS	DIATOMS	SECTION	METERS	GRAPHIC LITHOLOGY	DRILLING DISTURBANCE	SEDIMENTARY STRUCTURES	SAMPLES
						1	0.5, 1.0				*
						2					
						3					*
						4					
		B	B	B		5					
						6					
						7					
						CC					XRD

LITHOLOGIC DESCRIPTION

CLAY with MINOR ASH

- Colors: primarily greenish gray (5GY 5/1). Section 5 and top Section 6 olive gray (5Y 5/2) to grayish brown (10YR 5/2). Ash at Section 1, 15 cm dark gray (5Y 4/1); Section 2, 21 cm, grayish green (10GY 4/2); Section 3, 130–140 cm, olive (5Y 4/3). Section 5 has greenish gray (5G 6/1) streaks with specks of dark gray (N4) ash.
- Core is mottled with dark gray (N4) ash speckles, small streaks, and disaggregated layers. Some with associated greenish gray (5G 6/1) alteration haloes. Largely swirled, mixed, and deformed by drilling, which has mutilated any traces of original bioturbation.

SMEAR SLIDE SUMMARY (%):

	1, 60 D	3, 125 D
Texture:		
Sand	1	1
Silt	7	4
Clay	92	95
Composition:		
Quartz	2	1
Feldspar	4	4
Heavy minerals	1	Tr
Clay	85	90
Volcanic glass	8	5
Carbonate unspec.	Tr	Tr

$CaCO_3$ Bomb (%):
2, 116 = 0.0
6, 70 = 0.0

SITE 543 HOLE CORE 14 CORED INTERVAL 5759.5–5769.0 (mbsl) 132.5–142.0 (mbsf)

TIME – ROCK UNIT	BIOSTRATIGRAPHIC ZONE	FORAMINIFERS	NANNOFOSSILS	RADIOLARIANS	DIATOMS	SECTION	METERS	GRAPHIC LITHOLOGY	DRILLING DISTURBANCE	SEDIMENTARY STRUCTURES	SAMPLES
		B	B	B		1, 2, 3, 4, 5, 6, CC	0.5, 1.0	VOID, IW			*, *, XRD

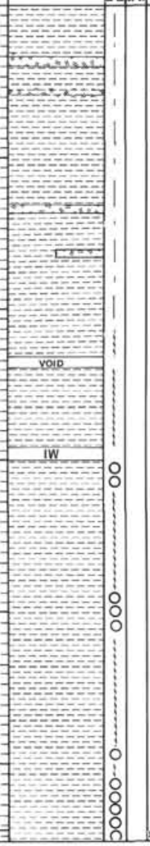

LITHOLOGIC DESCRIPTION

CLAY, VITRIC MUD, and MUD

- Colors: primarily greenish gray (5GY 5/1) with minor zones or lumps of olive gray (5Y 5/2) to grayish olive brown (10YR 5/2).
- Ash: Section 1, 52–57 cm: black (N2.5) burrowed; Section 1, 73–75 cm: gray (N5); Section 2, 50–55 cm: dark gray to black (N4–N2.5) mottled. Clay with minor ash beds in Sections 1 and 2. Sections 3, 4, and 5 consist of compacted mud breccia produced by drilling with minor soupy sections. Section 6 consists of soupy clay. Sections 1 and 3 somewhat disrupted by piano wire and may have rotational shear surfaces.

SMEAR SLIDE SUMMARY (%):

	1, 90	3, 80	5, 84
	D	D	D
Texture:			
Sand	2	1	Tr
Silt	6	5	4
Clay	92	94	96
Composition:			
Quartz	1	1	–
Feldspar	4	3	4
Heavy minerals	1	Tr	1
Clay	92	95	93
Volcanic glass	2	1	2

$CaCO_3$ Bomb (%):
2, 80 = 0.0
5, 110 = 0.0

SITE 543 HOLE CORE 15 CORED INTERVAL 5778.5–5788.0 (mbsl) 142.0–151.5 (mbsf)

TIME – ROCK UNIT	BIOSTRATIGRAPHIC ZONE	FORAMINIFERS	NANNOFOSSILS	RADIOLARIANS	DIATOMS	SECTION	METERS	GRAPHIC LITHOLOGY	DRILLING DISTURBANCE	SEDIMENTARY STRUCTURES	SAMPLES
		B	B	B		1, 2, 3, CC	0.5, 1.0				*, *, XRD

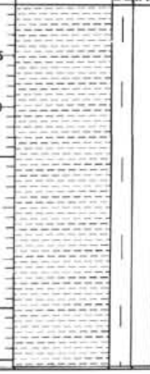

LITHOLOGIC DESCRIPTION

CLAY

- Colors: primarily greenish gray (5GY 5/1) mottled with dark greenish gray (5GY 4/1) and olive (5Y 5/1) areas in Sections 2 and 3.
- Clay is quite firm. Quite deformed by drilling and has a scaly surface owing to disruption by the piano wire.
- Core-Catcher contains a shell fragment at 15 cm.

SMEAR SLIDE SUMMARY (%):

	1, 90	3, 30
	D	D
Texture:		
Sand	Tr	Tr
Silt	5	5
Clay	95	95
Composition:		
Quartz	1	1
Feldspar	4	5
Heavy minerals	1	–
Clay	93	93
Volcanic glass	1	1

$CaCO_3$ Bomb (%):
CC = 0.0

SITE 543 HOLE CORE 16 CORED INTERVAL 5778.5–5788.0 (mbsf) 151.5–161.0 (mbsf)

TIME – ROCK UNIT | BIOSTRATIGRAPHIC ZONE | FOSSIL CHARACTER: FORAMINIFERS, NANNOFOSSILS, RADIOLARIANS, DIATOMS | SECTION | METERS | GRAPHIC LITHOLOGY | DRILLING DISTURBANCE | SEDIMENTARY STRUCTURES | SAMPLES

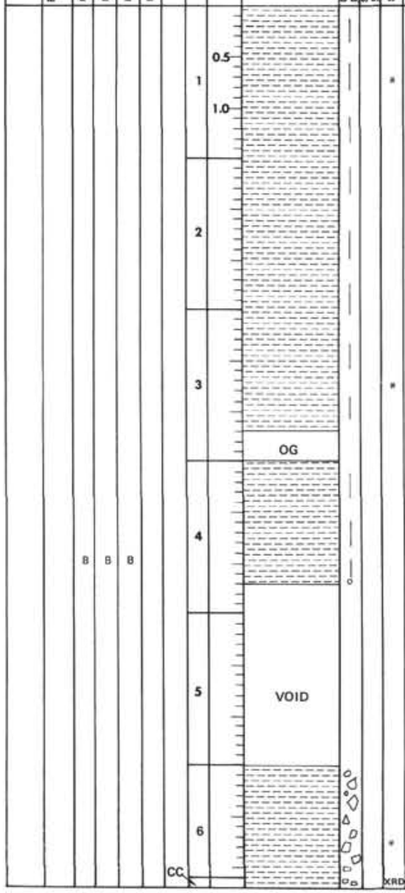

LITHOLOGIC DESCRIPTION

CLAY

- Colors: primarily greenish gray (5GY 5/1) with gradational layers and faint mottles of olive gray (5Y 5/2), olive (5Y 5/3), dark greenish gray (5GY 4/1) and dusky yellow green (5GY 5/2). The clay is faintly mottled. Sections 1 and 2 are moderately deformed by drilling and have scaly surface disruption from the piano wire. Sections 3 and 4 have less surface disruption than Sections 1 and 2. Sections 2 and 3 contain ashy, dark gray (N5) burrows. Section 5 consists of compacted clay breccia produced by drilling.

SMEAR SLIDE SUMMARY (%):

	1, 75 D	3, 75 D	6, 75 D
Texture:			
Sand	2	1	1
Silt	5	5	8
Clay	93	94	91
Composition:			
Quartz	1	1	1
Feldspar	4	5	5
Heavy minerals	1	5	1
Clay	89	92	83
Volcanic glass	5	2	10

$CaCO_3$ Bomb (%):
2, 92 = 0.0
4, 23 = 0.0

SITE 543 HOLE CORE 17 CORED INTERVAL 5788.0–5797.5 (mbsl) 161.0–170.5 (mbsf)

TIME – ROCK UNIT | BIOSTRATIGRAPHIC ZONE | FOSSIL CHARACTER: FORAMINIFERS, NANNOFOSSILS, RADIOLARIANS, DIATOMS | SECTION | METERS | GRAPHIC LITHOLOGY | DRILLING DISTURBANCE | SEDIMENTARY STRUCTURES | SAMPLES

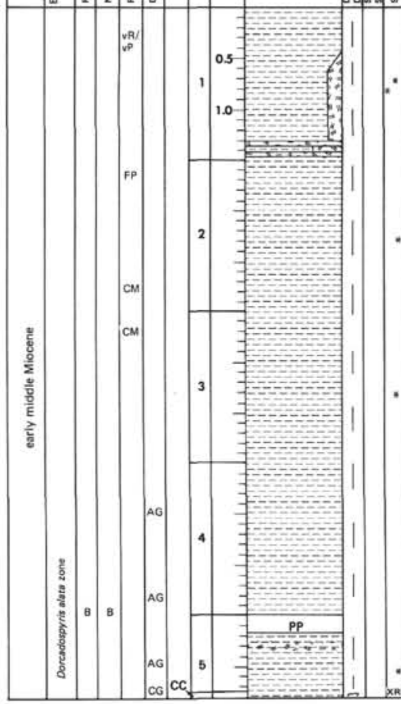

LITHOLOGIC DESCRIPTION

CLAY and MINOR ASH

- Colors: primarily greenish gray (5GY 5/1) with gradational color changes to small "layers" of olive (5Y 5/3), olive greenish gray (5GY 5/1–5Y 5/3), olive gray (5Y 5/2). There are 1–2 cm thick layers of pale green (10G 6/2) in Sections 2 and 4, alteration next to ashy spots. Section 1 contains gray burrow mottling.
- Ash: Section 1, 130–135 cm: black (5Y 2.5/1) bed; Section 1, 140–143 cm: very dark gray (5Y 3/1) bed; Section 5, 32–36 cm: dark gray (N3) layer. In addition there ashy specks often surrounded by pale green (10G 6/2) alteration. There is a small percent of radiolarians in Section 2 and below. The clay is quite firm and the surface has been disrupted by splitting with a piano wire.

SMEAR SLIDE SUMMARY (%):

	1, 75 D	1, 80 D	2, 80 D	3, 82 D	5, 57 D
Texture:					
Sand	1	5	2	3	4
Silt	5	7	8	5	6
Clay	94	88	90	92	90
Composition:					
Quartz	1	1	1	1	1
Feldspar	5	4	5	3	5
Heavy minerals	1	Tr	Tr	Tr	Tr
Clay	89	85	88	92	89
Volcanic glass	4	10	5	2	2
Diatoms	–	–	–	–	Tr
Radiolarians	–	–	1	2	3

$CaCO_3$ Bomb (%):
1, 65 = 0.0
6, 99 = 0.0

SITE 543 HOLE CORE 18 CORED INTERVAL 5797.5–5807.0 (mbsl) 170.5–180.0 (mbsf)

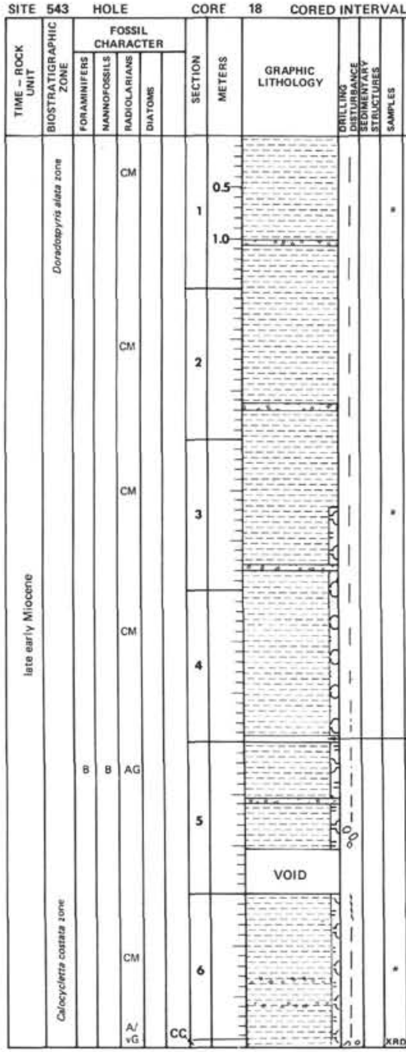

LITHOLOGIC DESCRIPTION

CLAY, RADIOLARIAN CLAY, and ASH

- Colors: primarily greenish gray (5GY 6/1) to grayish green (10GY 6/2) with some intervals more olive gray (5Y 5/2).
- Ash: beds Section 1, 57 cm: black (N2.5); 106–109 cm: black (N2.5) with pale blue green (5BG 7/2) area below ash; has a flat lower contact and a bioturbated upper contact; Section 2, 110–120 cm: grayish black (N2.5; Section 3, 125–130 cm: black (N2.5); Section 5, about 49–56 cm: black (2.5Y/2.5; and Section 6: black (2.5).
- Top part of core is clay, bottom is radiolarian clay; both have ash layers. Ash layers have well-defined lower contacts and bioturbated upper contacts. Bioturbation faint except near ash layers. Surface disrupted and core partially fractured by piano wire during splitting.

SMEAR SLIDE SUMMARY (%):

	1, 75	3, 75	6, 75
	D	D	D
Texture:			
Sand	3	10	10
Silt	5	5	5
Clay	92	85	85
Composition:			
Quartz	1	Tr	1
Feldspar	4	3	3
Heavy minerals	Tr	Tr	Tr
Clay	91	85	83
Volcanic glass	Tr	2	3
Radiolarians	4	10	10

$CaCO_3$ Bomb (%):
1, 65 = 0.0
6, 99 = 0.0

SITE 543 HOLE CORE 19 CORED INTERVAL 5807.0–5816.5 (mbsl) 180.0–189.5 (mbsf)

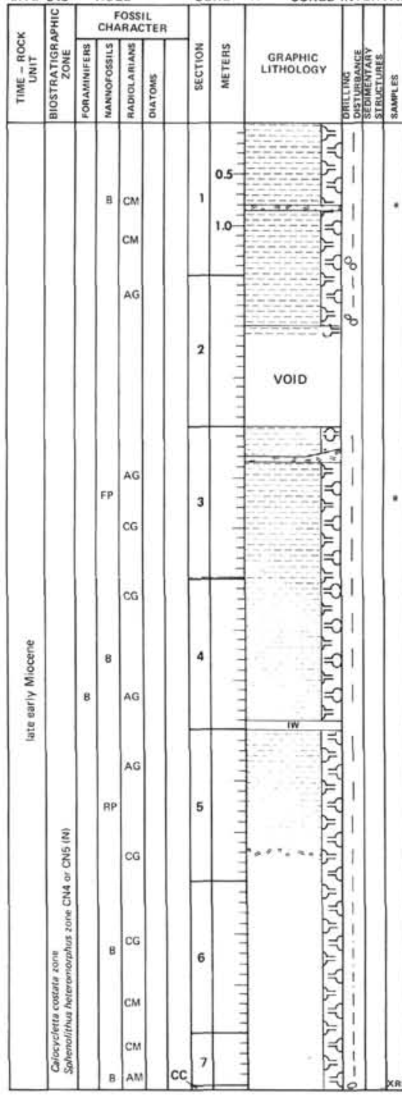

LITHOLOGIC DESCRIPTION

RADIOLARIAN CLAY and MINOR ASH

- Colors mostly light olive gray (5Y 6/2) and gray (5Y 5/1). Minor brownish black (5YR 2/1) ashes, some with alteration haloes of greenish gray (5G 6/1). Olive (5Y 5/3) mud at Section 1, 100 cm.
- Radiolarian clay, structureless except for ash beds. Disturbed by drilling and by piano wire.

SMEAR SLIDE SUMMARY (%):

	1, 82	3, 70
	M	D
Texture:		
Sand	10	8
Silt	80	42
Clay	10	50
Composition:		
Quartz	Tr	1
Feldsapr	15	–
Heavy minerals	Tr	–
Clay	10	50
Volcanic glass	75	25
Radiolarians	Tr	20

$CaCO_3$ Bomb (%):
3, 80 = 0.0
3, 93 = 0.0
6, 13 = 0.0

SITE 543 HOLE CORE 20 CORED INTERVAL 5816.5–5826.0 (mbsl) 189.5–199.0 (mbsf)

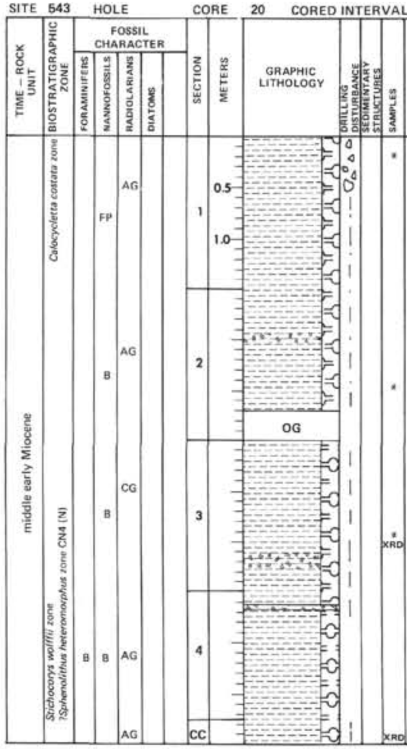

LITHOLOGIC DESCRIPTION

RADIOLARIAN CLAY and MINOR ASH

- Colors are mainly olive (5Y 5/3) and subordinate greenish gray (5GY 6/1) and olive gray (5Y 5/2). Dark gray (5Y 4/1) ash with alteration halo greenish gray (5G 5/1) at Section 2, 50 cm and Section 3, 110 cm. Gradational change from 5Y 5/3 down to light brown/strong brown (7.5YR 6/4–5/6) in Section 3. Section 4 is pale brown (10YR 6/3) to light yellowish brown (10YR 6/4).
- Core is mottled and swirled, locally ashy. Cavings breccia in top 60 cm of Section 1.

SMEAR SLIDE SUMMARY (%):

	1, 120	2, 95	3, 92
	D	D	D
Texture:			
Sand	4	2	2
Silt	25	18	15
Clay	71	80	83
Composition:			
Feldspar	3	2	1
Clay	71	80	83
Volcanic glass	Tr	Tr	–
Radiolarians	26	18	16
Fish remains	–	Tr	–

$CaCO_3$ Bomb (%):
2, 98 = 0.0
3, 88 = 0.0

Note: Core 21, 5826.0–5835.5 (mbsl) 199.0–208.5 (mbsf): no recovery.

SITE 542 HOLE CORE 22 CORED INTERVAL 5835.5–5845.0 (mbsf) 208.5–218.0 (mbsf)

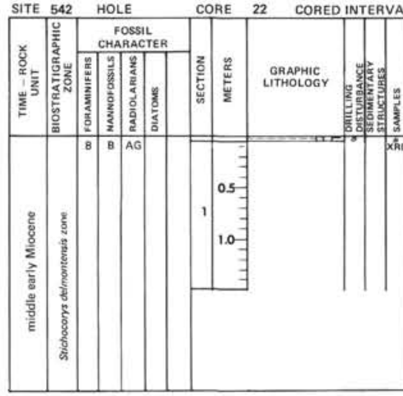

LITHOLOGIC DESCRIPTION

No recovery except for small sample scraped from the top of the core barrel.

- Light brownish gray (2.5Y 6/2) to pale olive (5Y 6/3) radiolarian mud.

SMEAR SLIDE SUMMARY (%):

	CC
	D
Texture:	
Sand	4
Silt	25
Clay	71
Composition:	
Feldsapr	2
Clay	71
Radiolarians	27

SITE 543 HOLE CORE 23 CORED INTERVAL 5845.0–5854.5 (mbsl) 218.0–227.5 (mbsf)

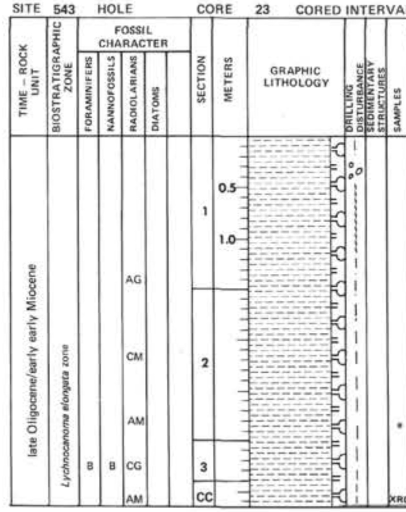

LITHOLOGIC DESCRIPTION

RADIOLARIAN CLAY

- Colors mainly pale olive (5Y 6/3), greenish gray (5GY 5/1); subordinately pale brown (10YR 6/3), olive (5Y 5/3), greenish gray (5G 6/1 and 5/1), light olive gray (5Y 6/2), and olive gray (5Y 5/2).
- Swirled variegated mud, slightly foraminiferal, locally radiolarian. Top of Section 1 brecciated (this probably represents Cores 21 and 22).

SMEAR SLIDE SUMMARY (%):

	2, 135
	D
Texture:	
Sand	1
Silt	12
Clay	87
Composition:	
Feldspar	1
Clay	87
Radiolarians	12

$CaCO_3$ Bomb (%):
1, 138 = 0.0
2, 99 = 0.0

SITE 543 HOLE CORE 24 CORED INTERVAL 5854.5–5864.0 (mbsl) 227.5–237.0 (mbsf)

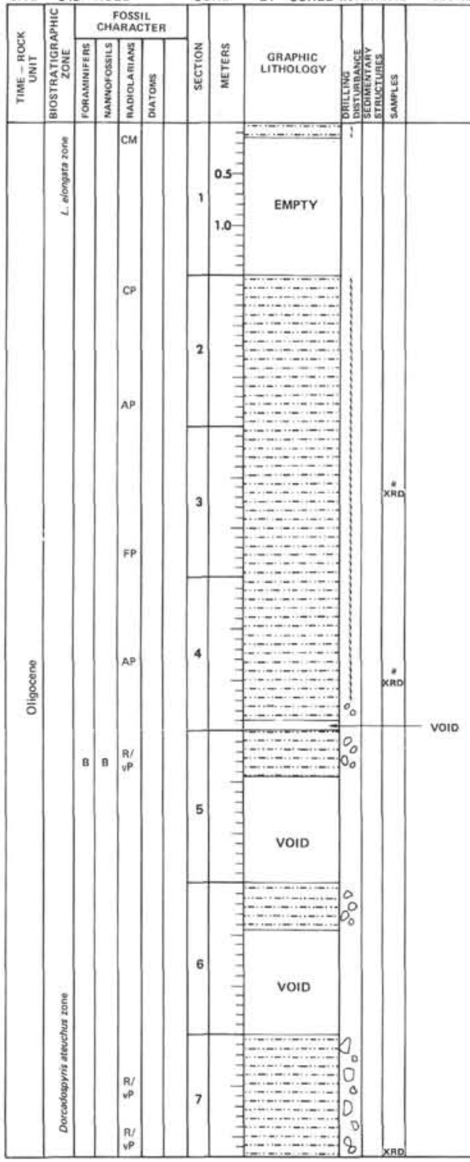

LITHOLOGIC DESCRIPTION

MUD

- Colors are greenish gray (5G 6/1) and olive gray (5Y 5/2) with light olive gray (5Y 6/2).
- Swirled, variegated mud: swirling is all a drilling effect. Olive gray and light olive gray predominate. Boundaries between different colors are gradational. Locally radiolarian. Thin rhodochrosite layer at Section 4, 94 cm.
- Drilling breccia below Section 4, 130 cm (slightly firmer clasts in a soupy matrix). Sections were cut at the bottom of each of the voids, artifically lengthening the core. The voids were each actually shorter than shown here.

SMEAR SLIDE SUMMARY (%):

	3, 60 D	4, 92 M
Texture:		
Sand	1	–
Silt	15	–
Clay	85	–
Composition:		
Feldspar	Tr	–
Heavy minerals	2	–
Clay	84	–
Volcanic glass	12	–
Radiolarians	2	–
Rhodochrosite	–	100

$CaCO_3$ Bomb (%):
2, 108 = 0.0
4, 103 = 0.0

SITE 543 HOLE CORE 25 CORED INTERVAL 5864.0–5873.5 (mbsl) 237.0–246.5 (mbsf)

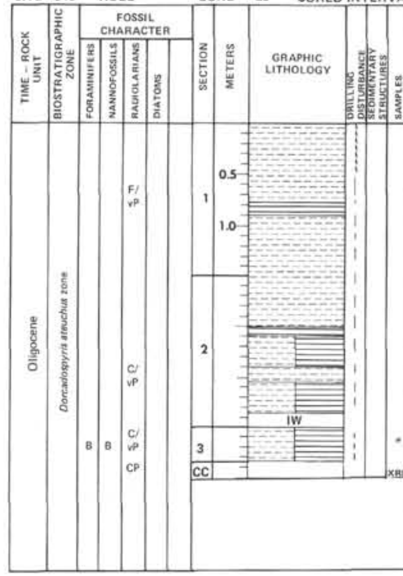

LITHOLOGIC DESCRIPTION

CLAY transitional to PELAGIC CLAY

- Colors of terrigenous clay are olive gray (5Y 5/2), greenish gray (5GY 6/1, 7/1, and 5/1), and light olive gray (5Y 6/2). Colors for clay-pelagic clay mixtures and pelagic clay are grayish brown 2.5Y 5/2 and 6/2), and brown (10YR 5/3, 6/2), and 7.5Y 5/4. Variegated mottled clay, swirled by drilling in upper part, with remains of horizontal layering. Colors in layers 10–20 cm thick with burrowed contacts. Slightly radiolarian. Few specks of rhodochrosite.

SMEAR SLIDE SUMMARY (%):

	3, 15 D
Texture:	
Sand	Tr
Silt	4
Clay	96
Composition:	
Feldspar	Tr
Clay	96
Carbonate unspec.	Tr
Radiolarians	4
Fish remains	Tr

$CaCO_3$ Bomb (%):
1, 11 = 0.0
2, 55 = 0.0

SITE 543 HOLE CORE 26 CORED INTERVAL 5873.5–5883.0 (mbsl) 246.5–256.0 (mbsf)

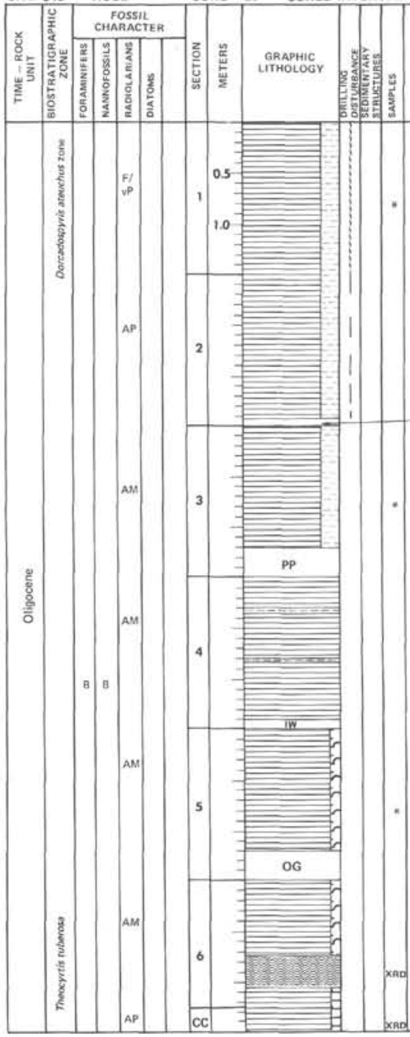

LITHOLOGIC DESCRIPTION

PELAGIC CLAY and RADIOLARIAN PELAGIC CLAY

- Colors: brown (10YR 5/3) mainly, with undertones of greenish gray (5GY 6/1). Beginning in Section 6: light yellowish brown (10YR 6/4), reddish yellow (7.5YR 6/6), and black (10YR 2.5/1). Mn-stained.
- Mottled brown clay: drilling breccia in Section 1. Then rotational shear surfaces every 2–4 cm; becoming more reddish downwards. Mn staining begins in Section 6.

SMEAR SLIDE SUMMARY (%):

	1, 80 D	3, 80 D	5, 80 D
Texture:			
Silt	5	10	10
Clay	95	90	90
Composition:			
Quartz	Tr	1	1
Feldsapr	5	5	5
Heavy minerals	Tr	–	–
Clay	91	87	76
Volcanic glass	1	8	–
Radiolarians	3	5	10

$CaCO_3$ Bomb (%):
2, 54 = 0.0
5, 55 = 0.0

SITE 543 HOLE CORE 27 CORED INTERVAL 5883.0–5892.5 (mbsl) 256.0–265.5 (mbsf)

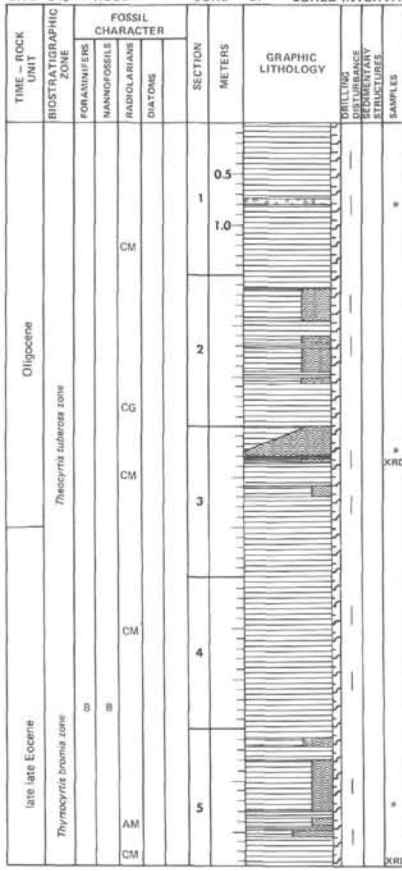

LITHOLOGIC DESCRIPTION

PELAGIC CLAY and MANGANIFEROUS PELAGIC CLAY

- Colors: light yellowish brown (10YR 6/4) and light brown (7.5YR 6/4). Minor colors (streaks, swirls, and mottles) gray (10YR 5/2), grayish brown (10YR 5/2), very pale brown (10YR 7/3 and 7/4), dark grayish brown (10YR 4/2), dark gray, (10YR 4/1), and black (10YR 2.5/1). Burrow-mottled light brown clay, swirled at top, rotational shear surfaces every 2–5 cm, more obvious toward base. Darker brown toward base.

SMEAR SLIDE SUMMARY (%):

	1, 80 D	3, 28 D	5, 70 D
Texture:			
Sand	1	2	–
Silt	10	12	–
Clay	89	86	–
Composition:			
Quartz	1	Tr	–
Feldspar	5	5	–
Clay	84	85	–
Radiolarians	10	10	–

$CaCO_3$ Bomb (%):
3, 120 = 0.0
5, 83 = 0.0

SITE 543 HOLE CORE 28 CORED INTERVAL 5892.5–5902.0 (mbsl) 265.5–275.0 (mbsf)

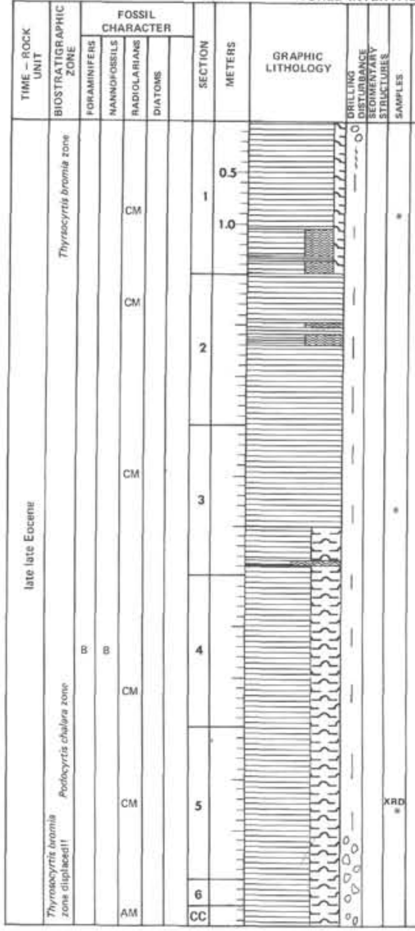

LITHOLOGIC DESCRIPTION

PELAGIC CLAY and RADIOLARIAN PELAGIC CLAY

- Colors mainly light yellowish brown (10YR 6/4). Mottles of brown (7.5YR 5/4), dark brown (7.5YR 4/2), very dark gray (N3) and yellowish red (5YR 4/8) increasing downwards.
- Burrow mottled light yellowish brown to variegated clay.
- Rotational shear surfaces every 2–4 cm.
- Drilling breccia at base.

SMEAR SLIDE SUMMARY (%):

	1, 80	3, 80	5, 80
	D	D	D
Texture:			
Sand	6	3	15
Silt	10	8	10
Clay	84	84	75
Composition:			
Quartz	1	1	1
Feldspar	5	4	4
Heavy minerals	1	–	–
Clay	83	88	68
Volcanic glass	Tr	2	–
Radiolarians	10	5	25

$CaCO_3$ Bomb (%):
1, 71 = 0.0
3, 59 = 0.0

SITE 543 HOLE CORE 29 CORED INTERVAL 5902.0–5911.5 (mbsl) 275.0–284.5 (mbsf)

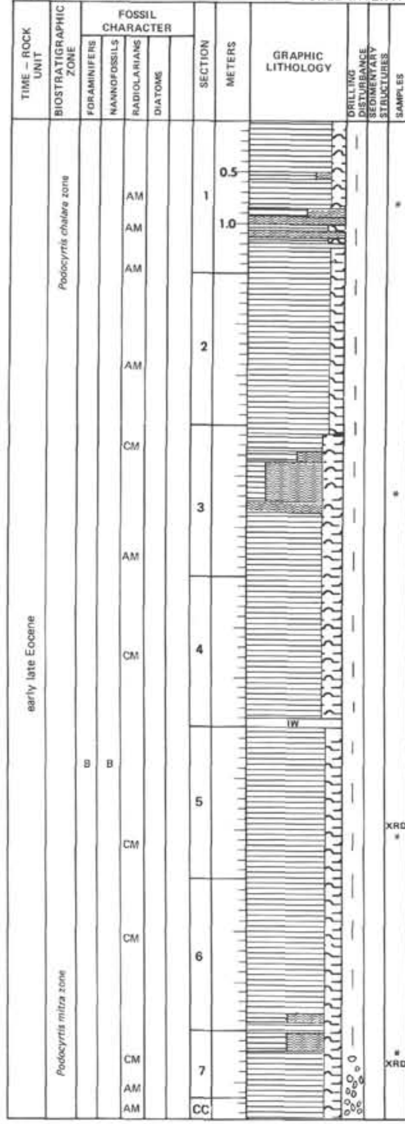

LITHOLOGIC DESCRIPTION

PELAGIC CLAY, RADIOLARIAN PELAGIC CLAY, and MANGANIFEROUS PELAGIC CLAY

- Colors mainly light yellowish brown (10YR 6/4) and very pale brown (10YR 7/3–7/4). Minor colors: dark gray (10YR 4/1), light brown (7.5YR 6/4). Mostly in Sections 3, 6, and 7 are black (10YR 2.5/1), dark gray (10YR 4/1) and grayish brown (10YR 5/2). In Sections 4 and 5 are light greenish gray (5GY 7/1), pale olive (5Y 6/3), and light gray (5Y 1/2).
- Light brown clay, burrowed variegated layers, local Mn-oxide staining. Faint mottling throughout. Rotational shear surfaces every 2–5 cm. Drilling breccia at base.

SMEAR SLIDE SUMMARY (%):

	1, 80	3, 70	5, 104	7, 24
	D	D	D	D
Texture:				
Sand	2	5	5	5
Silt	15	15	15	25
Clay	83	80	80	70
Composition:				
Quartz	1	1	1	1
Feldspar	5	5	4	5
Clay	78	69	58	63
Volcanic glass	–	–	2	–
Diatoms	1	Tr	Tr	1
Radiolarians	15	25	35	30

$CaCO_3$ Bomb (%):
2, 56 = 0.0
3, 61 = 1.0

SITE 543 HOLE CORE 30 CORED INTERVAL 5911.5–5921.0 (mbsl) 284.5–294.0 (mbsf)

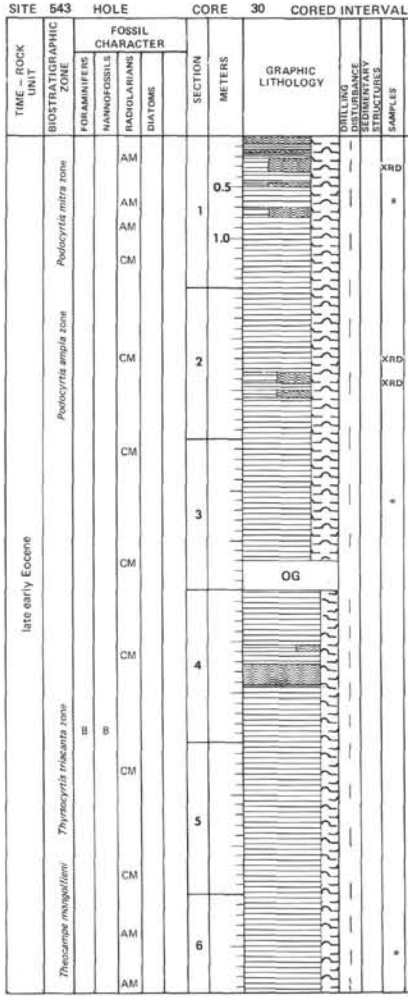

LITHOLOGIC DESCRIPTION

MARLY RADIOLARIAN OOZE, RADIOLARIAN CLAY, and MANGANIFEROUS RADIOLARIAN CLAY

- Colors: mainly very pale brown (10YR 7/4), also grayish brown (10YR 5/2), light brown (7.5YR 6/4) (as burrow fills), reddish yellow (5Y 6/6), dark grayish brown (10YR 4/2), light yellowish brown (2.4Y 6/4) in top 2 sections. Then: mainly pale brown (10YR 6/3) to light yellowish brown (10YR 6/4), with thin layers of brown (6.5YR 5/4) and black (10YR 2.5/1) manganese-oxide stains.
- Ooze and clay, variably stained by Mn-oxides (black).
- The brown layers are non-radiolarian and burrowed.
- Rotational shear surfaces every 3–6 cm.

SMEAR SLIDE SUMMARY (%):

	1, 65	3, 70	6, 60
	D	D	D
Texture:			
Sand	10	20	2
Silt	20	30	8
Clay	70	50	90
Composition:			
Quartz	1	1	Tr
Feldspar	4	4	4
Clay	55	45	76
Radiolarians	40	45	15

$CaCO_3$ Bomb (%):
5, 125 = 0.0
6, 82 = 0.0
6, 60

SITE 543 HOLE CORE 31 CORED INTERVAL 5921.0–5930.5 (mbsl) 294.0–303.5 (mbsf)

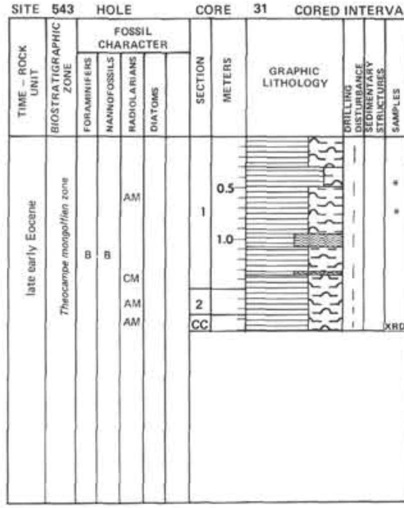

LITHOLOGIC DESCRIPTION

RADIOLARIAN CLAY and BROWN CLAY

- Colors: very pale brown (10YR 7/4) and brown (7.5YR 5/4), with very dark gray (10YR 3/1) and 10YR 4/1).
- Alternating very pale brown radiolarian clays and brown clays. Layers of each typically mottled by the other.
- Patchy Mn-oxide staining. Drilling breccia at very top.

SMEAR SLIDE SUMMARY (%):

	1, 46	1, 75
	M	D
Texture:		
Sand	2	8
Silt	5	32
Clay	93	60
Composition:		
Feldspar	1	Tr
Clay	93	60
Volcanic glass	2	—
Radiolarians	4	40

$CaCO_3$ Bomb (%):
1, 77 = 0.0
2, 8 = 0.0

SITE 543 HOLE CORE 32 CORED INTERVAL 5930.5–5940.0 (mbsl) 303.5–313.0 (mbsf)

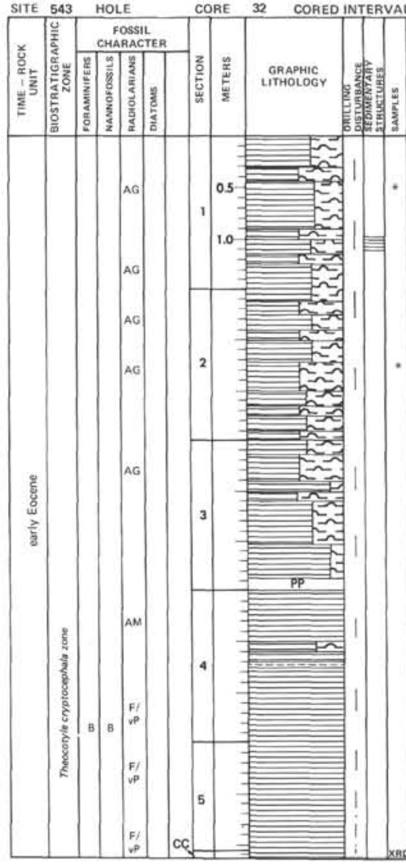

LITHOLOGIC DESCRIPTION

RADIOLARIAN CLAY

- Colors: 2.5YR 7/2; 5YR 4/4, 5/4, 4/3, 5/3, and 5/6; mainly brown 7.5YR 5/4, 6/4, and 5/2; 10YR 6/3, 7/2, 5/4, 6/4, and 6/2). Very minor light gray (5Y 6/1–5Y 7/2), light brownish gray (10YR 6/2) and light greenish gray (5GY 7/1). Variegated radiolarian clay: shades of brown (mainly), pale brown, reddish brown, yellowish red, and yellowish brown (yellow more important towards base). Layers of each color 5–20 cm thick; contacts graditional and intermittently burrowed (planolites type).

SMEAR SLIDE SUMMARY (%):

	1, 50	2, 75
	D	D
Texture:		
Sand	10	8
Silt	30	43
Clay	60	49
Composition:		
Quartz	Tr	1
Clay	60	49
Radiolarians	40	50

$CaCO_3$ Bomb (%):
1, 81 = 0.0
2, 8 = 0.0

SITE 543 HOLE CORE 33 CORED INTERVAL 5940.0–5949.0 (mbsl) 313.0–322.5 (mbsf)

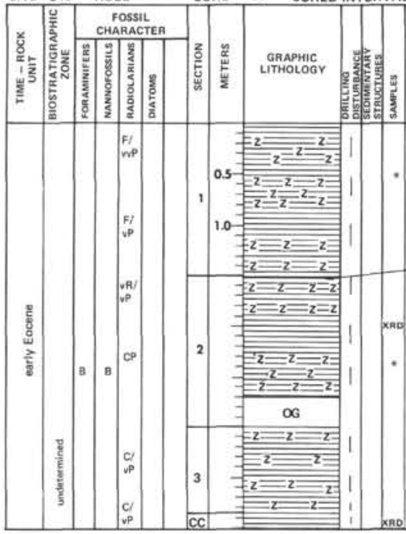

LITHOLOGIC DESCRIPTION

ZEOLITIC PELAGIC CLAY

- Colors: alternating light yellowish brown to pale brown (10YR 6/4–6/3) and yellowish red (5YR 4/6–5/6).
- All zeolitic, light yellowish brown more so.
- Firm clay constitutes drilling biscuits, softer remolded clay constitutes matrix. Some biscuits preserve laminations and bioturbation. Surface disrupted by piano wire.

SMEAR SLIDE SUMMARY (%):

	1, 50	2, 90
	D	M
Texture:		
Sand	3	Tr
Silt	5	10
Clay	92	90
Composition:		
Feldspar	Tr	–
Heavy minerals	Tr	Tr
Clay	92	90
Volcanic glass	1	–
Zeolite	4	10
Radiolarians	2	Tr

$CaCO_3$ Bomb (%):
1, 148 = 0.0

SITE 543 HOLE CORE 34 CORED INTERVAL 5949.5–5959.0 (mbsl) 322.5–332.0 (mbsf)

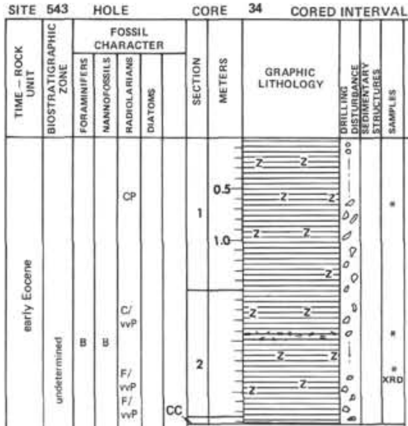

LITHOLOGIC DESCRIPTION

PELAGIC CLAYSTONE and ZEOLITIC PELAGIC CLAYSTONE

- Colors: yellowish red (5YR 5/5), reddish brown (5YR 5/4 and 4/4), pale olive (5Y 6/3), yellowish brown (5YR 5/6), (Core-Catcher) reddish yellow (7.5YR 6/6), (ash Section 2, 43 cm) greenish gray (5GY 6/1). Chunks of red/light brown (less/more zeolitic) claystone in a matrix of smaller brecciated pieces and mush.
- Chunks preserve lamination and bioturbation. Thin altered ash at Section 2, 43 cm.

SMEAR SLIDE SUMMARY (%):

	1, 67	2, 44	2, 80
	D	M	D
Texture:			
Sand	–	2	–
Silt	3	10	10
Clay	97	88	90
Composition:			
Quartz	Tr	1	–
Feldspar	–	5	Tr
Heavy minerals	–	–	Tr
Clay	98	81	90
Volcanic glass	–	3	–
Zeolite	2	10	10
Radiolarians	–	Tr	–
Fish remains	Tr	–	Tr
Fe-oxides	Tr	–	Tr

SITE 543 HOLE A CORE 1 CORED INTERVAL 5627.0–5637.0 (mbsl) 0.0–10.0 (mbsf)

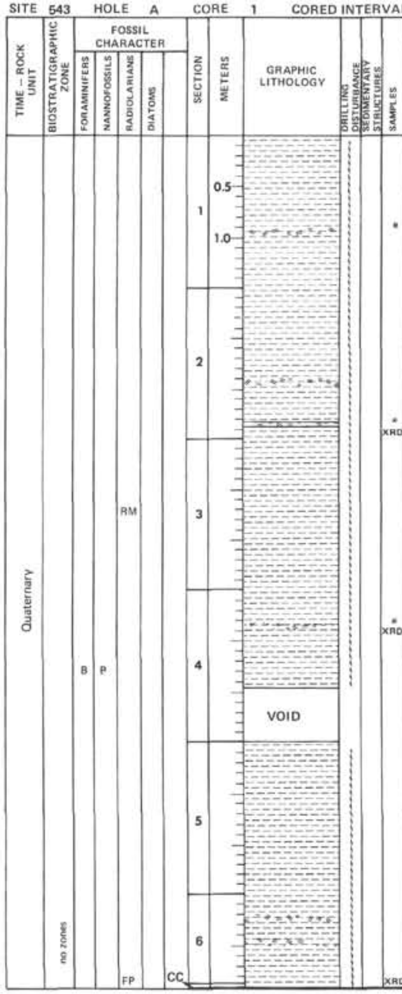

LITHOLOGIC DESCRIPTION

CLAY AND VITRIC CLAY

- Colors: brown (10YR 5/3), patches of yellowish brown (10YR 5/4), dark grayish brown (10YR 4/2 and 4/1), grayish brown (10YR 5/2) and light yellowish brown (10YR 6/4). Ash at Section 2, 135 cm is light brownish gray (10YR 6/2).
- Thoroughly swirled brown clay, with yellower and grayer ashy intervals and streaks.

SMEAR SLIDE SUMMARY (%):

	1, 90	2, 135	4, 30
	D	M	M
Texture:			
Sand	2	40	3
Silt	3	55	25
Clay	95	5	72
Composition:			
Feldspar	2	40	1
Heavy minerals	Tr	2	Tr
Clay	95	5	72
Volcanic glass	3	40	2
Radiolarians	Tr	–	Tr
Ferromagnesians	–	13	–
Pyrolusite	–	–	25

SITE 543 HOLE A CORE 2 CORED INTERVAL 5959.0–5968.5 (mbsl) 332.0–341.5 (mbsf)

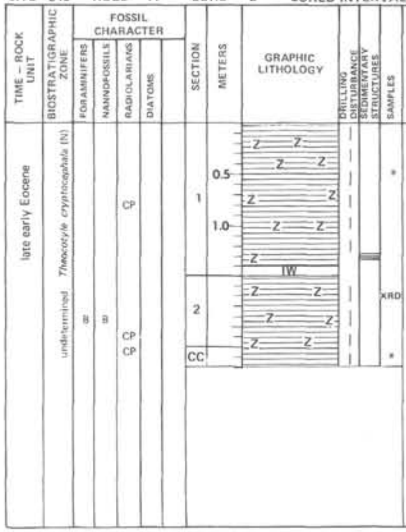

LITHOLOGIC DESCRIPTION

ZEOLITIC PELAGIC CLAY AND CLAYSTONE

- Colors: thinly alternating light yellowish brown (10YR 6/4) and yellowish red (5YR 4/6). Thin layers of greenish gray (5GY 6/1) at Section 1, 50 and 86 cm, Section 2, 50 and 61 cm, and Core-Catcher, 16 cm.
- Zeolitic clay and claystone. Firm and hard chunks in a highly sheared matrix. Rotational shear surfaces every 2 cm from Section 1, 60–140 cm.

SMEAR SLIDE SUMMARY (%):

	1, 50	CC, 19
	D	D
Texture:		
Silt	10	10
Clay	90	90
Composition:		
Quartz	1	1
Feldspar	5	6
Heavy minerals	Tr	Tr
Clay	84	84
Volcanic glass	–	1
Zeolite	10	8

$CaCO_3$ Bomb (%):
2, 52 = 0.0
CC = 0.0

SITE 543 HOLE A CORE 3 CORED INTERVAL 5968.5–5978.0 (mbsl) 341.5–351.0 (mbsf)

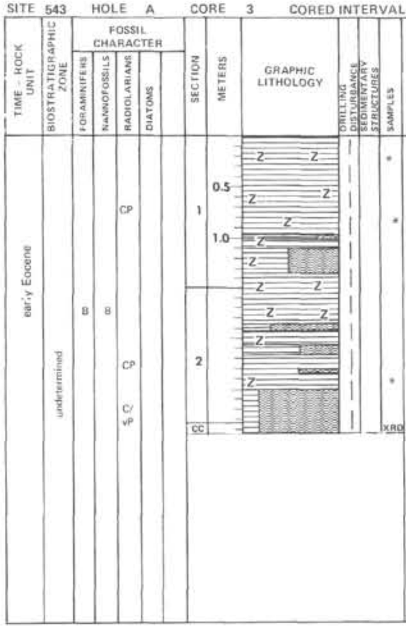

LITHOLOGIC DESCRIPTION

ZEOLITIC PELAGIC CLAY AND MANGANIFEROUS PELAGIC CLAY

- Colors: mainly yellowish brown (10YR 5/4), dark yellowish brown (10YR 4/4). Subordinately dark gray to very dark grayish brown (10YR 3/1) (Mn-stain); light greenish gray (5G 7/1) near top.
- Firm zeolitic pelagic clay with sporadic manganese oxide staining.
- Rotational shear surfaces every 2–5 cm.
- In uppermost 40 cm, coherent lumps are separated by cm-thick shear zones.
- Dark Mn-staining occurs as thin to very thin wavy layers except at base of Section 2 where 33 cm of clay is Mn-stained with large lighter-colored oval patches.

SMEAR SLIDE SUMMARY (%):

	1, 25	1, 83	2, 90
	D	D	D
Texture:			
Silt	8	10	15
Clay	92	90	85
Composition:			
Quartz	1	1	1
Feldspar	6	5	6
Heavy minerals	–	Tr	–
Clay	84	84	88
Volcanic glass	1	Tr	Tr
Zeolite	8	10	5

$CaCO_3$ Bomb (%):
1, 148 = 0.0
2, 101 = 0.0

SITE 543 HOLE A CORE 4 CORED INTERVAL 5978.0–5987.5 (mbsl) 351.0–360.5 (mbsf)

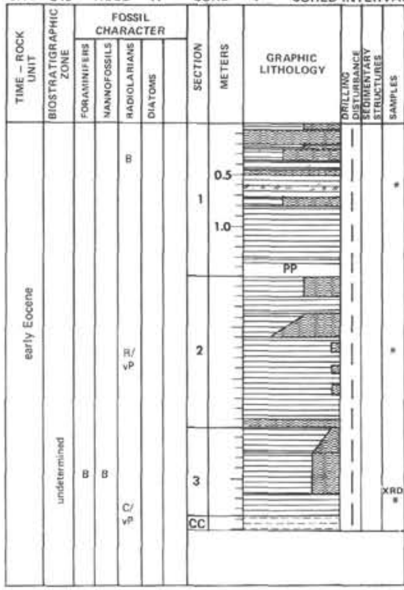

LITHOLOGIC DESCRIPTION

PELAGIC CLAY AND MANGANIFEROUS PELAGIC CLAY

- Colors: mainly yellowish brown (10YR 5/4), minor dark brown (10YR 4/3) increases downwards. Very dark grayish brown (10YR 3/2) (Mn-stained). One bit of light greenish gray (5GY 7/1) at Section 1, 60 cm.
- Claystone, sporadically Mn-oxide stained.
- Rotational shear surfaces every 3–5 cm.
- Mn-staining occurs as thin to medium parrallel-sided or irregular layers.
- Darker layers may contain lighter oval patches.

SMEAR SLIDE SUMMARY (%):

	1, 62	2, 70	3, 75
	M	D	D
Texture:			
Sand	–	1	1
Silt	8	7	5
Clay	92	92	94
Composition:			
Quartz	Tr	Tr	Tr
Feldspar	5	6	6
Heavy minerals	1	–	–
Clay	87	92	90
Volcanic glass	5	2	4
Zeolite	2	Tr	Tr

$CaCO_3$ Bomb (%):
1, 6 = 0.0
3, 36 = 0.0

SITE 543 HOLE A CORE 5 CORED INTERVAL 5987.5–5997.0 (mbsl) 360.5–370.0 (mbsf)

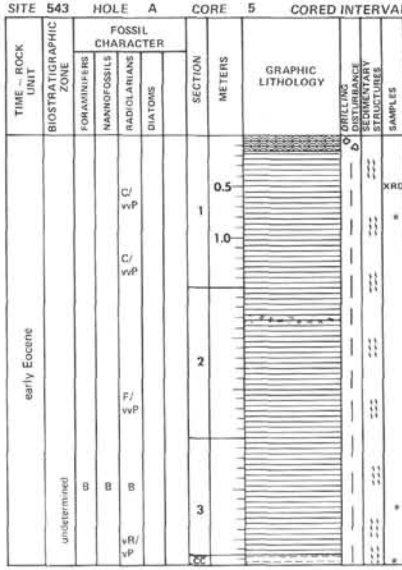

LITHOLOGIC DESCRIPTION

PELAGIC CLAYSTONE

- Colors: alternating reddish brown (2.5YR 4/4) and brown (7.5YR 4/4).
- Core clearly becomes redder downwards.
- Few patches and one thin bed of light greenish gray (5GY 7/1).
- Claystone, burrowed, rotational shear surfaces every 2–5 cm. Breccia at very top of Mn-stained cavings from further up hole.

SMEAR SLIDE SUMMARY (%):

	1, 80	3, 70	CC
	D	D	D
Texture:			
Sand	–	Tr	–
Silt	5	8	5
Clay	95	92	95
Composition:			
Quartz	Tr	Tr	Tr
Feldspar	4	4	5
Heavy minerals	Tr	Tr	–
Clay	94	94	93
Volcanic glass	2	2	2

$CaCO_3$ Bomb (%):
1, 84 = 0.0
2, 58 = 0.0

SITE 543 HOLE A CORE 6 CORED INTERVAL 5997.0–6006.5 (mbsl) 370.0–379.5 (mbsf)

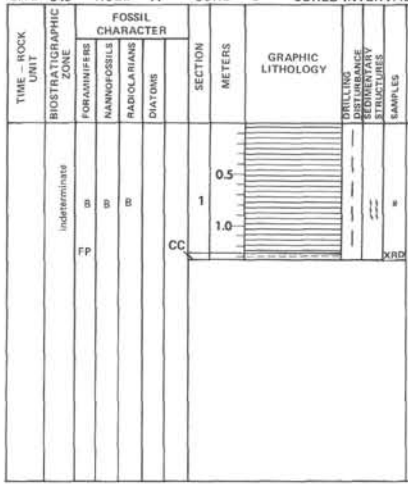

LITHOLOGIC DESCRIPTION

PELAGIC CLAY
- Uniform reddish brown (2.5YR 4/5) clay.
- Rotational shear surfaces every 3–5 cm.
- Core above is lower Eocene, core below is upper Cretaceous.

SMEAR SLIDE SUMMARY (%):

	1, 80
	D
Texture:	
Silt	9
Clay	91
Composition:	
Quartz	2
Feldspar	5
Heavy minerals	1
Clay	89
Volcanic glass	3
Calc. nannofossils	Tr

$CaCO_3$ Bomb (%):
1, 49 = 0.0

SITE 543 HOLE A CORE 7 CORED INTERVAL 6006.5–6016.0 (mbsl) 379.5–389.0 (mbsf)

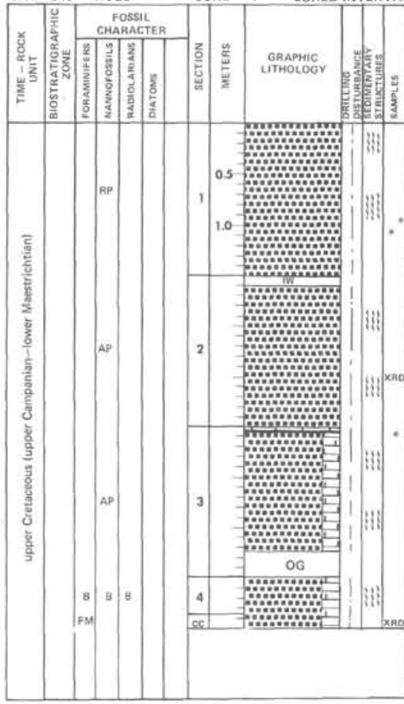

LITHOLOGIC DESCRIPTION

FERRUGINOUS MUDSTONE, CALCAREOUS FERRUGINOUS MUDSTONE, and MINOR CHALK
- Color mainly dark brown to dark reddish brown (7.5YR 3/2–5YR 3/3). Minor irregular patches and laminations of dark reddish brown (2.5YR 3/4) and reddish brown (5YR 4/3, 4/4), and brown (7.5YR 5/4); also light brown (5YR 5/6), the latter nannofossil-rich.
- Bioturbated, ferruginous, slightly dolomitic (from XRD) locally calcareous mudstone.
- Pancake shaped fragments embedded in a brecciated sheared matrix. Larger fragments preserve burrows (planolites, few zoophycus, tiny chondrites). Some fragments thinly parallel laminated.
- Burrow fills lighter brown than surrounding sediment.
- Top of Section 3 has 5 cm of bluish white (5B 9/1) chalk also burrowed. Gray (5GY 5/1) reduction zone immediately below, about 1 cm thick. Cuts across burrows in ferruginous clay. Whole core cut by rotational shear surfaces every 2–4 cm.

SMEAR SLIDE SUMMARY (%):

	1, 96	1, 107	3, 5
	D	M	M
Texture:			
Sand	–	Tr	–
Silt	5	6	Tr
Clay	95	94	100
Composition:			
Feldspar	5	6	–
Heavy minerals	–	Tr	–
Clay	95	94	15
Foraminifers	–	–	Tr
Calc. nannofossils	–	–	85

$CaCO_3$ Bomb (%):
1, 96 = 0.0
3, 100 = 24.4

SITE 543 HOLE A CORE 8 CORED INTERVAL 6016.0–6025.5 (mbsl) 389.0–398.5 (mbsf)

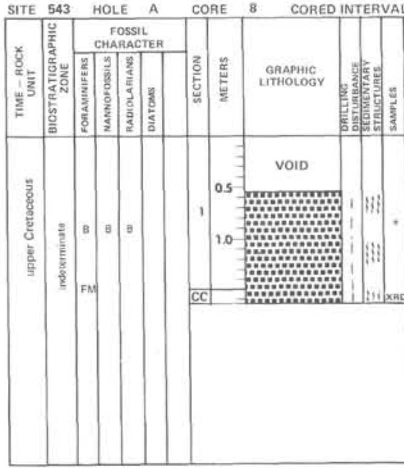

LITHOLOGIC DESCRIPTION

FERRUGINOUS CLAYSTONE
- Color predominantly reddish brown (5YR 4/3) with minor mottling of lighter brown (5YR 5/3).
- Ferruginous slightly dolomitic bioturbated claystone.
- Has drilling biscuits and rotational shear surfaces.
- Slightly calcareous.

SMEAR SLIDE SUMMARY (%):

	1, 84
	D
Texture:	
Silt	6
Clay	94
Composition:	
Feldspar	2
Clay	94
Dolomite	4

$CaCO_3$ Bomb (%):
1, 17 = 4.9
1, 87 = 5.4

SITE 543 HOLE A CORE 9 CORED INTERVAL 6025.5–6035.0 (mbsl) 398.5–408.0 (mbsf)

TIME – ROCK UNIT	BIOSTRATIGRAPHIC ZONE	FORAMINIFERS	NANNOFOSSILS	RADIOLARIANS	DIATOMS	SECTION	METERS	GRAPHIC LITHOLOGY	DRILLING DISTURBANCE	SEDIMENTARY STRUCTURES	SAMPLES
upper Cretaceous (middle–upper Campanian)	middle–upper Campanian	CM	CP	B		1	0.5	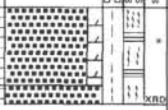			*
						CC					XRD

LITHOLOGIC DESCRIPTION

DOLOMITIC FERRUGINOUS CLAYSTONE

- Color dominantly reddish brown (5YR 4/3). Also reddish brown (5YR 4/4) and dark brown (7.5YR 3/2).
- Laminated, mottled, ferruginous, dolomitic claystone.
- Lighter and darker brown laminae have slightly wavy, burrowed margins. Burrowing decreases downwards and drilling disturbance increases downwards.

SMEAR SLIDE SUMMARY (%):

	1, 33
	D
Texture:	
Silt	2
Clay	98
Composition:	
Heavy minerals	Tr
Clay	90
Dolomite	8

$CaCO_3$ Bomb (%):
1, 50 = 28.8
1, 6 = 17.6

SITE 543 HOLE A CORE 10 CORED INTERVAL 6035.0–6044.5 (mbsl) 408.0–417.5 (mbsf)

TIME – ROCK UNIT	BIOSTRATIGRAPHIC ZONE	FORAMINIFERS	NANNOFOSSILS	RADIOLARIANS	DIATOMS	SECTION	METERS	GRAPHIC LITHOLOGY	DRILLING DISTURBANCE	SEDIMENTARY STRUCTURES	SAMPLES
upper Cretaceous (lower Campanian)	lower Campanian		CP	B		1		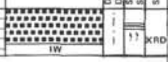			XRD
			CM	R/ vP				IW			

LITHOLOGIC DESCRIPTION

FERRUGINOUS NANNOFOSSIL CLAY

- Sediment 0–37 cm. IW sample 10 cm long was taken from below this but basalts were inadvertently placed in this interval during core preparation.
- Colors: reddish brown (5YR 4/4), yellowish red (5YR 5/4), and dark reddish brown (2.5YR 3/4).
- Horizontally laminated, burrow-mottled, ferruginous nannofossil clay. Burrows mainly planolites-like; few vertical burrows.

$CaCO_3$ Bomb (%):
1, 28 = 53.2

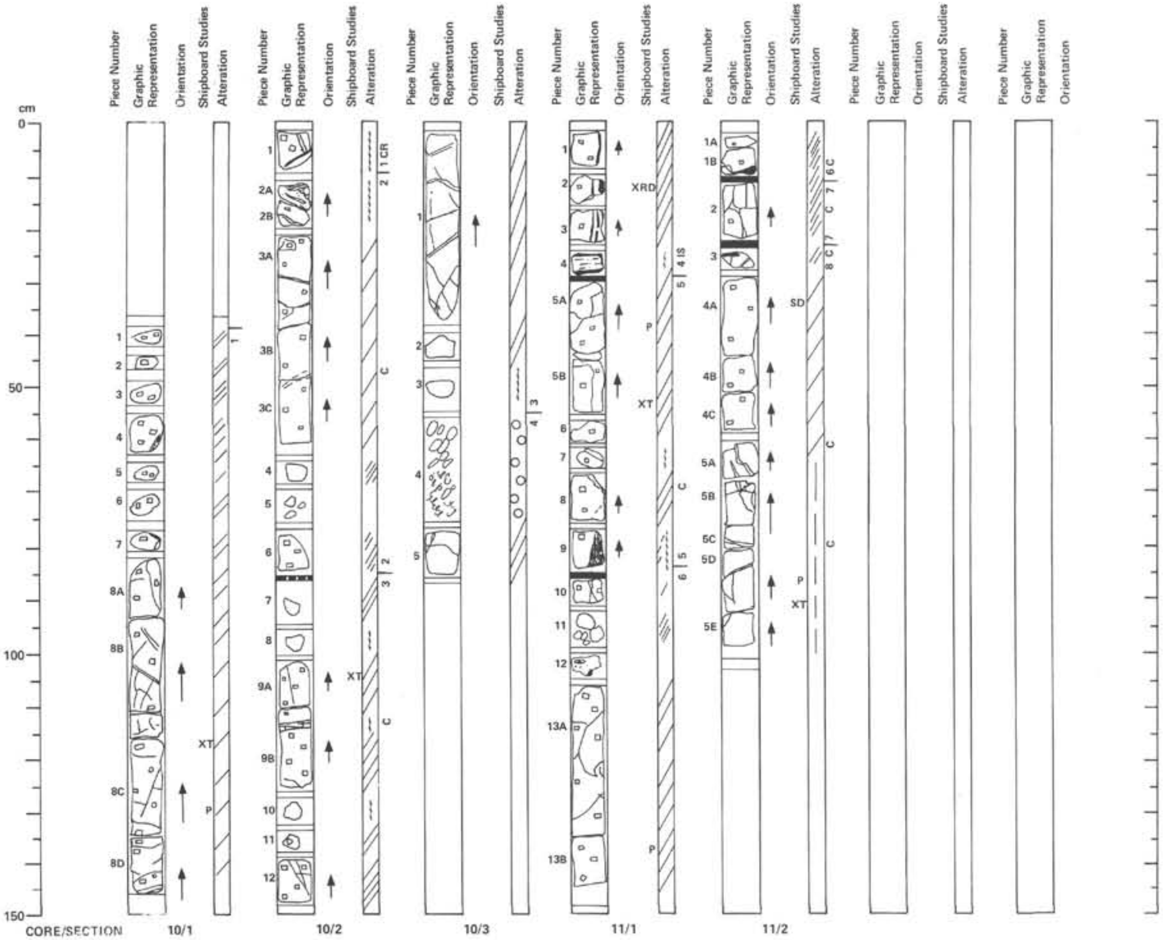

78A-543A-10

6048.0–6054.5 mbsl 411.0–417.5 mbsf

PLAGIOCLASE-OLIVINE MODERATELY PHYRIC BASALT

Four distinct cooling unit boundaries are present in this pillow sequence, as indicated by the numbers alongside the alteration columns. The basalts are moderately to extensively altered oxidatively to dark brown (10YR 4/3) and dark grayish brown (10YR 4/2), with alteration especially intense at the top of the core. There are abundant calcite veins in fractures in much of the core. The rocks have 5–10% plagioclase phenocrysts as 1) large irregular glomerocrysts up to 5 mm, 2) small glomerocrysts with tabular crystals, and 3) individual tabular or rounded phenocrysts. Olivine is pervasively altered to a light bluish green mineral (saponite?) or to reddish iron hydroxides and clays. Crack-filling limestones occurs in Section 2, piece 9B.

Thin Section Descriptions

78A-543A-10-1, 115–118 cm, piece 8C: Pillow interior. Sample has ~10% plagioclase phenocrysts and <1% altered olivine phenocrysts set in an altered microlitic groundmass. Some plagioclases are complexly zoned, and have spherulitic inclusions. Others are tabular or clumped into glomercrystt. Most are partially replaced with calcite, which forms a vein in part of the section, and fills vesicles. In the groundmass, clays replace pyroxenes and glass(?), and iron hydroxides replace titanomagnetite.

78A-534A-10-2, 112–115 cm, piece 9A: Pillow interior. The section has ~10% plagioclase phenocrysts and glomerocrysts, and <1% altered olivine phenocrysts, plus one grain of chromian spinel. It is intensely altered to reddish iron hydroxides in the groundmass, and is riddled with calcite. The phenocrysts have abundant altered or spherulitic formerly glassy inclusions, some are rounded, and many have skeletal margins. They are partially replaced by calcite and most are transformed to K-feldspar. The groundmass is microlitic to coarsely fan spherulitic in texture, but is mostly altered to clays and iron hydroxides.

78A-543A-11

6054.5–6057.0 mbsl 417.5–420.0 mbsf

ALTERED PLAGIOCLASE-OLIVINE MODERATELY PHYRIC TO SPARSELY PHYRIC BASALT

Portions of pillow cooling units 4–8 are in this core (right margin of alteration column), marked by distinctive altered glass. Glass occurs on the edge of pillow 4 and on both sides of an interpillow limestone (11-1, piece 4). Phenocrysts are mainly plagioclase, ranging up to 5% and diminishing in abundance downcore. Alteration is moderate to intense with rare olivine phenocrysts altered to clays and iron hydroxides. Glass is replaced by bluish clays. Calcite veins are prominent in a number of pieces.

Thin Section Descriptions

78A-543A-11-1, 50–52 cm, piece 5B: Pillow interior. The section has ~5% plagioclase phenocrysts and glomerocrysts, plus 2–3 altered olivines, and one chromian spinel with round, altered, glass inclusions. The groundmass is microlitic to somewhat spherulitic, and is partially oxidatively altered to clays and iron hydroxides. There is a calcite vein on one edge, and calcite in some vesicles. The vein was first lined with pale green clays. Plagioclase phenocrysts are partially replaced by clays and K-feldspar, especially near the vein.

78A-543A-11-2, 89–91 cm, piece 5D: Pillow interior. The section has only 1–2% small plagioclase phenocrysts set in a microlitic to spherulitic groundmass. Crystal size in the groundmass is smaller than in sections above. Alteration is pervasive, but not as intense as above with clays and iron hydroxides abundant in the groundmass and filling rare vesicles. Clays also largely replace the plagioclase phenocrysts and many microlites. Only one crystal (olivine?) is replaced by calcite.

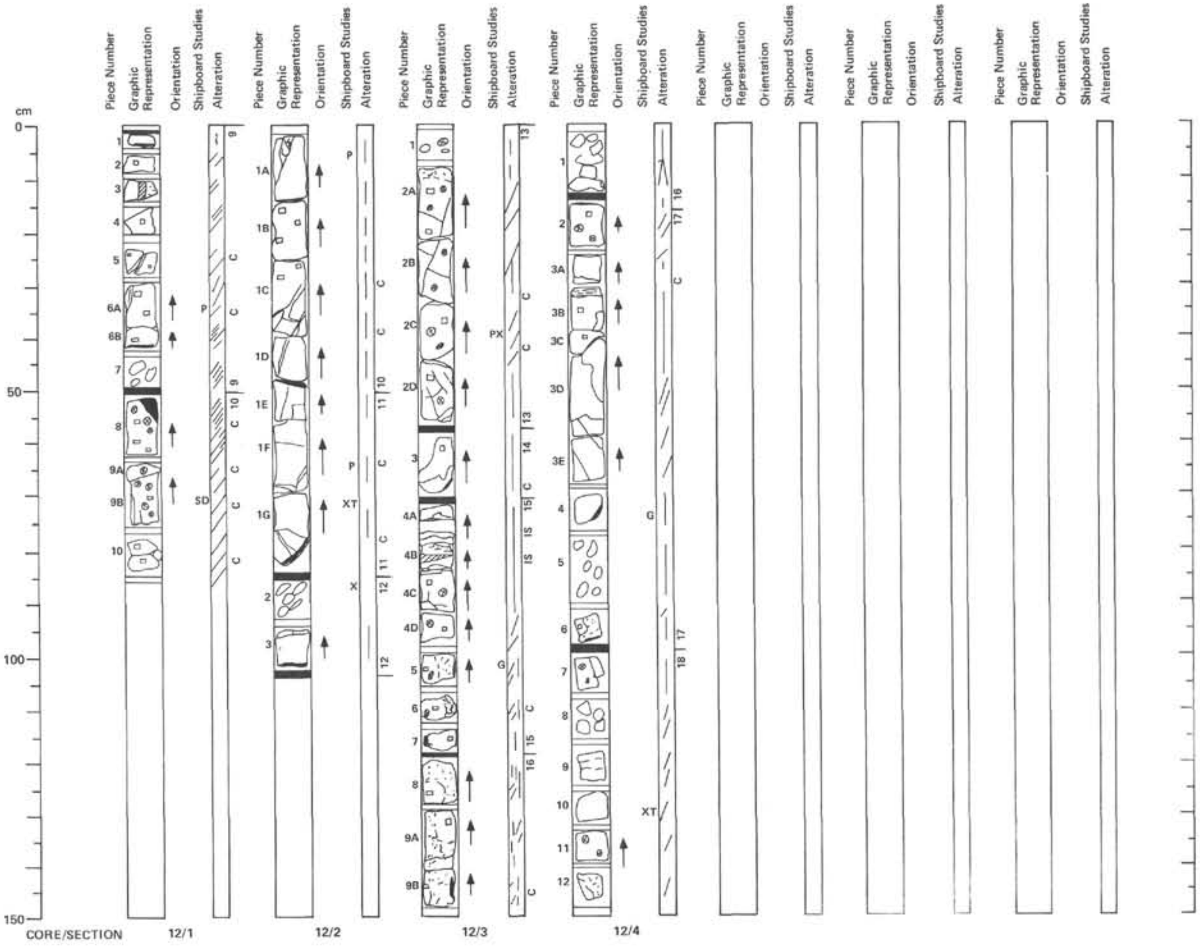

78A-543A-12

6057.0–6064.0 mbsl

420.0–427.0 mbsf

SPARSELY PLAGIOCLASE-OLIVINE PHYRIC BASALT

Pillow cooling units 9–18 were recovered in this core, along with interpillow mudstone and fracture-filling limestone in Sections 2 and 3 respectively. The pillow margins are defined by altered glass. Near several pillow margins are large, well-developed shperulites. The rocks are moderately to intensely altered, with calcite veins prominent in Sections 1 and 3, and a beautiful vein in Section 4, pieces 3A and B. Clay minerals are green and blue, and rare olivines are altered to iron hydroxides.

Thin Section Descriptions

78A-543A-12-2, 70–72 cm, piece 1G: Pillow interior. The section has < 1% tiny (< 1 mm) tabular plagioclase microphenocrysts in a microlitic, altered, groundmass. Crystals are aligned, and the piece of rock has an alteration rind. The basalt also had small euhedral olivines (< 0.5%) now altered to reddish iron hydroxides. The groundmass is partially replaced by green and orange clays, and iron hydroxides, which form discrete patches up to 0.5 mm across. The section has a thin crack lined with iron hydroxides.

78A-543A-12-4, 128–133 cm, piece 10: Pillow interior. The section contains 3–4% plagioclase phenocrysts, lesser altered olivine phenocrysts, and several chrome spinels. The groundmass consists of sprays of microlitic plagioclase separated by zones of brownish fine spherulitic material. The feldspars are tabular to subhedral, many having altered or devitrified glass inclusions. Most phenocrysts are at least partially altered to clays. Green clays replace a tabular ferromagnesian phenocrysts (CPX?) and fill a number of vesicles. Olivines are replaced by pale yellow clays. The groundmass textures are distinctively different from those in Core 11 and in Core 12, Section 2, piece 1G, indicating that this is a third petrographic and probably chemical type.

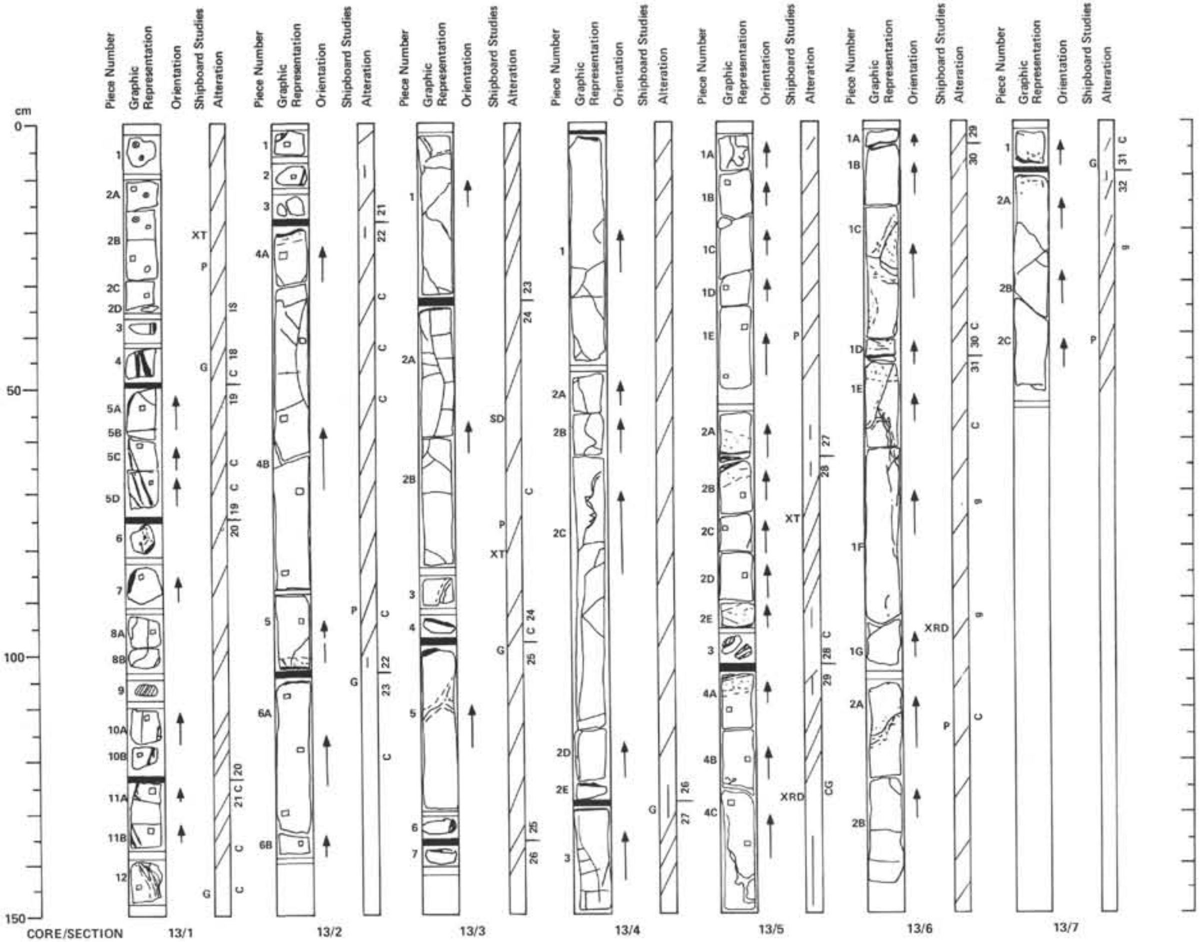

78A-543A-13

6064.0–6073.0 mbsl

427.0–436.0 mbsf

SPARSELY-MODERATELY PLAGIOCLASE-OLIVINE PHYRIC BASALT

Pillow cooling units 18–32 are represented by the core (see right margin of alteration column for sequence). Recovery was extremely high, hence portions of every cooling unit, and all of most of them, must have been retrieved. The core has well recovered curved portions of glassy pillow rinds, plus interpillow sediments in several pieces. There are prominent calcite veins and interpillow fillings, the latter preserving fresh glass. Alteration seems a mix of oxidative and non-oxidative, with iron hydroxides and blue green clays near glass and in large fractures, and pale green clays in small fractures and pillow interiors. Section 6 has brownish altered zones next to fractures.

Thin Section Descriptions

78A-543A-13-1, 18–20 cm, piece 2B: Pillow interior. The section has ~4% plagioclase phenocrysts and lesser olivines set in a groundmass of plumose plagioclase spherulites and microlites. The olivines are altered to clays, and the groundmass is altered to iron hydroxides concentrated in slightly more crystalline zones. The plagioclase phenocrysts are tabular and euhedral, sometimes forming clumps, and many have corners with dendritic projections into the groundmass. Most are replaced by clays.

78A-543A-13-3, 79–82 cm, piece 2B: Pillow interior. The section has <1% plagioclase microphenocrysts mainly tabular in form. The groundmass is microlitic, consisting of small plagioclase needles and tight bundes of plagioclase-clinopyroxene sheafs, with remaining islets dotted with titanomagnetite. The groundmass texture is distinctly different from that of immediately adjacent samples above, being as crystalline or moreso, but with small crystals. Alteration is restricted to a narrow vein of green clays and Mn-oxides(?).

78A-543A-13-5, 72–75 cm, piece 2C: Pillow interior. The section has ~5% plagioclase and altered olivine phenocrysts set in a sheaf spherulite matrix. The plagioclase phenocrysts occur as glomerocrysts with altered olivine, as individual anhedral crystals with skeletal interiors, and as either single crystals or loose clumps of tabular euhedra having corners with dendritic projections. Green clays and iron hydroxides line a narrow vein, fill vesicles, and replace olivines, with the green clay generally filling interiors of these (formed after the iron hydroxides). There are more large elongate microlites and tabular microphenocrysts in this than in the previous sample.

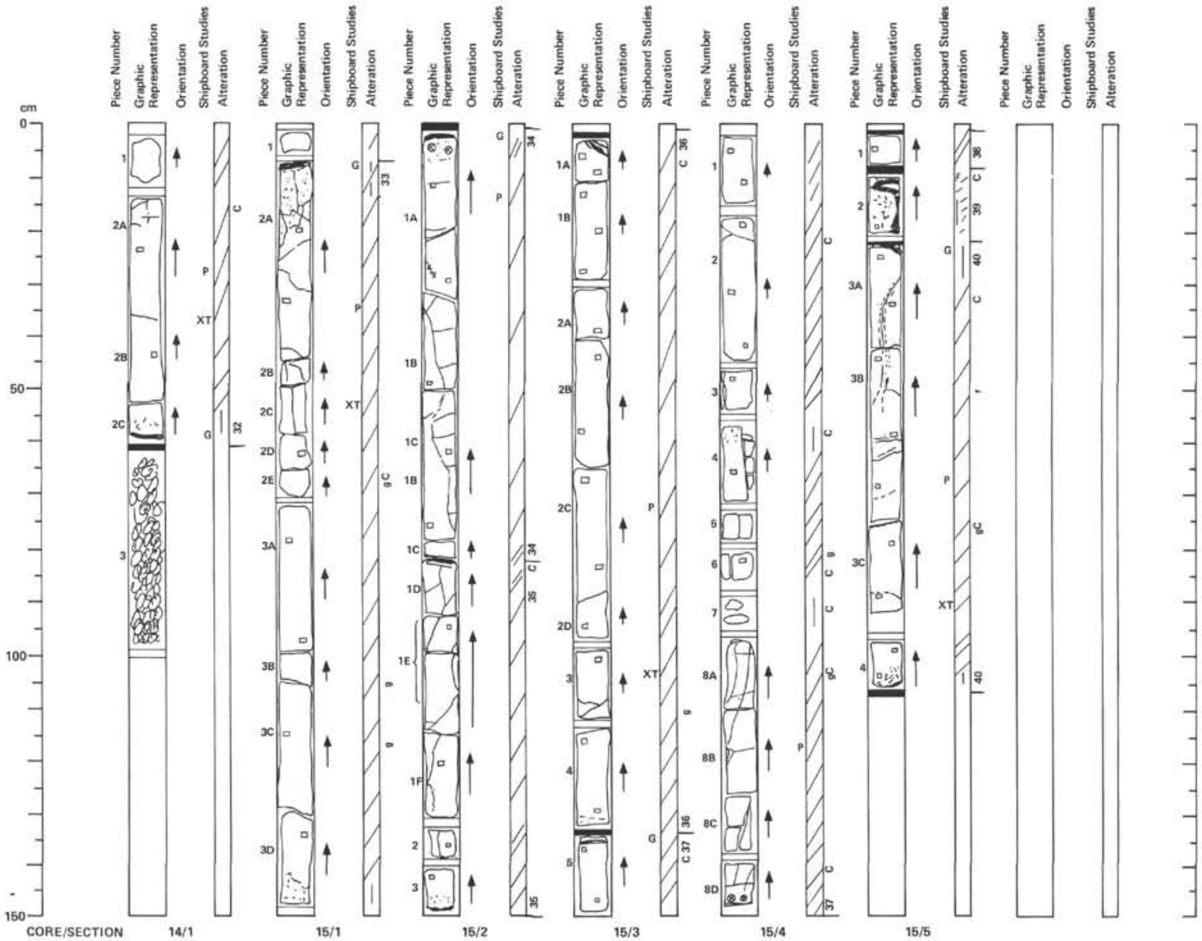

78A-543A-14

6073.0–6075.0 mbsl | 436.0–438.0 mbsf

SPARSELY PLAGIOCLASE-OLIVINE PHYRIC BASALT

This short core contains the remainder of pillow cooling unit 32 recovered in Core 13. There is glass at the bottom of piece 2C with a zone of oxidative alteration near the glass. Drilling breccia including basalt chips and brown claystone is at the base of the core.

Thin Section Description

78A-543A-14-1, 37–40 cm, piece 2B: Pillow interior. The section contains about 5% plagioclase phenocrysts and microphenocrysts, and rare altered olivines. The plagioclases occur as glomerocrysts of large anhedral to subhedral crystals, one of them including olivine, as large single tabular crystals, as single rounded crystals (resorbed xenocrysts), as single elongate euhedra, and as loose aggregates of elongate euhedra. The groundmass is fairly coarse grained, with plagioclase laths surrounded by anhedral clinopyroxene, but giving way to patches of microlites and spherulites with abundant titanomagnetites. Alteration occurs along one edge, where the altered olivines are replaced by clays and iron hydroxide, the groundmass is stained red, and a remnant of a vein lined with iron hydroxides can be seen.

78A-543A-15

6075.0–6082.0 mbsl | 438.0–445.0 mbsf

SPARSELY-MODERATELY PLAGIOCLASE OLIVINE PHYRIC BASALT

The core includes pillow units 33–40 (right margin of alteration column) with up to 5% plagioclase phenocrysts and rare altered olivine phenocrysts, and, in one or two pieces, green clinopyroxene phenocrysts. Alteration is moderate with calcite veins, fractures filled with green clays, and reddish oxidized zones next to some fractures and pillow margins. Calcite fills interpillow voids, thus preserving glass. In Section 5, cooling unit 39 is a confluence of two pillows with the irregular glass margin recovered intact.

Thin Section Descriptions

78A-543A-15-1, 49–51 cm, piece 2C: Pillow interior. The section has 2–3% plagioclase phenocrysts, including one large euhedral 5 mm megacryst. There is one plagioclase-olivine glomerocryst, with the olivine altered to clays and iron hydroxides. The groundmass consists of skeletal plagioclase microlites in a matrix of spherulitic clinopyroxene, titanomagnetite and altered glass. Alteration minerals include patches of green and blue-green clays, and iron hydroxides, distributed pervasively in the groundmass.

78A-543A-15-3, 100–102 cm, piece 3: Pillow interior. The sample contains a number of large (2–3 mm) plagioclase phenocrysts and glomerocrysts, some having devitrified glass inclusions, lesser altered olivine phenocrysts, and one large clinopyroxene megacryst. Most of the plagioclase phenocrysts are tabular, grouped in clusters, or anhedral. The cpx megacryst surrounds smaller plagioclase crystals. The groundmass consists of microlites of plagioclase, irregular, near-spherulitic sprays of clinopyroxene, with dark islands of altered glass and skeletal titanomagnetite in between. Olivines and portions of the groundmass are replaced by pale brown or dark brown clays.

78A-543A-15-5, 90–92 cm, piece 3C: Pillow interior. The section contains ~5% plagioclase phenocrysts and glomerocrysts, with lesser altered olivine phenocrysts (one containing two chromian spinels) and several clinopyroxene phenocrysts or portions of glomercrysts. The plagioclase phenocrysts include megacrysts with devitrified glass inclusions and tabular crystals forming loose clumps or individual crystals. The clinopyroxene crystals are somewhat rounded. The groundmass is similar to that of Core 15, Section 3, piece 3 except it is more altered to brown clays, and is traversed by 3 veins, one earlier formed and filled with brown clays, two later formed and filled with calcite.

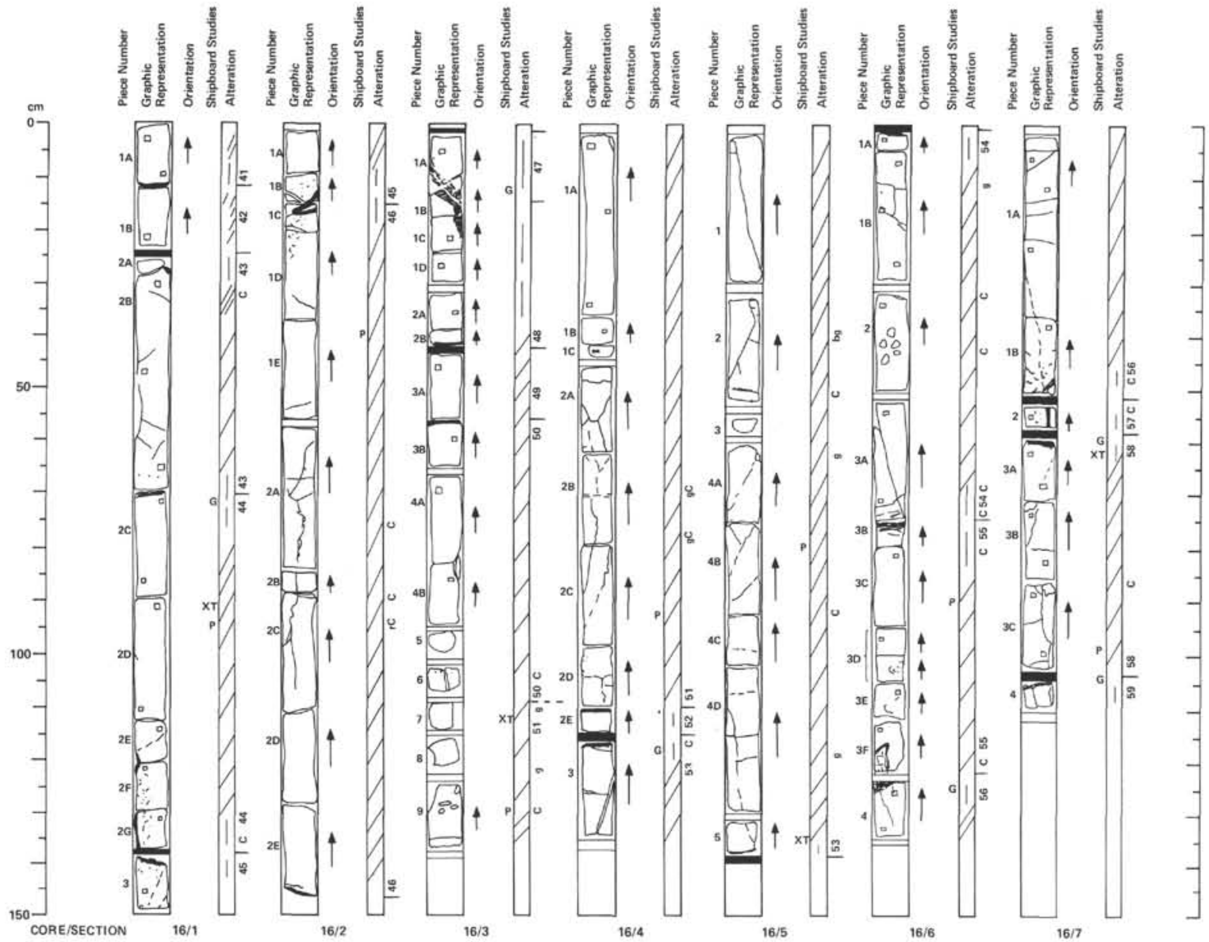

78A-543A-16

6082.0–6092.0 mbsl

445.0–455.0 mbsf

SPARSELY PLAGIOCLASE-OLIVINE PHYRIC BASALT

Pillow cooling units 41–59 were recovered in this core (numbers at right margin of alteration column). Plagioclase phenocrysts form up to 5% of the rock and there are rare, altered, olivine phenocrysts. The contact between pillow cooling units 45 and 46 was recovered intact. Alteration is moderate, with brownish zones next to glass, and fractures lined with calcite, green clays, and iron hydroxides. There is a groundmass textural contrast in Section 3, suggesting contrasting chemical types (between pieces 6 and 7). Calcite preserves glass at pillow margins.

Thin Section Descriptions

78A-543A-16-1, 89–92 cm, piece 2D: Pillow interior. The section contains ~3% plagioclase phenocrysts and glomerocrysts, with rare altered olivine phenocrysts and portions of glomerocrysts. Plagioclase phenocrysts may contain devitrified glass inclusions and form crystals up to 3 mm long. Most, however are tabular, euhedral, and elongate. The groundmass consists of elongate skeletal plagioclase microlites separated by a fine grained mesostasis of spherulitic clinopyroxene, titanomagnetite, and altered glass, dark brown in color. Rare vesicles are filled with green and/or brown clays, and calcite fills alteration voids in olivines. A calcite vein crosses one corner of the section, and the basalt is more altered near it.

78A-543A-16-3, 108–111 cm, piece 7: Pillow interior. The section has 2–3% large plagioclase megacrysts with 1–2% additional elongate, tabular phenocrysts. There are also a few altered olivine phenocrysts. The plagioclase megacrysts have devitrified glass inclusions. The groundmass has about 20% very elongate skeletal plagioclase microlites, with the remainder either intersecting sheaf spherulites, or more crystalline sprays of augite between which occur altered glass and titanomagnetite. Olivines are replaced by brown or vivid green clays. Pale brown and pale green clays also fill or partly fill vesicles in concentric layers. One vesicle also has calcite.

78A-543A-16-7, 60–64 cm, piece 3A: Pillow rim. The section has a 1 cm glassy edge and successive more crystalline spherulite zones away from the glass. There are several large plagioclase megacrysts and glomerocrysts, plus scattered tabular phenocrysts. One megacryst in the glass is riddled with glass inclusions. A glomerocryst near the glass has had olivine almost entirely altered to clays, and plagioclase to zeolite, with a single large chromian spinel still preserved. Some fresh, small, olivines and clinopyroxenes are still retained in the glass, and there is one plagioclase-clinopyroxene glomerocryst. A few plagioclases are beautifully rounded. Alteration is mainly oxidation of spherulitic zones, which are dark reddish brown as a result, and formation of clay-zeolite veins in the glass. Vesicles in the spherulitic zones are filled with calcite.

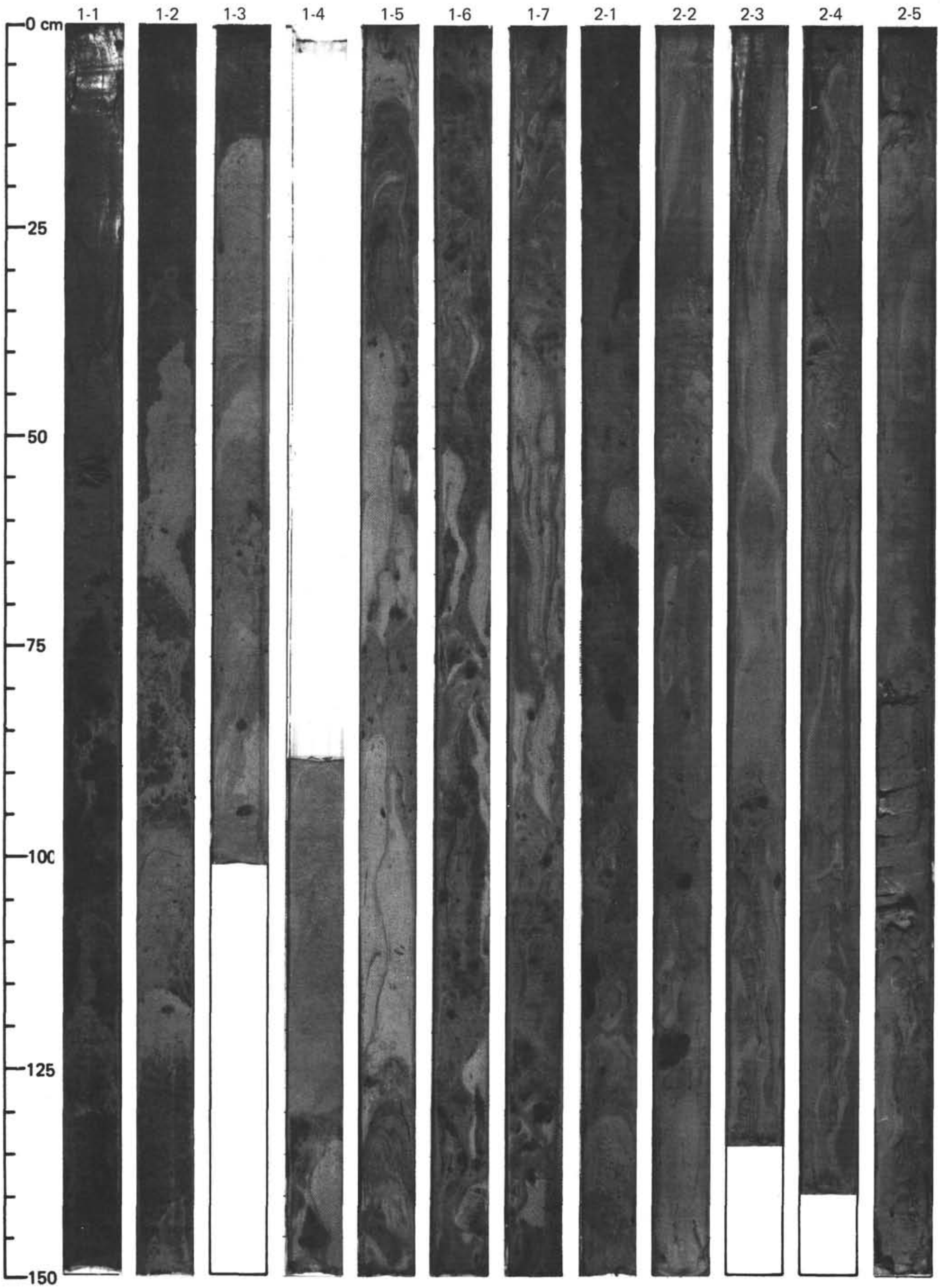
1-1
1-2
1-3
1-4
1-5
1-6
1-7
2-1
2-2
2-3
2-4
2-5
0 cm
25
50
75
100
125
150

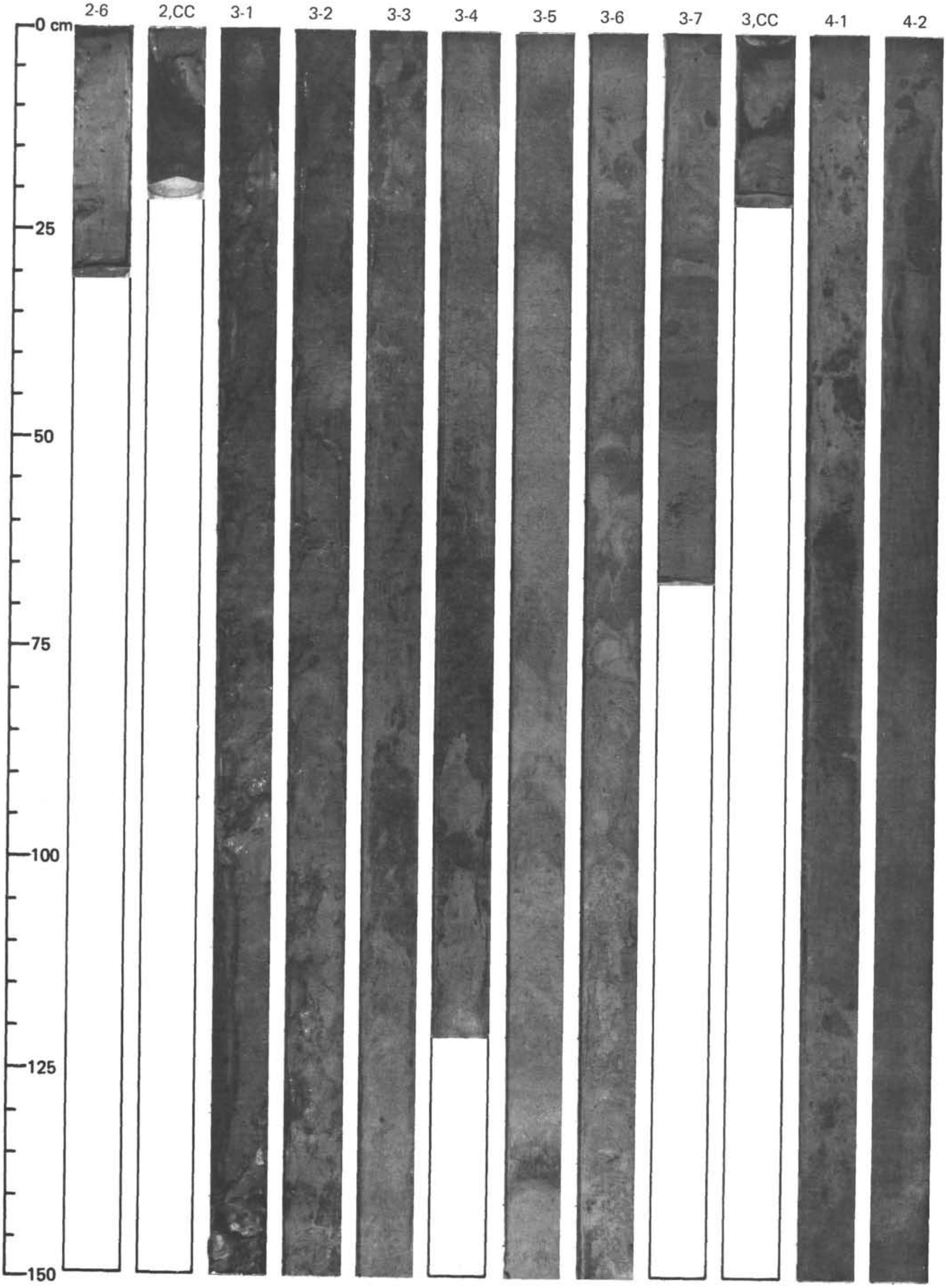
0 cm
25
50
75
100
125
150
2-6
2,CC
3-1
3-2
3-3
3-4
3-5
3-6
3-7
3,CC
4-1
4-2

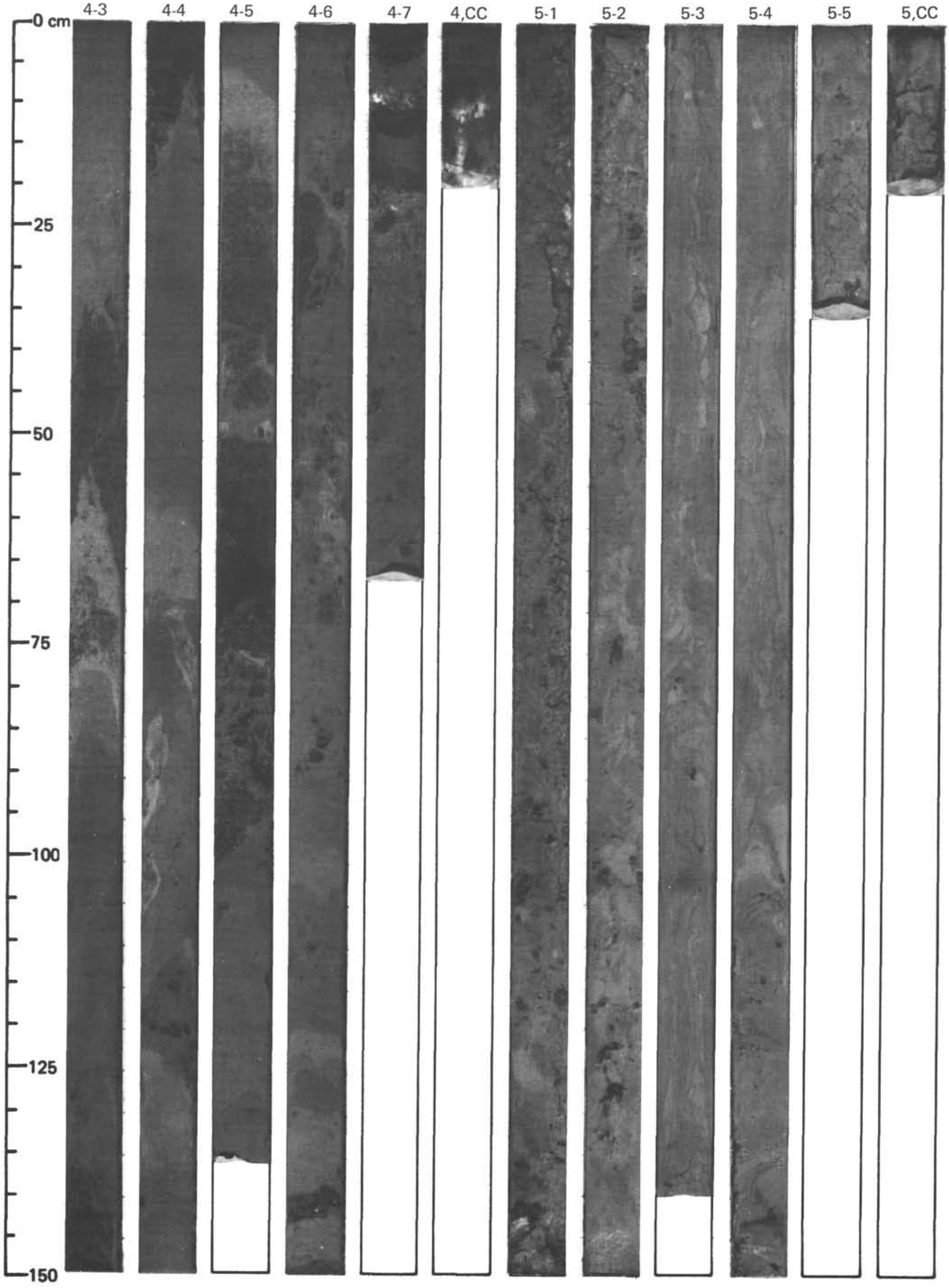
4-3
4-4
4-5
4-6
4-7
4,CC
5-1
5-2
5-3
5-4
5-5
5,CC
0 cm
25
50
75
100
125
150

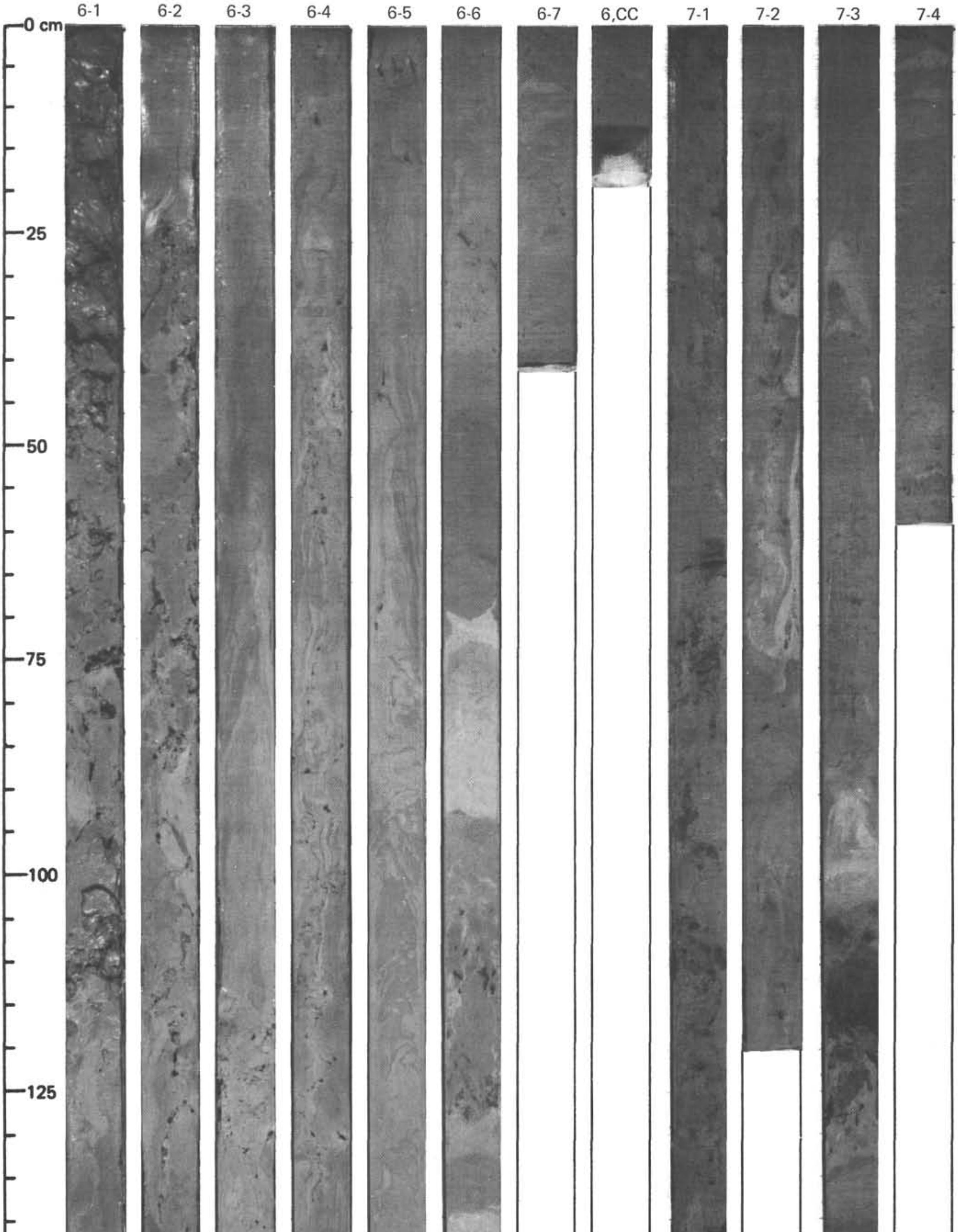

6-1
6-2
6-3
6-4
6-5
6-6
6-7
6,CC
7-1
7-2
7-3
7-4
0 cm
25
50
75
100
125
150

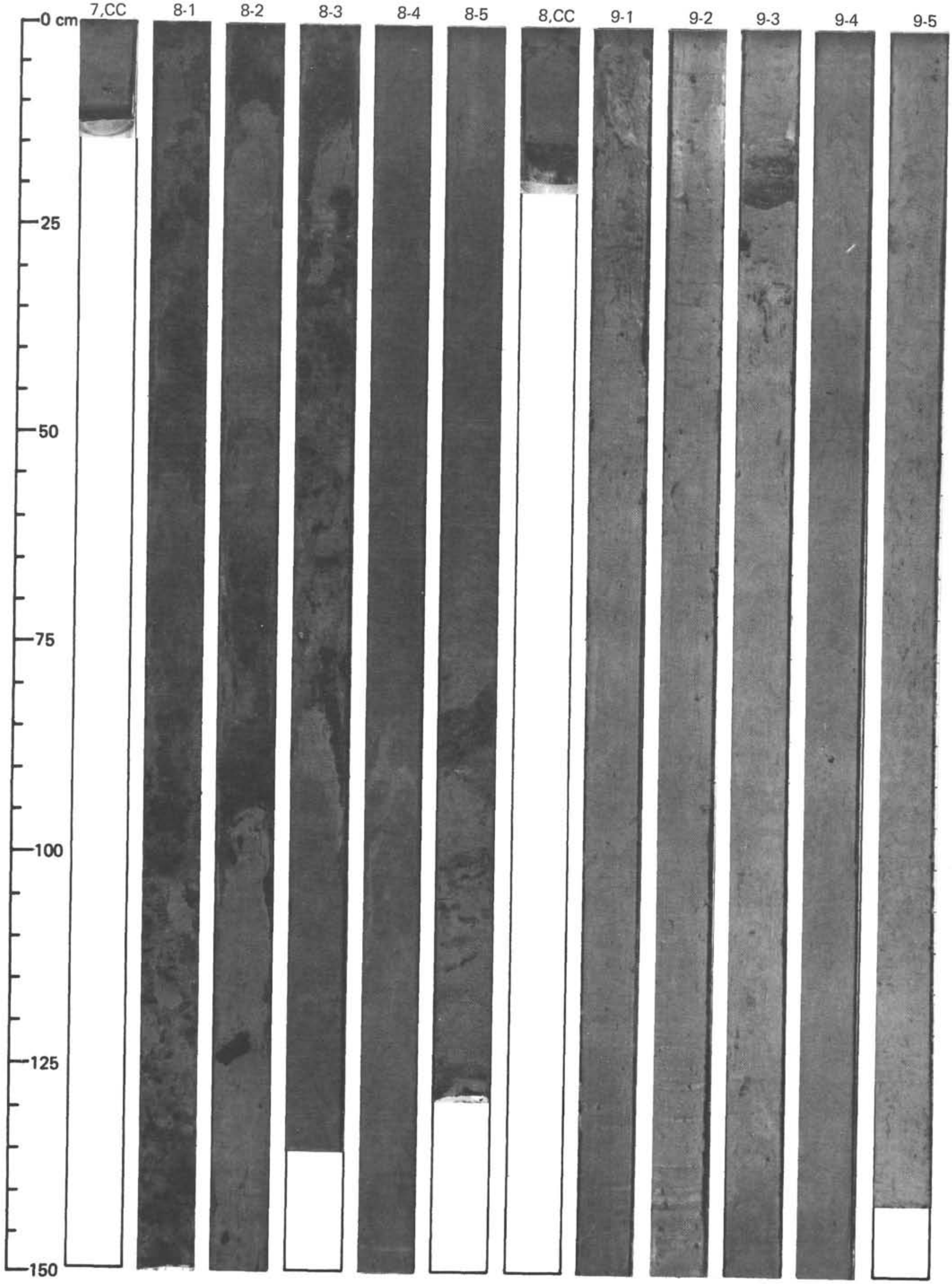
7,CC
8-1
8-2
8-3
8-4
8-5
8,CC
9-1
9-2
9-3
9-4
9-5
0 cm
25
50
75
100
125
150

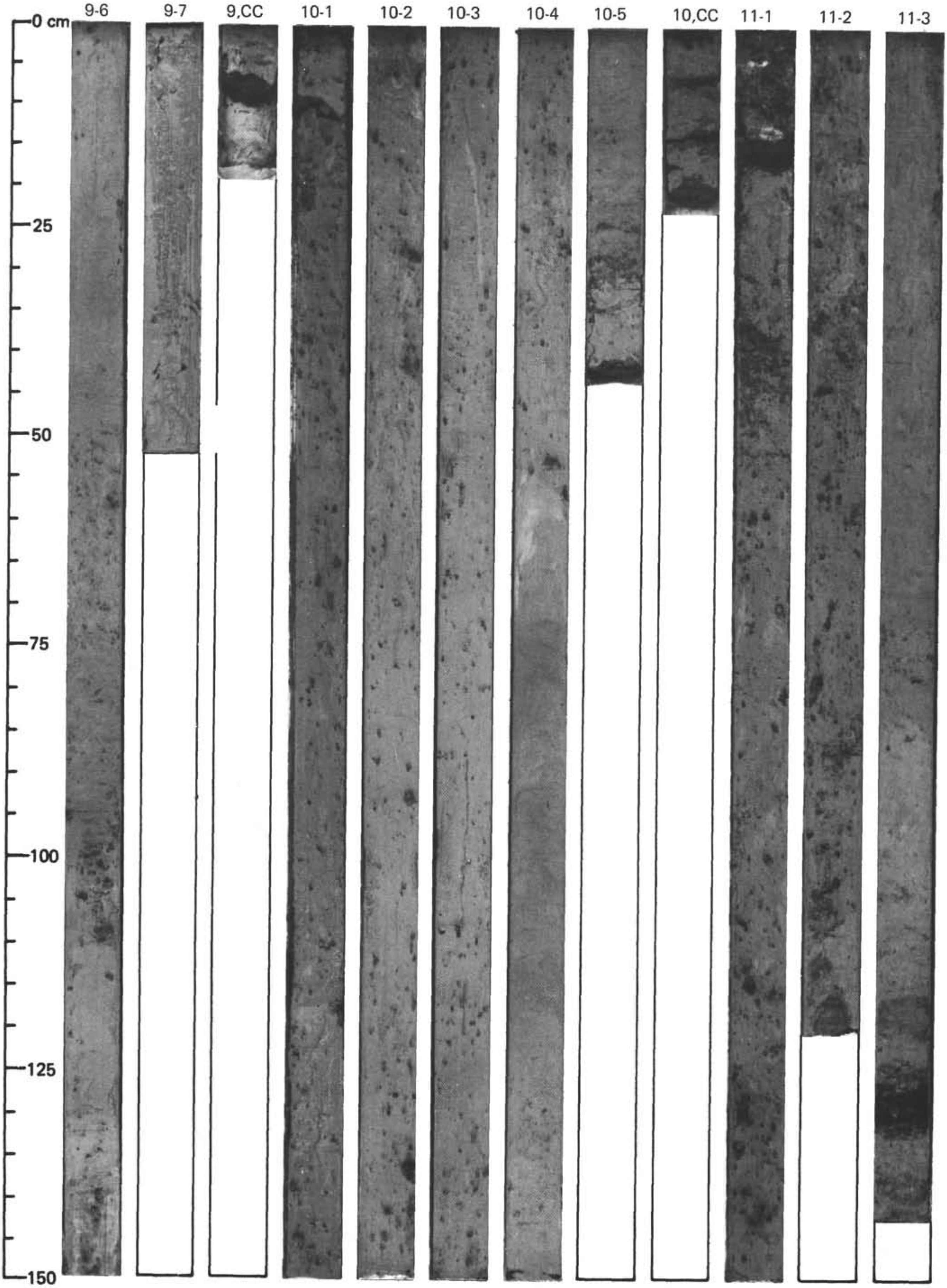
9-6
9-7
9,CC
10-1
10-2
10-3
10-4
10-5
10,CC
11-1
11-2
11-3
0 cm
25
50
75
100
125
150

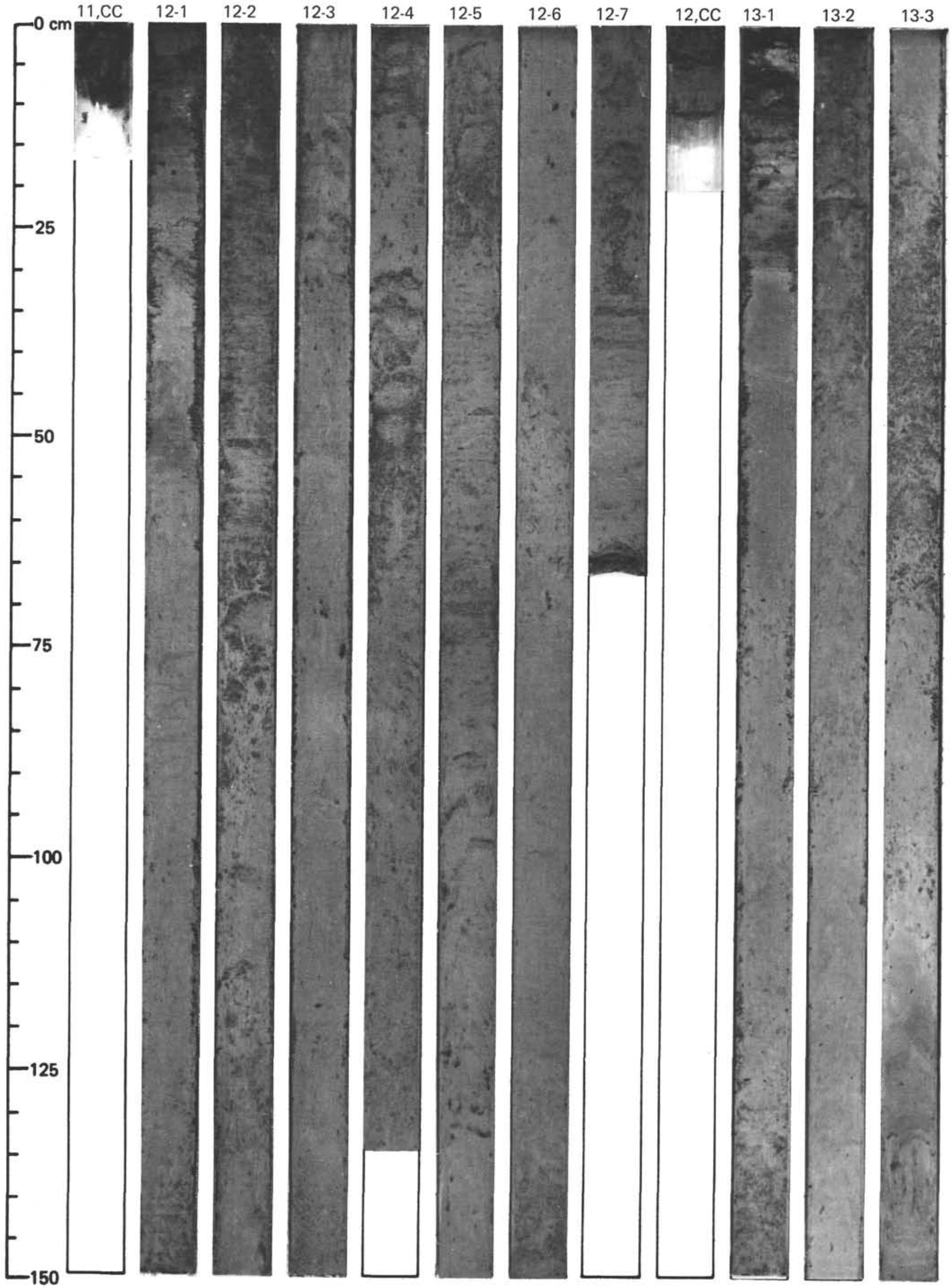
11,CC
12-1
12-2
12-3
12-4
12-5
12-6
12-7
12,CC
13-1
13-2
13-3
0 cm
25
50
75
100
125
150

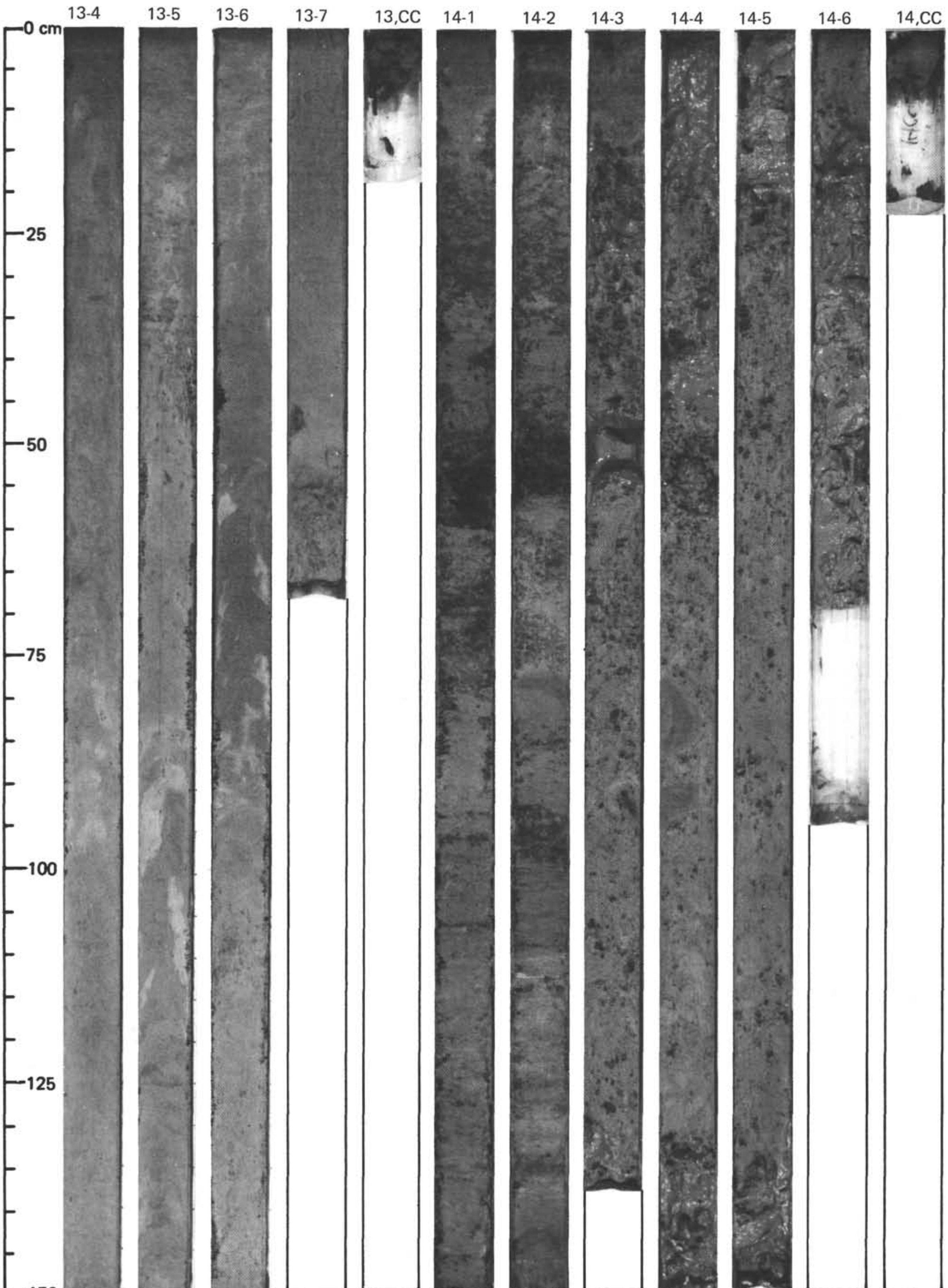
13-4
13-5
13-6
13-7
13,CC
14-1
14-2
14-3
14-4
14-5
14-6
14,CC
0 cm
25
50
75
100
125
150

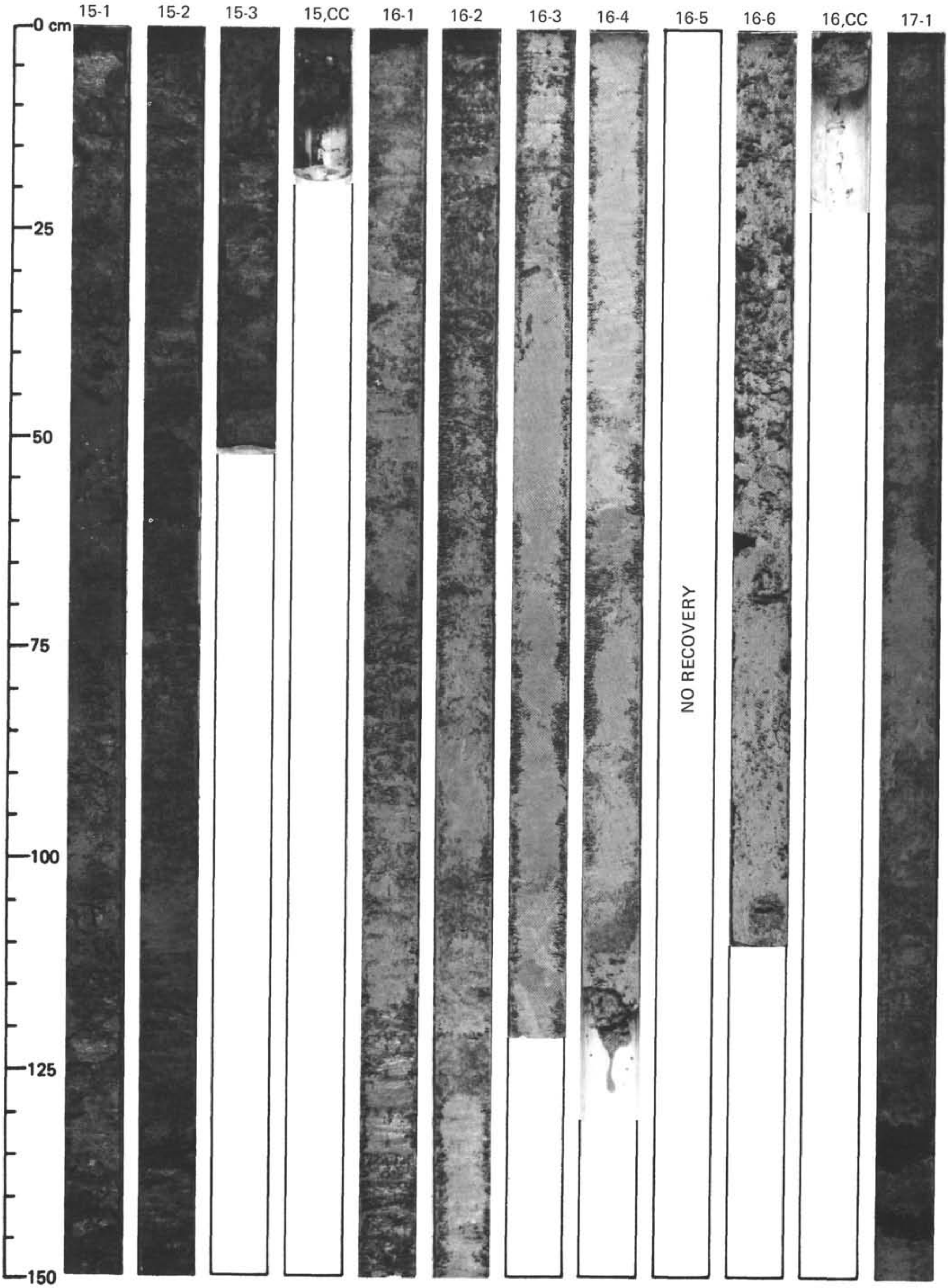
15-1
15-2
15-3
15,CC
16-1
16-2
16-3
16-4
16-5
16-6
16,CC
17-1
0 cm
25
50
75
100
125
150
NO RECOVERY

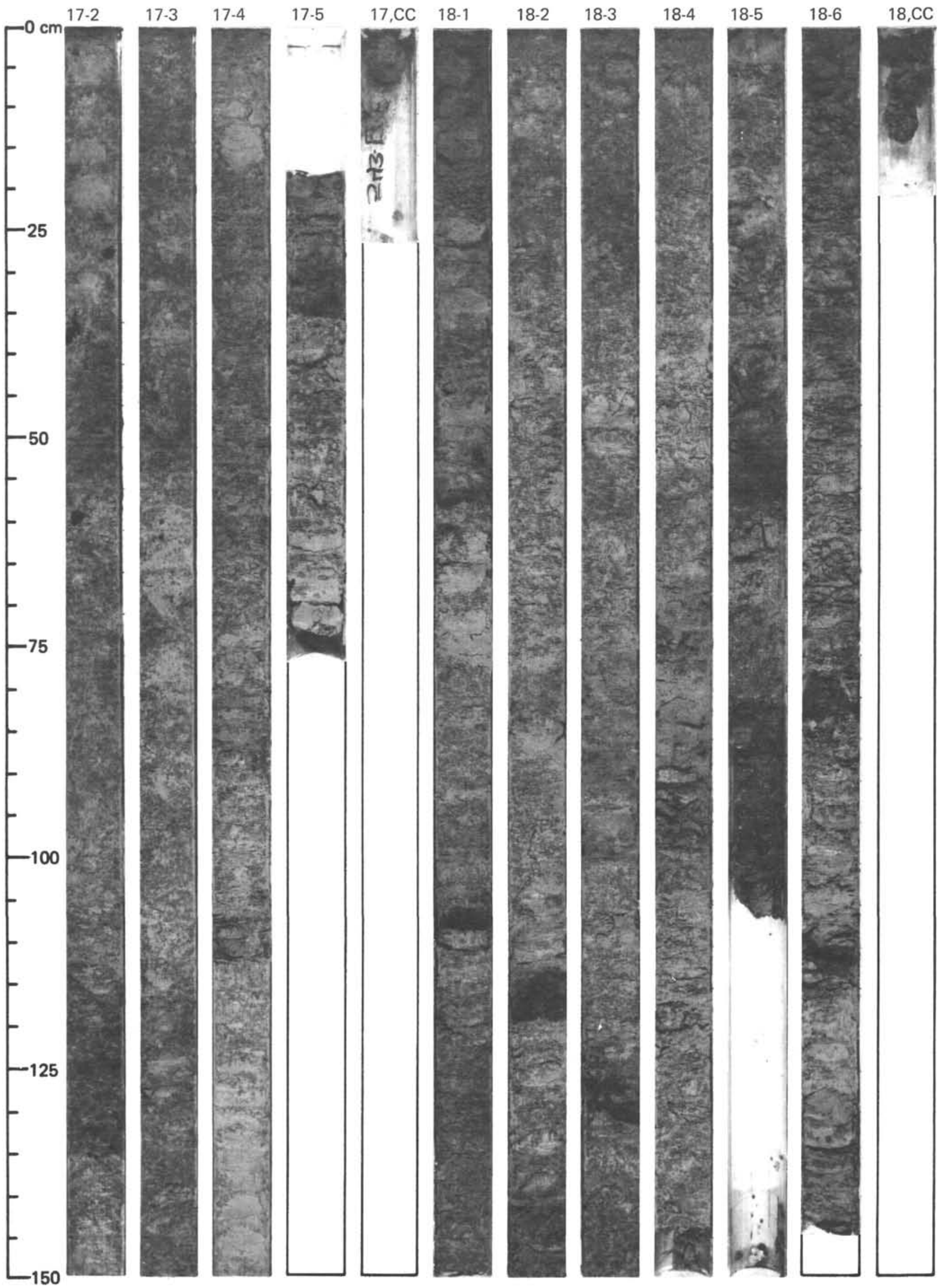
17-2
17-3
17-4
17-5
17,CC
18-1
18-2
18-3
18-4
18-5
18-6
18,CC
0 cm
25
50
75
100
125
150

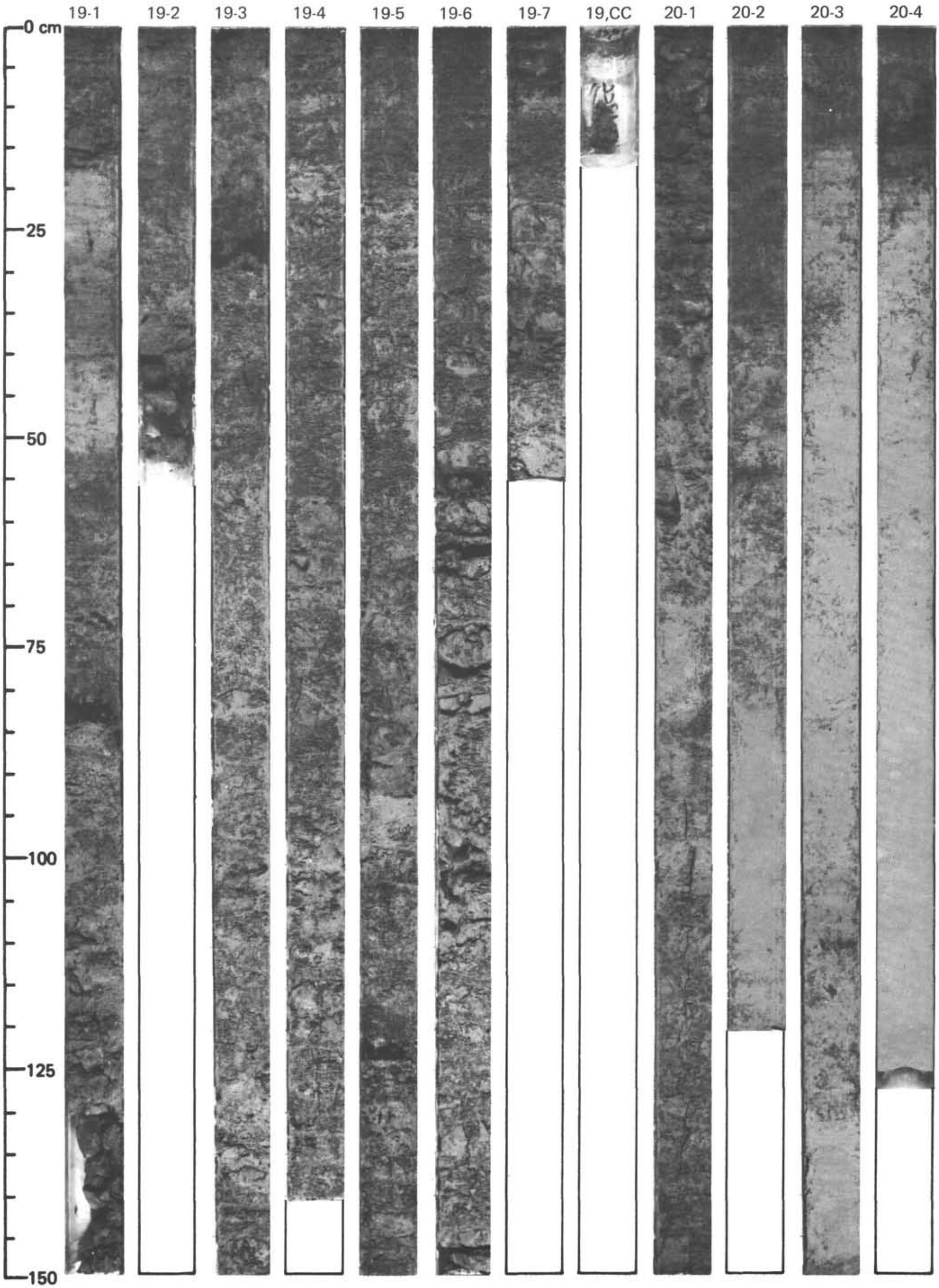
19-1
19-2
19-3
19-4
19-5
19-6
19-7
19,CC
20-1
20-2
20-3
20-4
0 cm
25
50
75
100
125
150

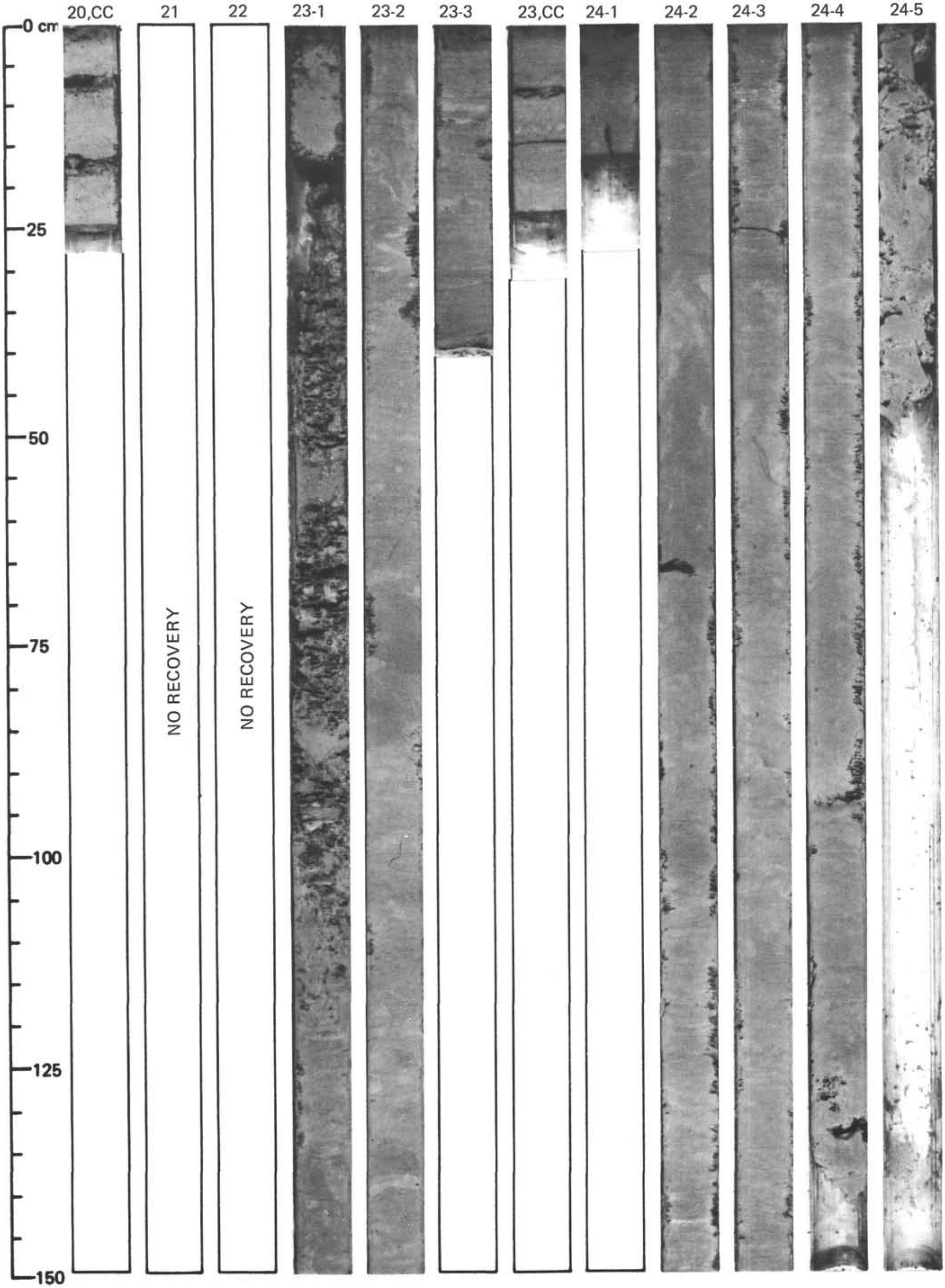
0 cm
25
50
75
100
125
150
20,CC
21
22
23-1
23-2
23-3
23,CC
24-1
24-2
24-3
24-4
24-5
NO RECOVERY
NO RECOVERY

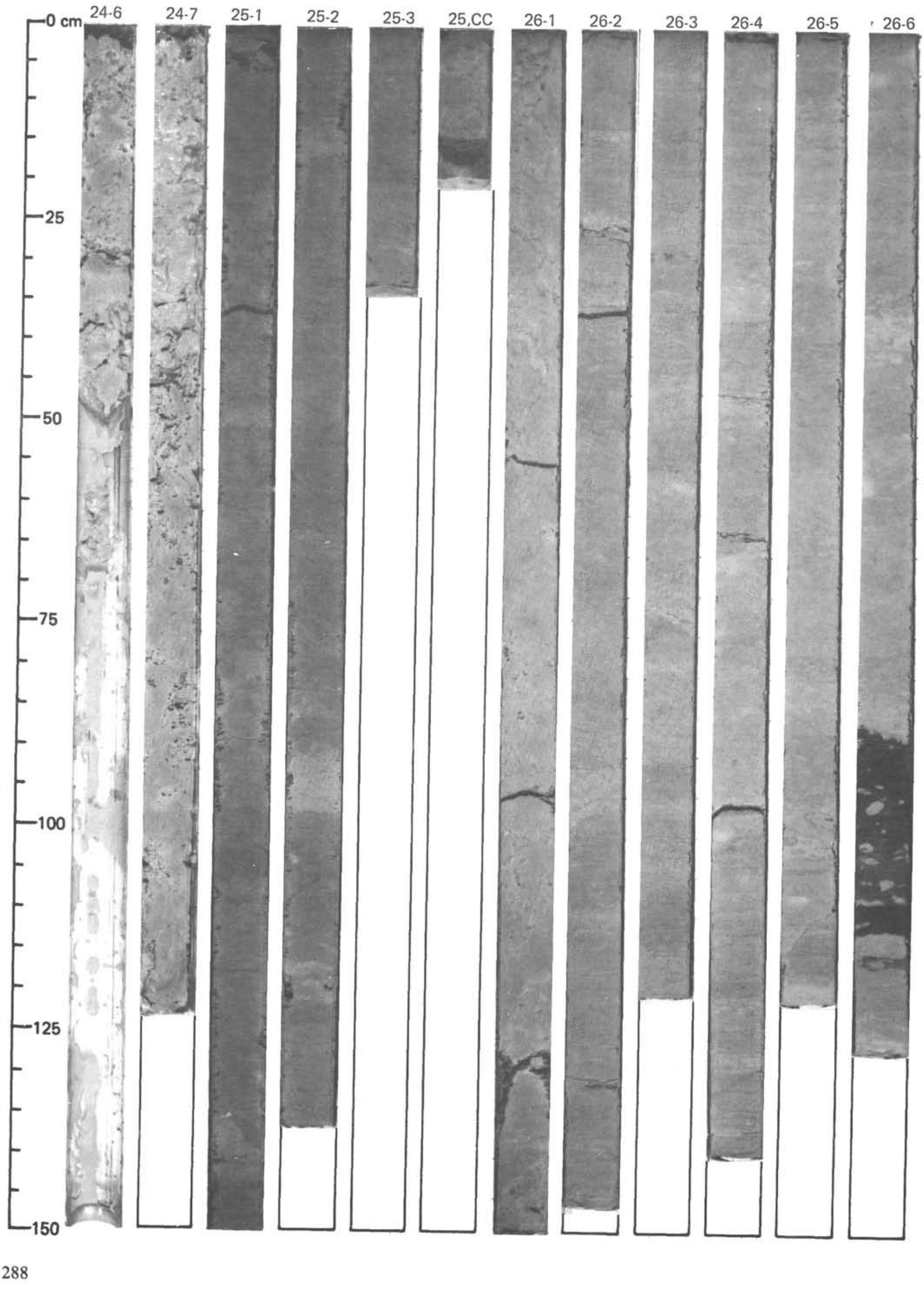
0 cm
25
50
75
100
125
150
24-6
24-7
25-1
25-2
25-3
25,CC
26-1
26-2
26-3
26-4
26-5
26-6

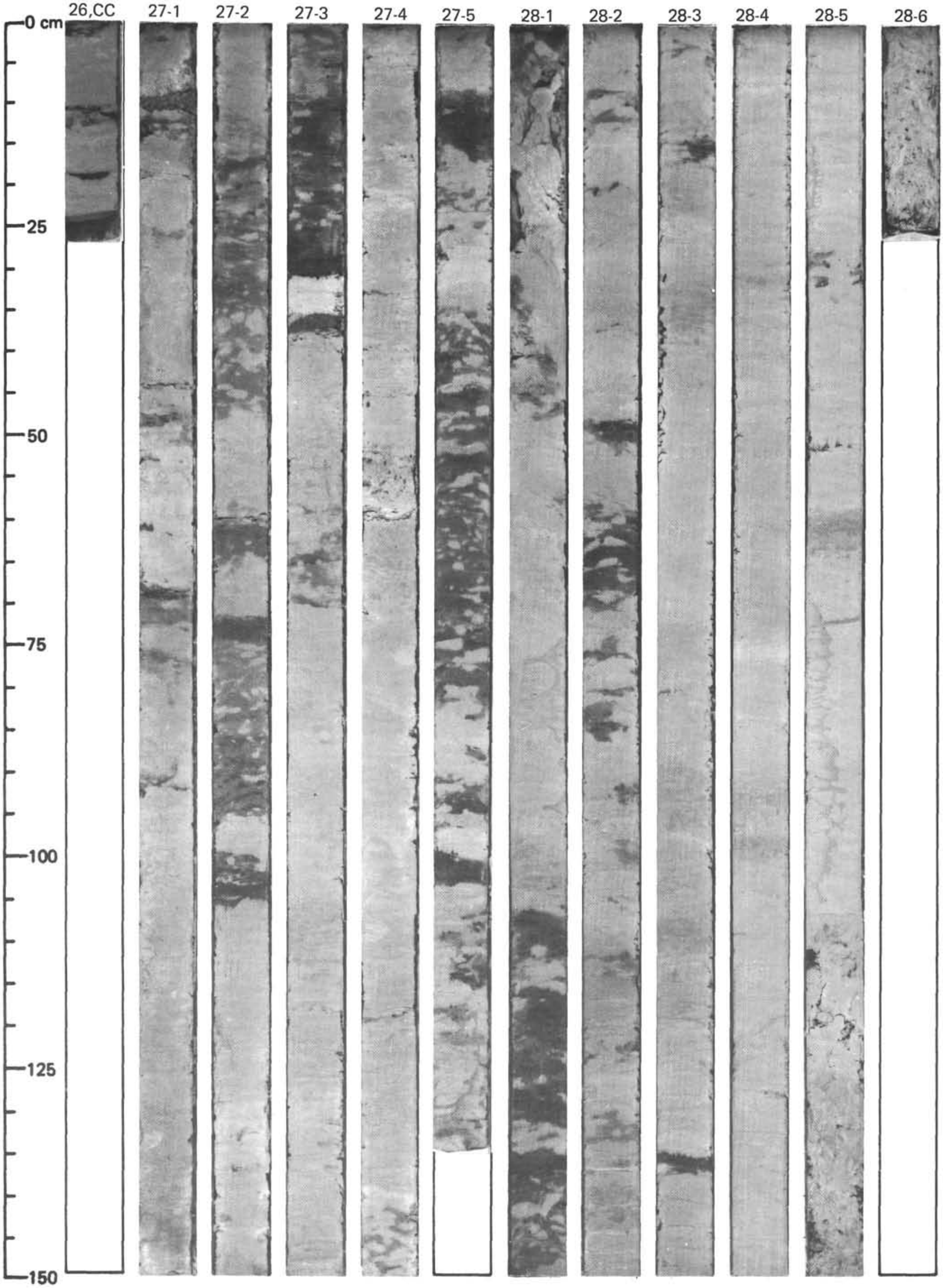
26,CC
27-1
27-2
27-3
27-4
27-5
28-1
28-2
28-3
28-4
28-5
28-6
0 cm
25
50
75
100
125
150

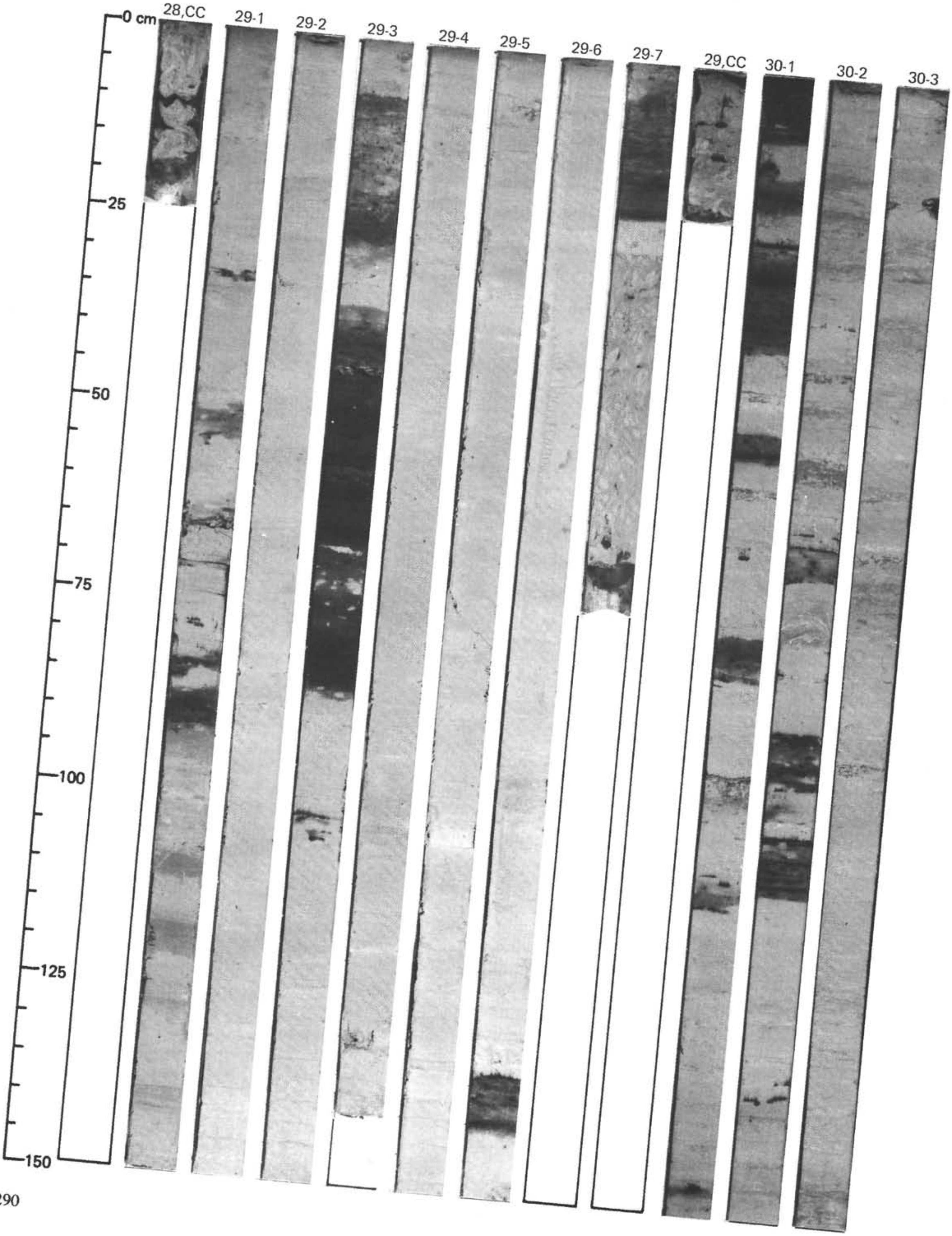
0 cm
25
50
75
100
125
150
28,CC
29-1
29-2
29-3
29-4
29-5
29-6
29-7
29,CC
30-1
30-2
30-3

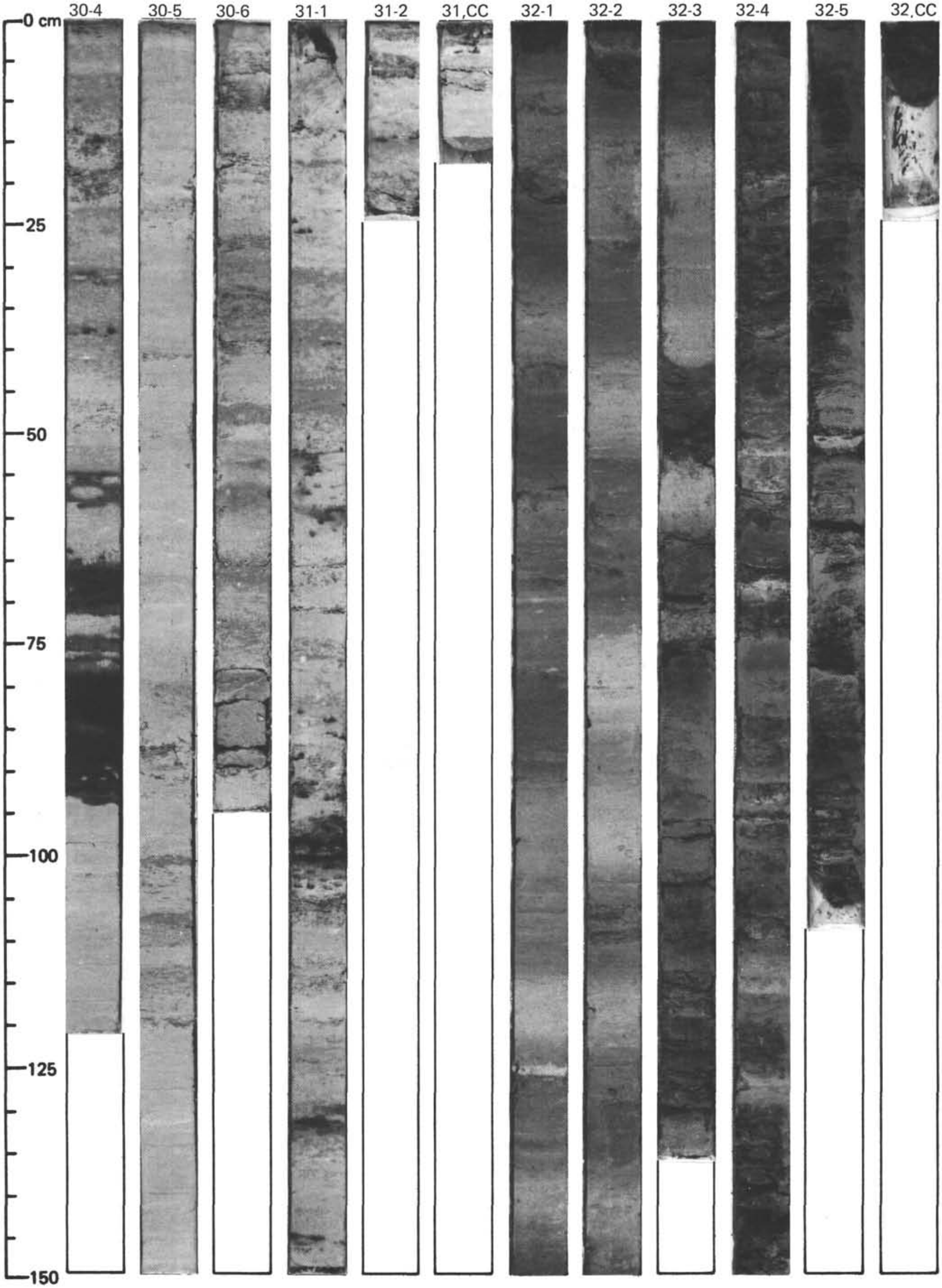
30-4
30-5
30-6
31-1
31-2
31,CC
32-1
32-2
32-3
32-4
32-5
32,CC
0 cm
25
50
75
100
125
150

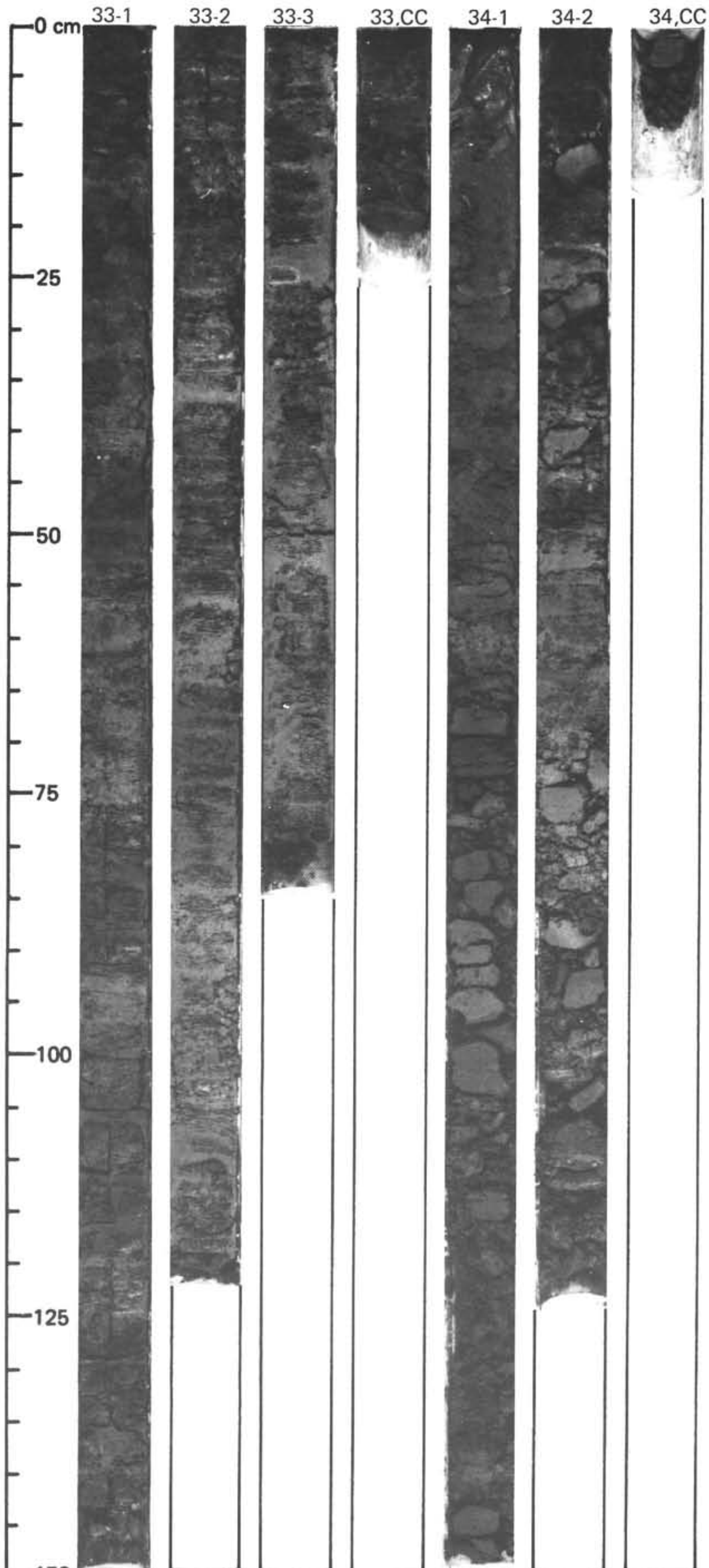
33-1
33-2
33-3
33,CC
34-1
34-2
34,CC
0 cm
25
50
75
100
125
150

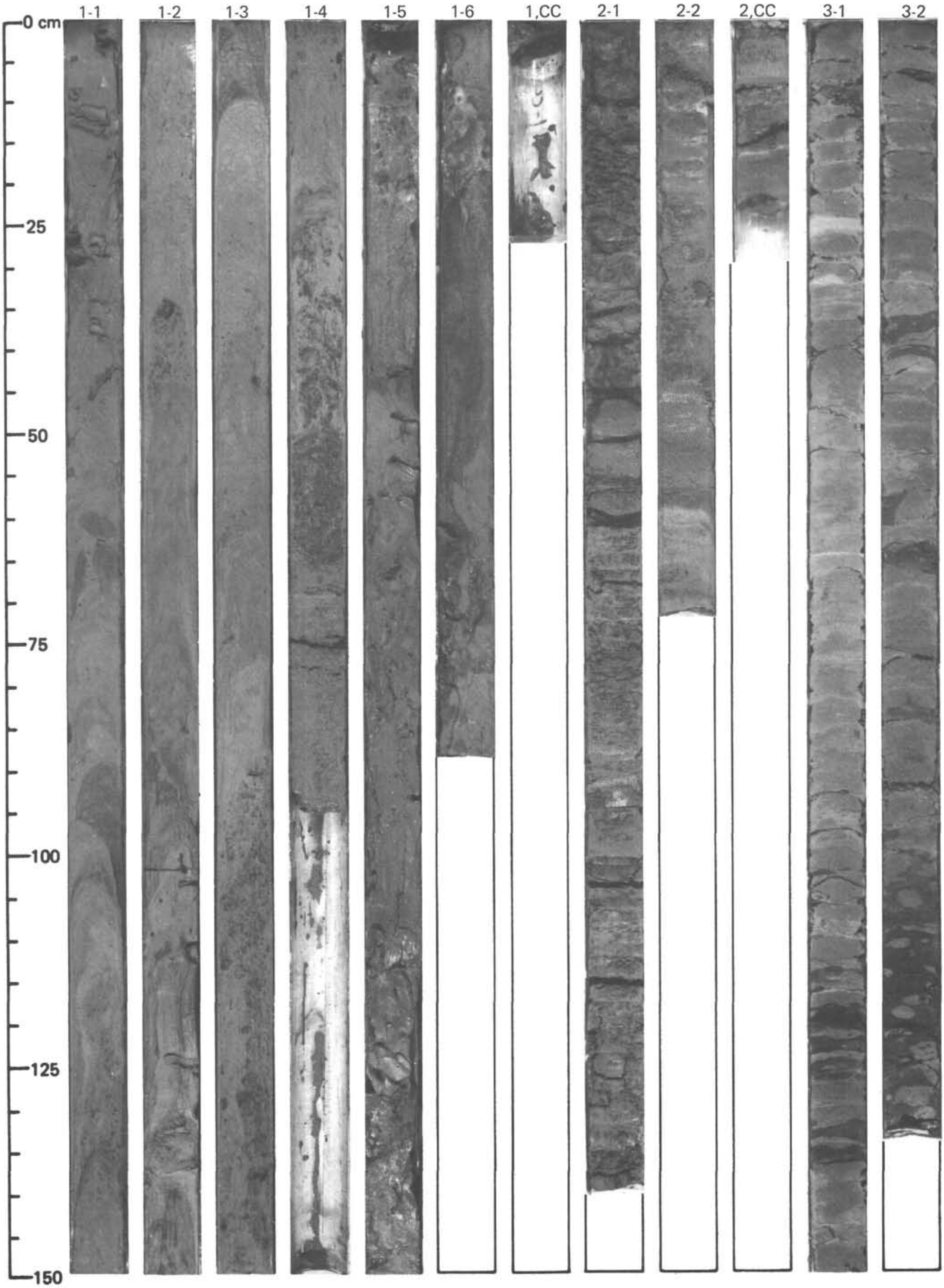
1-1
1-2
1-3
1-4
1-5
1-6
1,CC
2-1
2-2
2,CC
3-1
3-2
0 cm
25
50
75
100
125
150

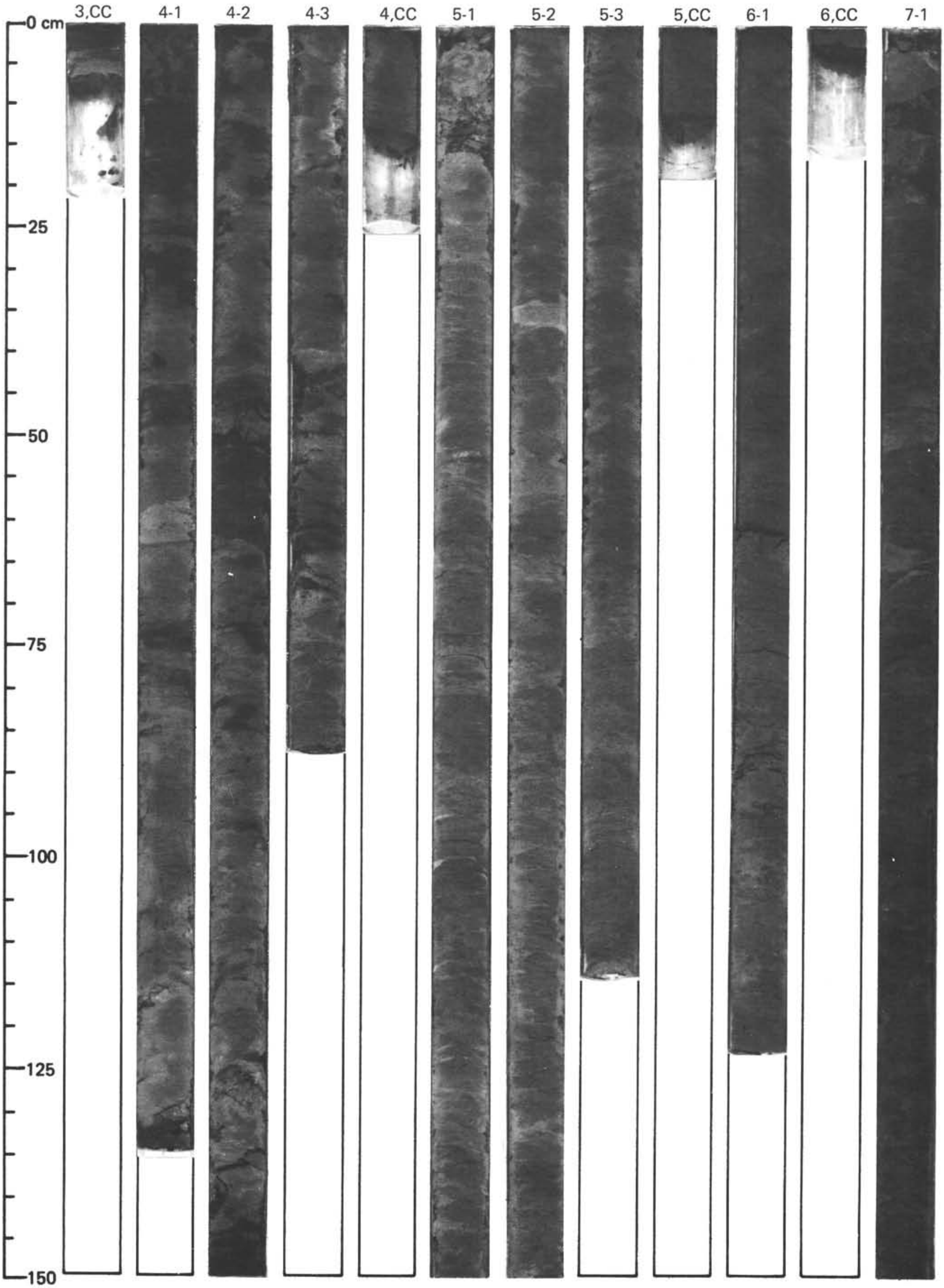
3,CC
4-1
4-2
4-3
4,CC
5-1
5-2
5-3
5,CC
6-1
6,CC
7-1
0 cm
25
50
75
100
125
150

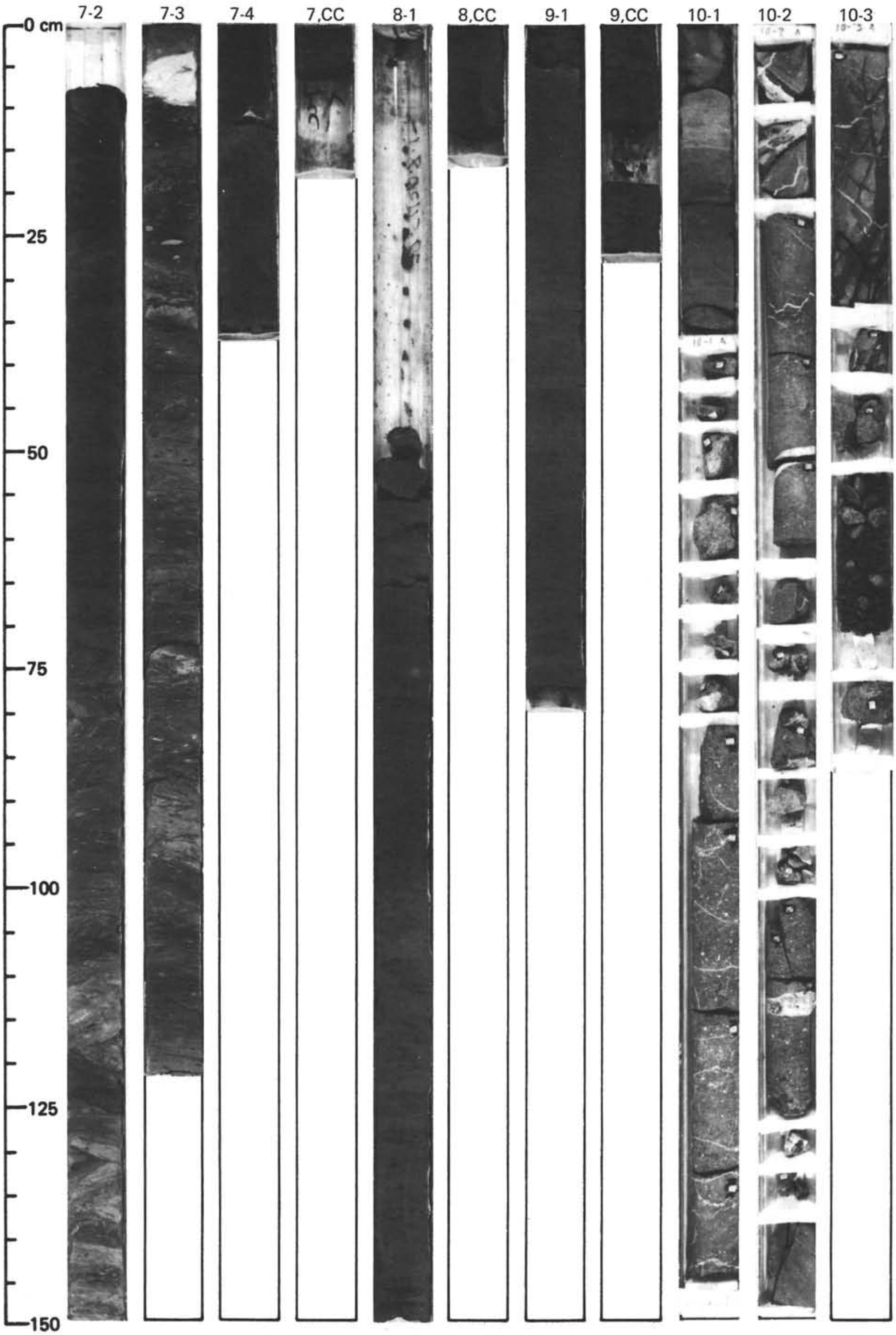
0 cm
25
50
75
100
125
150
7-2
7-3
7-4
7,CC
8-1
8,CC
9-1
9,CC
10-1
10-2
10-3

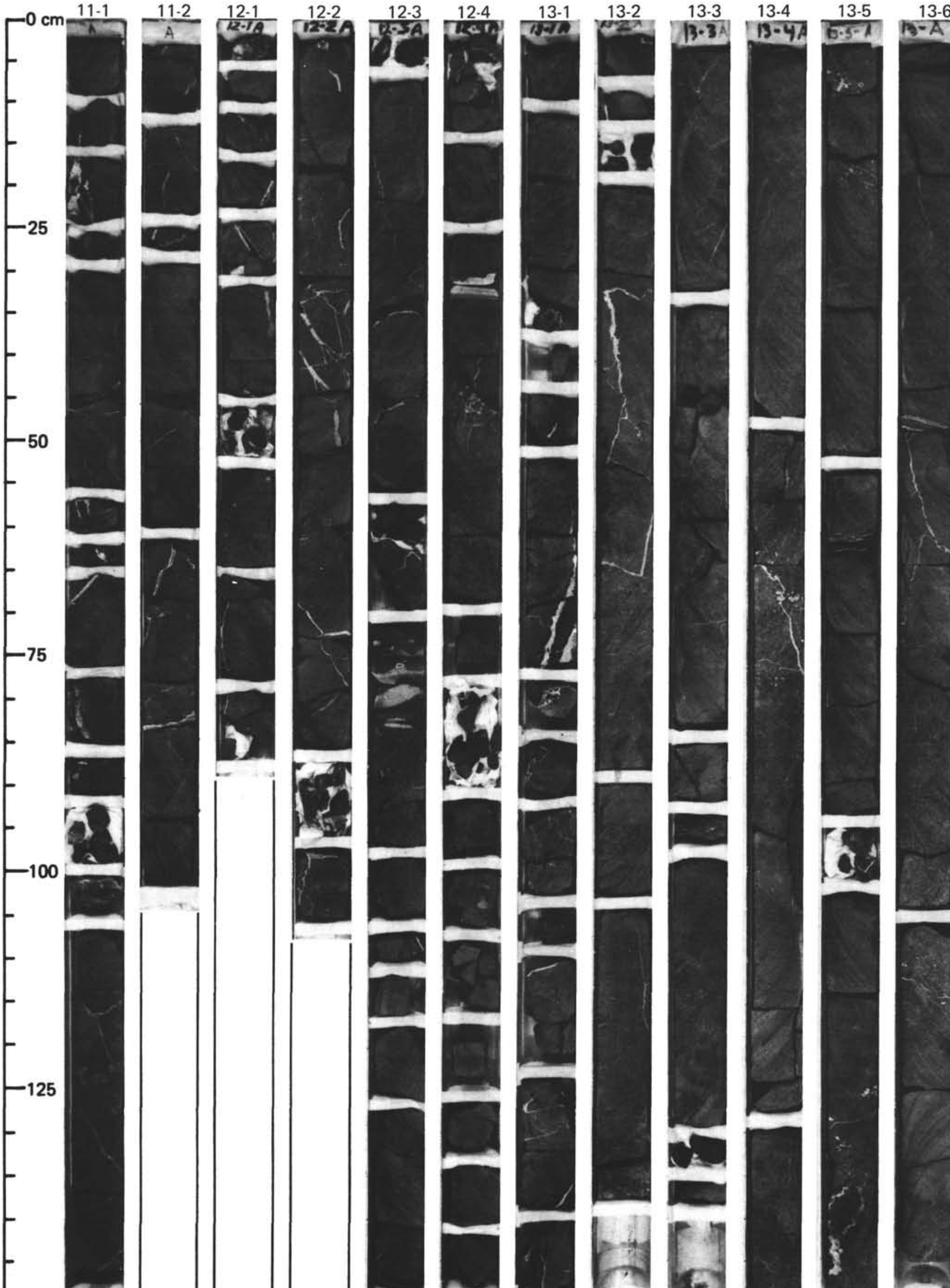
0 cm
25
50
75
100
125
150
11-1
11-2
12-1
12-2
12-3
12-4
13-1
13-2
13-3
13-4
13-5
13-6

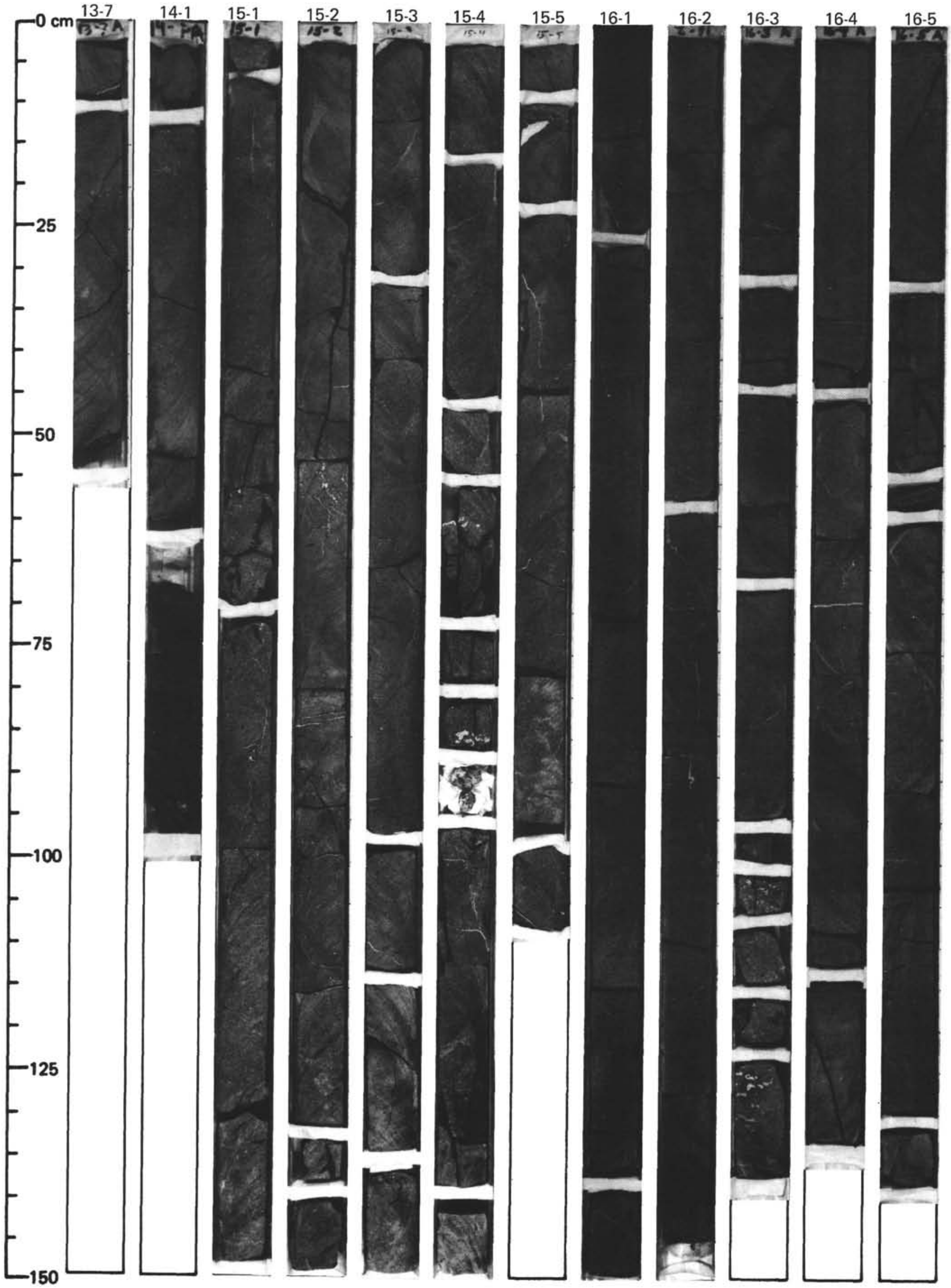

0 cm
25
50
75
100
125
150
13-7
14-1
15-1
15-2
15-3
15-4
15-5
16-1
16-2
16-3
16-4
16-5

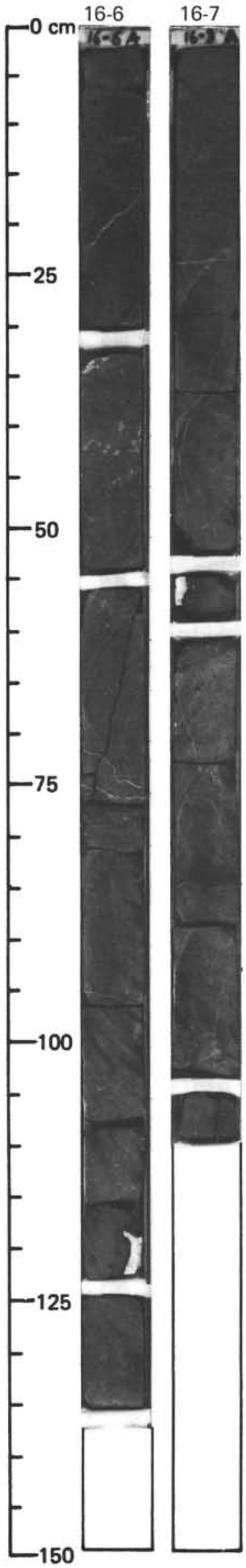
16-6
16-7
0 cm
25
50
75
100
125
150